

Spatial Modeling for Building Design Evaluation: from Visual Landscape Quality Assessment to Devaluation Risk Estimation

Présentée le 21 mai 2024

Faculté de l'environnement naturel, architectural et construit
Laboratoire d'économie urbaine et de l'environnement
Programme doctoral en architecture et sciences de la ville

pour l'obtention du grade de Docteur ès Sciences

par

Adam Robert SWIETEK

Acceptée sur proposition du jury

Prof. M. Andersen, présidente du jury
Prof. Ph. Thalmann, directeur de thèse
Prof. L. Barrage, rapporteuse
Dr S. Tobias, rapporteuse
Prof. A. Alahi, rapporteur

Acknowledgements

This dissertation would not have been possible without the support and expertise of my supervisor, Prof. Philippe Thalmann. I am grateful for the opportunity and academic freedom to explore and learn.

I have been fortunate to meet many inspiring and talented researchers throughout my journey. I thank the members at LEURE for listening, discussing, and challenging my work. In particular, thank you to Sigit, Marc, Fleance, Abdul, Sascha, Margarita, Sergey, Vincent, Gino, Paola and Taka. A special thanks to the countless experts who have enriched my learning, including my collaborator Marius Zumwald, the team at Wüest Partner, and my jury: Marilyne Andersen, Alexandre Alahi, Lint Barrage, and Silvia Tobias, for their generous support, ideas and continuous encouragement.

Thank you to my family for their endless support and love. To my parents, Wojciech and Marzena, without you I would not have the patience nor resilience to make this possible. To Conrad, Theresa, David, Tatiana thank you for always having an open ear, and for supporting me along this unconventional path. Hartwig und Marga, ich danke euch für eure endlose Ermutigung, Großzügigkeit und euer offenes Herz. Viele der Ideen in diesem Werk gehen auf einen Dachboden in Neustadt zurück.

Finally, I owe my curiosity and confidence to you, Judith. Your love and strength are the basis of everything I have accomplished. I dedicate this work to my newborn son, Henry, who has given me the opportunity to rediscover the world from a new perspective.

ABSTRACT

Zoning reform is a crucial tool for cities to adapt to contemporary challenges. However, its implementation remains challenging. Property owners, with a vested interest in the value of their neighborhoods, are sensitive to local developments and the potential unforeseen effects on environmental amenities.

Where complete information exists, environmental amenities and risks are priced into real estate valuations. Yet, there remains a lack of forward-looking micro-scale environmental data. Moreover, methods to incorporate such information into urban and building design evaluation are limited to the macro-scale: e.g. climate change risk. These hinder the markets' ability to effectively price discriminate, especially concerning uninsured local risks like zoning reform. Addressing this gap, this thesis leverages advancements in spatial modeling and geographical artificial intelligence (GeoAI) to estimate the financial impact of such risks, with a focus on the devaluation risk of visual impact from urban densification.

This thesis introduces spatial modeling for building design evaluation as four parts: *(i) Performance Simulation*, *(ii) Design Evaluation*, *(iii) Environmental Valuation*, and *(iv) Design Impact*. The concept of design performance, its economic evaluation, and its exposure and sensitivity are introduced by relating building performance simulations and real estate economics.

This work explores the impact of environmental risks on real estate valuation and proposes the concept of local area devaluation risk estimation. It focuses on visual impact resulting from nearby land-use changes as the variable of interest due to (1) the influence window views have on property valuations and on public opposition to densification and (2) the lack of methods to measure building-level visual quality in a comprehensive manner. It presents methods for the *(i)* 3D-CAD simulation of viewpoint visual shares and the *(ii)* statistical analysis of Visual Capital, a unique approach that estimates building level visual landscape quality by modeling income-sorting. Further, it introduces the *(iii)* hedonic pricing of Visual Capital and its application in an *(iv)* integrated impact analysis of computationally generated urban scenarios through Architectural Design Appraisal. Design Appraisal forecasts prices of procedurally generated building designs, using the learned estimates of financial preference of design performance. Applied within a regional simulation, it introduces a property-level environmental impact assessment to study local area devaluation risk.

This work represents the first-time that financial valuation is integrated within building design evaluation. The main results illustrate the potential of large-scale 3D data and GeoAI to (1) capture difficult to assess urban amenities (e.g. the view) and risks (e.g. obstruction), and to (2) inform urban design and land-use by incorporating market information into design simulations. This thesis concludes with a discussion of how these new concepts facilitate preference-driven generative design optimization and site selection.

ZUSAMMENFRASSUNG

Die Reform der Flächennutzungsplanung ist ein wichtiges Instrument für Städte, um sich an den Herausforderungen der Gegenwart zu stellen. Ihre Umsetzung bleibt jedoch eine Herausforderung. Grundstückseigentümer, die ein ureigenes Interesse am Wert ihres Viertels haben, reagieren empfindlich auf lokale Bauprojekte und die daraus hervorgehenden unvorhergesehenen Auswirkungen auf die Umwelt.

Wenn vollständige Informationen vorliegen, können Umweltvorteile und -risiken in die Immobilienbewertung einbezogen werden. Dies ist jedoch selten der Fall. Es mangelt nach wie vor an zukunftsorientierten Umweltdaten auf Mikroebene. Darüber hinaus sind die Methoden, die solche Informationen in die Bewertung von Städten und Gebäuden einbeziehen, auf die Makroebene beschränkt: z. B. das Risiko des Klimawandels. Dies schränkt die Fähigkeit der Märkte ein, eine wirksame Preisdiskriminierung vorzunehmen, insbesondere in Betracht nicht versicherbarer lokaler Risiken, wie sie zum Beispiel solche, die aus einer Flächennutzungsreform hervorgehen. Um diese Lücke zu schließen, nutzt diese Arbeit Fortschritte in der räumlichen Modellierung und der geografischen künstlichen Intelligenz (GeoAI), um die finanziellen Auswirkungen solcher Risiken abzuschätzen, wobei der Schwerpunkt auf dem Abwertungsrisiko von Gebäuden liegt, welches auf visuelle Veränderungen bedingt durch städtische Verdichtung zurückzuführen ist.

In dieser Arbeit wird die räumliche Modellierung für die Bewertung von Gebäudedesigns in vier Teilen vorgestellt: (i) Leistungssimulation, (ii) Designbewertung, (iii) Umweltbewertung und (iv) Auswirkungen des Designs. Das Konzept der Designbezogenen Gebäudeleistung, ihre wirtschaftliche Bewertung sowie ihre Exposition und Sensibilität werden neu eingeführt, indem Simulationen der Gebäudeleistung direkt mit der wirtschaftlichen Bewertung einer Immobilie in Zusammenhang gebracht werden.

In dieser Arbeit werden die Auswirkungen von Umweltrisiken auf die Immobilienbewertung untersucht und das Konzept der Risikoabschätzung für die Abwertung lokaler Gebiete eingeführt. Die Arbeit konzentriert sich auf visuelle Auswirkungen, die sich aus nahegelegenen Landnutzungsänderungen ergeben, als Variable von Interesse aufgrund (1) des Einflusses, den Fensteransichten auf Immobilienbewertungen und auf den öffentlichen Widerstand gegen eine Verdichtung haben, und (2) des Mangels an Methoden zur umfassenden Messung der visuellen Qualität einzelner Gebäude. Es werden Methoden vorgestellt, die die (i) 3D-CAD-Simulation der visuellen Anteile von Aussichtspunkten und die (ii) statistische Analyse von Visual Capital erlauben. Letzteres ist ein neuer Ansatz, der die visuelle Landschaftsqualität auf Gebäudeebene durch Modellierung der Einkommenssortierung einschätzt. Darüber hinaus wird (iii) die Auswirkung von Visual Capital auf Immobilienpreise mithilfe des hedonischen Preismodells bestimmt und die daraus hervorgehenden Koeffizienten für eine (iv) integrierte Wirkungsanalyse (Architectural Design Appraisal) genutzt, die Computer-erzeugte urbane Designszenarien finanziell bewertet. Im Rahmen einer regionalen Simulation wird eine Umweltverträglichkeitsprüfung individuell abgeänderter Grundstücke eingeführt, um das Risiko der finanziellen Abwertung eines lokalen Gebiets aufgrund von Bauprojekten zu untersuchen.

Diese Arbeit stellt, zum ersten Mal, eine Methode vor, die die finanzielle Bewertung einer Immobilie in die Bewertung von Gebäudedesigns integriert. Die Ergebnisse veranschaulichen welches Potenzial die großflächige Nutzung von 3D-Daten und GeoAI, bietet, um (1) schwer zu bewertende städtische Annehmlichkeiten (z. B. die Aussicht) und

Risiken (z. B. Einschränkung der Aussicht) zu bewerten und um (2) Stadtplanung und Flächennutzung durch die Einbeziehung von Marktinformationen in Designsimulationen zu optimieren. Diese Arbeit schließt mit einer Diskussion darüber, wie diese neuen Konzepte die präferenzgesteuerte generative Designoptimierung und Standortauswahl erleichtern können.

TABLE OF CONTENTS

<i>1</i>	<i>Introduction</i>	<i>15</i>
1.1	Real Estate and Environmental Risk	15
1.1.1	Transition Risks	16
1.1.2	Mitigating Risk with Insurance and Risk Transfer Mechanisms	17
1.1.3	Adaptation to Uninsured Risks	18
1.1.4	Local Effects of Urban Adaptation	20
1.1.5	Local Amenities and Risk	21
1.2	Evaluating Environmental Risks	23
1.2.1	Modeling Physical Climate Risk	25
1.3	Modeling Local Area Risk	27
1.3.1	Land Use Change as a Hazard to Property Valuations	27
1.3.2	Addressing the Challenges with 3D GIS and the View Metrics	28
1.4	Motivation	31
1.4.1	Background on Design Simulations	32
1.4.2	Background on Building Performance Evaluation	33
1.4.3	Background on Environmental Valuation	36
1.4.4	Background on Design Impact Assessment	37
<i>2</i>	<i>Visual Capital: Evaluating Building Level Visual Quality at Scale</i>	<i>39</i>
2.1	Introduction	40
2.2	Literature Review	42
2.2.1	Spatial Feature Extraction	42
2.2.2	Evaluation of view-metrics	43
2.3	Data & Methods	44
2.3.1	Viewpoint Visual Share Data	45
2.3.2	Developing Building-Level View-Metrics	47
2.3.3	Measuring Visual Capital	54
2.3.4	Measuring Regional Difference of Visual Capital	57
2.3.5	Drawing New Geographic Boundaries of High Visual Capital	57
2.4	Results	58
2.4.1	Distribution of building-level view-metrics across the Swiss building stock	58
2.4.2	Model	60
2.4.3	Visual Capital	62
2.5	Discussion	68
2.6	Conclusion	72
<i>3</i>	<i>Automated Design Appraisal: Estimating Real Estate Price Growth and Value at Risk due to Local Development</i>	<i>73</i>
3.1	Introduction	74
3.2	Literature Review	76
3.2.1	Economic Performance Metrics	76
3.2.2	Devaluation Risk	77
3.2.3	Visibility Simulation and Visual Capital	78
3.3	Material and Methods	79
3.3.1	Pricing Model	80
3.3.2	Design Simulation	81

3.3.3	Integrated Impact Assessment	83
3.4	Results	86
3.4.1	Value of a View	86
3.4.2	Single Hazard	89
3.4.3	Multi Hazard	91
3.5	Discussion	96
3.6	Conclusion	99
4	<i>Conclusion & Outlook</i>	<i>100</i>
4.1	Main Contribution & Findings	100
5	<i>Future Outlook</i>	<i>103</i>
5.1	Addressing Limitations	103
5.2	Towards Preference Driven Design	103
6	<i>Supplements</i>	<i>106</i>
6.1	Mini-Study: UEQ, Urban Health, Energy Consumption	106
6.2	How view determines well-being and value	109
6.3	Supplementary Material for Visual Capital Article	115
7	<i>References</i>	<i>125</i>

LIST OF TABLES

Table 1: To explore the concept of devaluation risk, this thesis adopts the following terms that define the determinates of risk (IPCC, 2023).....	23
Table 2 Data Types common to Urban Analytics	28
Table 3 Landscape Elements and Distance Considered	47
Table 4 Definitions for Visual Composition and Configuration Metrics	49
Table 5 - Summary Statistic for Visual Composition Indicators for 33 million viewpoints.	50
Table 6 Summary Statistics for Visual Configuration Indicators	52
Table 7- Summary of Commune-Level Income Statistics for Agglomerations Used in Training Sample	55
Table 8: Regression results across four models, where the dependent variable is the natural logarithm of the transacted price. Column (1) presents the regression results of the model that includes only the variable of interest, visual capital (VC). Column (2) presents the results of the model containing VC conditional on the agglomeration. Column (3) incorporates the fully specified model with an unconditional VC . Column (4) presents results for the fully specified model with VC conditioned on lake-side agglomeration. Robust standard errors are shown in brackets and statistical significance is denoted at the following levels *** $p < 0.01$, ** $p < 0.05$, * $p < 0.1$	87
Table 9 Urban environmental quality metrics and their underlying data source.	106
Table 10 Environmental features (including solar irradiance, road noise, air quality, thermal comfort, view metrics) help to partly explain the spatial structure of the YPLLG in Geneva	107

LIST OF FIGURES

Figure 1 Abstract Definition of Environmental Risks, adapted from IPCC, EEA report.....	23
Figure 2 Schematic summarizing the visual share dataset. Data collected from each Viewpoint (VP) is illustrated with a representative Viewpoint Image. The actual database contains values representing the proportion of each landscape element visible from a single VP.....	46
Figure 3 Schematic summarizing the developed methodology.....	46

- Figure 4 ECDF of maxVSH elements across the Swiss building stock. Figure indicates that building-level views of elements vary in abundance, where abundant elements are seen (maxvsh >0%) by more than half of the building stock and scarce elements are visible in less than half. 59
- Figure 5 Scatterplot of commune-level predictions against commune-level net-income. Plot illustrates the dispersion of commune-level prediction increases against net-income, where the 95th percentile and Mean score are shown in Red and Blue. 60
- Figure 6 Impact of view-metrics on a single building's prediction. (A) Summary plot illustrates the SHAP value of a single instance and directionality of impact of the view-metric, where high and low feature values are shown in Red and Blue. The impact of the top 6 features are shown, the remaining, less influential metrics (by absolute mean) can be found in the Supplementary material Fig S7. Interaction plots show that prediction influence of (B) nature views vary across visual access to water, (C) views of buildings vary against sky exposure, (D) larger views of a waterbodies in the same scenery, as well as views of far-distance, have larger predictions than smaller views of waterbodies, and (E) vegetation varies across distance inequality. 62
- Figure 7 Scatterplot of Commune-level prediction for the 10 largest Swiss urban agglomerations. A fitted line, and its slope shown in blue and the agglomeration's mean prediction is shown in orange. The plot and computed slope describe the degree to which income sorting can explain residential sorting variations across Switzerland. A steeper slope, e.g. Lausanne, implies that the visual environment can describe the difference between low- and high-income communes; whereas in Bern smaller differences in visual capital between the high- and low- income communes, i.e. flatter slopes, suggests visual landscape to be less important to the residential income sorting process. 63
- Figure 8 Spatial Distribution of Visual Capital across Swiss agglomerations. Standardized VC values are used to illustrate the spatial dispersion of above and below average within and across agglomerations. 64
- Figure 9 Choropleth depicting visual capital of the Swiss building stock shows higher levels of visual capital are found nearby lakes and on the foothills of the Alps. Comparison of the distribution of building-level average net-income and Visual Capital values for Zurich and Geneva reveals that VC captures intra-communal differences in building-level view quality. 65
- Figure 10 Heatmap depicts the average VC (left) and skewness of VC (right) when stratified by urban and natural form; i.e. building density

- (100 m radius) and terrain slope (1 km area). Urban/Natural form conditions with less than 1000 buildings are excluded (greyed). 66
- Figure 11 Computed boundaries of high visual capital (HVC) are shown in blue. Communes with darker shades of green indicate higher income levels, grey communes were excluded from the training-sample because no income data was readily available, and the red border indicates high-income communes as labeled by a secondary data source. HVC appears in all held-out validation samples; including Jouxkens-Mezery. HVC spills past administrative boundaries of high-income neighborhood, including St.Sulpice and Pully. 68
- Figure 12 (a) Abstract schematic of the proposed Automated Design Appraisal algorithm: step 1.) define the set of design parameters of interest; step 2.) update buildings within 3D city model according to design parameters, thereby creating an alternative design scenario; step 3.) compute building performance metrics using building and micro-climate simulations – in this paper, we utilize a viewpoint visual share visibility simulation to generate a set of view-metrics and subsequently calculate the visual landscape quality, i.e. Visual Capital; step 4.) update vector of building attributes to include new performance metrics; step 5.) use fitted model to predict price of building with updated performance metrics. (b) Abstract schematic showing the application of ADA for a visual impact assessment in Lausanne. The proposed development, shown in red, represents the point of modification within a reference 3D city model. The spatial distribution of price impact, computed via ADA, is shown, with darker red representing greater impact on a building’s predicted price. 82
- Figure 13: Spatial distribution and abstract representation of the integrated impact assessment metrics used to visualize the distribution of impacts on maxVSH Sky, i.e. the maximum visible proportion of sky from a single viewpoint across all of a building’s viewpoints. Reference is the as-built condition of the city, Direct Effect (DE) express the gain in Sky Exposure as a result of the up zoning, Cumulative Local Effects (CLE) describes the gross cost imposed on its neighbors due up zoning at a given building, and Exposure to Local Effects (ELE) expresses the maximum potential loss across all of the unzoning scenarios tested. 86
- Figure 14: Price Effect of Visual Capital by agglomeration while holding the other model parameters constant. The black line represents the actual range of values used during model training. For comparison, Lausanne (the agglomeration used in the case studies), is shown in red. 89
- Figure 15: (a) ECDF of relative change of maximally exposed view-metric and predicted price for all buildings in the sample region. Maximum

visual impact is defined as the maximum relative change across a building’s vector of view-metrics between the two design scenarios. Heavily skewed distribution indicates concentrated losses. (b) Summary of log fold changes of view-metrics for all buildings between two design scenarios, the design scenario with the proposed development versus the baseline, as-built condition. (c) Barplot of the proportion of aggregate value lost for each level of price sensitivity, relative to the sample share of corresponding buildings. (d) Dot plot comparing the exposed view-metrics of buildings with Positive and Negative price sensitivity, suggesting some building benefits from additions to the ‘Sky-Line’ (Panoramic and Element Richness). (e) Series of effect-size maps following the developed method: 4-view metrics (lake-view, nature view, far-distance, and sky-exposure). (f) Effect size map of the predicted price impact the proposed development site has on neighboring buildings (development shown in black). (g) Top ranked view-metric contributing to price risk at a given building. 90

Figure 16 Barplot of the share of (a) altered buildings with newly gained or enlarged existing views (direct effects) of specific landcover elements. (b) Share of exposed buildings with partial or full obstruction by view metric. (c) Spatial distribution of Lake-View direct effects, relative direct effect ranks, local exposure, and relative exposure ranks. (d) Boxplot of the Price effect across all design scenario; including direct (DE), cumulative local (CLE), exposure (ELE), and net effect. (e) Spatial distribution of Price Effects (DE and ELE); illustrating spatial variability of the number of impacted building to a specific hazard and the count of hazards a building is exposed to (Visual Risk). (f) Correlation plot of price effect metric and Urban and Environmental form attributes, with correlation values shown for significant values $p < .05$ 92

Figure 17: Change in top weighted view-metrics for 2 separate properties, EGID 796374 from a region of high price gain and EGID 280091437 representing a region from high price risk. Points in grey represent the values for the reference scenario, or as-built condition; Blue points represent visual share value after alteration at the property; and the set of Red points represent the values after the modification it’s set of neighbors. Change in visual share (%) of view-metric is expressed for DE with green dashed line, and ELE with red dashed line. The relative change in listed in brackets. For example, the maximum visual share of water (maxVSH:Water) for EGID 280091437 in the reference scenario is ~2.3%; whereas it drops to .3% when EGID 280026324 builds up an addition floor, and rises to 8% when EGID 280091437 itself build up an additional floor. 95

Figure 18: Predictive importance rank of view-metrics in driving (a) price gain and (d) price risk as a proportion of buildings. (b+e) Maps illustrate

the spatial distribution of the first ranked view-metric, and the spatial distribution of (c +f) of the view-metric with largest impact on price: (c) maximum visual share of water and (f) and maximum visual share of sky	96
Figure 19: illustrates the outcomes of a Generative Design simulation, where grey circles represent generated building designs and the black line delineates the Pareto Front of optimal designs. The left figure displays the traditional two objective functions found in Architectural Design Optimization literature: minimizing Material Cost (which encompasses efficiency, sustainability, etc.) and maximizing Engineering Performance (encompassing structural, thermal, etc. aspects). The right figure introduces the expanded dimensions made possible by integrating a property valuation model: maximizing property valuation (predicted price) and minimizing social cost (including local devaluation risk, NIMBY acceptability, etc.)	105
Figure 20: Effect of Building Level Urban Environmental Indicators on Renovation Propensity.	107
Figure 21 Schematic of the Viewpoint Visual Share geodatabase	111
Figure 22 Plotting the geographic footprint of lake-view buildings, colored by the size of their respective largest view, reveals the differences in supply of lake-view buildings, between Lake Geneva and Lake Zürich.	112
Figure 23 The x-axis shows the highest value (share as %) per building of the respecting view element. The y-axis shows the predicted valuation (in thousands of CHF) of a single-family home with a given visual share, while controlling for other predictors used in our hedonic model. Left: Marginal effect of a view of building elements in distance (1km). Right: Effect of lake-view on transaction prices.	113

1 Introduction

The overarching goal of this thesis is to add to the growing body of literature on environmental risk modeling (see section 1.1 and 1.2) by developing a spatial modeling approach to estimate local area risk in real estate. For reasons identified in Section 1.3, I narrow the context of the approach to a specific scope: the visual impact of land use change as a hazard to property values. Section 1.4 summarizes the four foundation parts to environmental risk modeling in real estate, and presents the unique and outstanding challenges for the chosen hazard. The remainder of the thesis aims to contribute to the existing economic, environmental, and design literature by addressing the following challenges:

1. Generating building simulations to capture both spatial and aspatial characteristics of a view
2. Developing a single measure of visual landscape quality
3. Creating a pricing model fitted on building-level visual landscape quality metrics, which allows constructing an integrated impact analysis.
4. Simulating and evaluating the direct and indirect effects of potential land-use change scenarios on real estate valuations.

Applying these challenges to local area risk estimation brings us one step closer to addressing a broader question and a longstanding challenge in the field of architectural design optimization:

5. Preference-driven generative design

1.1 Real Estate and Environmental Risk

Among the factors that drive devaluation in real estate, changes to the environment are an increasing concern. Consequently, understanding environment-related risks are seen as a priority for property owners (ULI & Heitmann, 2019). This concern stems from the actual and perceived potential impact of a changing environment on property valuations. Between 1930 and 2010 in the United States, the profound effects of natural disasters on local communities

included two notable consequences: Firstly, there was an estimated 1.5 percentage point net increase in the number of people moving away from areas hit by severe weather events. Secondly, these areas experienced a decrease in property values following such disasters. These in turn led to reduced tax revenues and expenditures (Boustan et al., 2020). In a forward looking study, Zillow projects that a 6 foot rise in sea-level by 2100 could affect 2% of U.S. homes with an aggregate potential impact of \$916 billion; Miami (\$217.3B), New York City (\$123.2B), and Tampa(\$40.6B) being the hardest hit (Bretz, 2017). Extreme events such as Hurricane Harvey and Sandy have already led to elevated delinquency rates for commercial (Holtermans et al., 2023) and for residential mortgages (Kousky et al., 2020). Similarly, mortgage delinquency and foreclosures rose following California fires from 2000 to 2018 (Issler et al., 2020). Importantly, following a peril or catastrophic event, lenders restrict the supply of credit to susceptible properties (Garmaise & Moskowitz, 2009), whereby doing so directly negatively affects property valuations.

1.1.1 Transition Risks

Environmental risk in real estate isn't limited to physical hazards. Often, risk is depicted as either *physical* or *transitional* (European Central Bank, 2020). The distinction lies in whether there is a direct impact on properties within a given location. Transitional risks describe the cost of transitioning to a lower-carbon economy (US EPA, 2022), it includes changes to regulation and energy cost, as well as changes to market preference, i.e. market risk. Keys et al. show that homes sales volume fell by 16-20% for flood-prone areas prior to a fall in home prices, suggesting a shift in attitude towards buying in vulnerable environments (Keys & Mulder, 2020). Yet, attitudes towards long-run climate risk remains heterogenous. Flood-prone homes sell at a discount in 'climate-believer' neighborhoods compared to 'non-believer' (Baldauf et al., 2020). In the largest study of its kind, Fairweather et al use the Redfin home-search platform to conduct a nationwide field experiment, testing home buyer search decision in the face of home-specific flood-risk information (Fairweather et al., 2023). This study randomly placed users into either a group that sees the flood-risk score (*treatment*) or does not (*control*),

finding a negative price effect for properties not already classified as risky by FEMA or properties not located on the waterfront. This suggests users implicitly consider risks where information is readily available. Thus, information on risks plays a critical role when delivered as ‘new news’, or in situations where estimating risk is complicated and not readily available. Moreover the complexity of measuring the variety of environmental risks, such as the visual quality, at the property level further inhibits a buyer’s ability to price discriminate.

1.1.2 Mitigating Risk with Insurance and Risk Transfer Mechanisms

Despite an increased awareness and concrete evidence of environmental risk on real estate, there is a continued investment of resources into regions deemed to be vulnerable. Redfin finds that in 2022 more people are moving into than out of disaster-prone (flooding, wild-fire, and heat) areas, and suggests “*the consequences of climate change haven’t fully sunk into American because oftentimes, homeowners and renters don’t foot the whole bill when disaster strikes. Insurers and government programs frequently subsidize the cost of rebuilding after storm hits, and mortgages mean homeowners are ceding some risk to lenders*” (Katz & Bokhari, 2023). This financial risk transfer mechanism represents an important factor in driving continued investments in risk-prone areas. Pooling by insurers and lenders allow individual investors to financially diversify away from risk-prone areas by simply paying a premium to banks (Kahn, 2024). The market price of the charged premium should reflect the risk of vulnerable areas. Yet, while lenders have the capacity to more readily assess the risk related to sea level rise (SLR) and other environment-related risks, financial securitization of insurance costs, federally-backed loans as well as an ‘underwrite to securitize’ lending attitude all subsidize this cost, driving the continued funding of climate-vulnerable areas (Hurst et al., 2019; Taylor, 2020). Indeed, Katz & Bokhari note that many insurers have either failed or backed out of the high-risk state of Louisiana, subsequently causing homeowner insurance premiums to substantially increase forcing the state to further subsidize its state-mandated insurance program. As Fairweather notes “*...with natural disasters intensifying and insurers pulling out of disaster-prone areas including Florida and California, American may start feeling a greater sense*

of urgency to mitigate climate dangers – especially if their home’s value is at risk of declining.” (Katz & Bokhari, 2023). Insurance-Linked-Securities, ILS, diversify the financial exposure to high-impact and low-probability events allowing insurers to continue to provide short-term coverage policies to developers, lenders, and investors, ultimately allowing them to proceed with ‘business as usual’ (Taylor, 2020). Moreover, it has been shown that government sponsored enterprise (GSEs) (Fannie Mae, Freddie Mac, and the FHA), when pricing these securities, do not factor in the regional variation of climate risk which suggests significant mispricing, and only recently announced plans to update its underwriting practices (Olick, 2023). ILS instruments, such as Catastrophe bonds (CAT-bonds), are important instruments cities can take advantage of to enhance their financial resilience to various environmental risks; however, considering that these securities are globalizing mispriced local-risks, it does little to address the underlying issue.

Insurances are designed to manage random impacts of predictable severity; however, with statistical non-stationarity, evident by an increasing frequency and severity (Herweijer et al., 2009), these instruments are relied upon to fund increasingly vulnerable assets. Thus as a form of climate adaptation, banks are increasingly securitizing and off-loading at-risk mortgages to GSEs as evidence of adverse selection grows (Ouazad & Kahn, 2022, 2023), and increased leverage in disaster-prone area (L. Bakkensen et al., 2023)

1.1.3 Adaptation to Uninsured Risks

Where complete information exists, environmental risks will be priced into real estate valuations. Those willing to take on the risk, may bid on homes with an intention to upgrade or adapt them to a climate-ready state (Shogren & Stamland, 2002), whereas the risk averse and those without technical or economic capacity will relocate. In addition to partisan beliefs, the latter may describe the factors driving residential climate sorting (Bernstein et al., 2022). Yet, as discussed in section 1.1.1, home buyers do not have complete information regarding emerging risks. In fact, a growing body of evidence points to the market risk of repricing

property due to newly revealed property level environmental information. For example, Gao et al show that new information about local pollution levels elicited an outward migration from polluted cities, and a near doubling of the marginal effect of pollutants on property prices (Gao et al., 2023). As such, detailed information is critical to capture existing and future risks to property valuation. Despite the existing financial incentives for real estate stakeholders to diversify against physical environmental risks (described in section 1.1.2), the available set of financial risk transfer mechanisms do not address the underlying and growing issue of these risks. Further, it is evident that transitional risks cannot be overlooked. Unlike physical risks, most transitional risks are not insurable and thus directly affect the valuation and potential financial performance of every stakeholder throughout the life-cycle. Importantly, information on transitional risks are difficult to evaluate and quantify for individual stakeholders.

The lack of coverage for transitional risks leaves a gap in risk management strategies for property owners. Exposure to uninsured transitional risks is not an abstract concern; for property owners, it has concrete implications at the local, or neighborhood level. Stakeholders, especially homeowners, are acutely aware of the potential for these risks to translate into financial losses (Fischel, 2001). Among these risks is the devaluation due to local land use change or development of unwanted land use (Schively, 2007). For example, Thibodeau showed that the development of a high-rise building had a negative effect on the property values of adjacent neighbors (within 2,500 meters) (Thibodeau, 1990). As visual obstruction and similar localized risks are not insurable, property owners find themselves without a safety net, nor mechanism to financially diversify, which understandably influences their subjective risk perception to proposed changes within their local neighborhoods (Sandman, 1986).

This local-level reaction is best depicted by the ‘not in my backyard’ (NIMBY) phenomena. NIMBYism is characterized by a collective opposition to local developments, including waste or industrial facilities (Lu, 2023; Schively, 2007), wind farms (van der Horst, 2007; Warren et al., 2005), social services (Davidson & Howe, 2014), and residential housing projects (Basolo & Hastings, 2003). This

response to the uninsured risks of property ownership – opposition to local land use change – is a rational option (Fischel, 2001). Home owners have a majority of their net worth tied to a single asset, as such, changes to the neighborhood pose a risk to local property values. This raises the question: if homeowners were offered insurance against devaluation risk, would there still be NIMBYs? Renters are seldom considered NIMBYs, perhaps because they are financially diversified; in the event of adverse local changes, they have the ability to relocate without suffering substantial financial losses. In theory, an insurance contract against home value loss could compensate property owners. In practice however, the lack of information to properly estimate risks and costs hinder its applications. This dilemma is known as the price-index problem and the moral hazards problem (Fischel, 2001).

Since property owners are exposed and sensitive to the indirect, or spillover, effects of new development, the NIMBY movement can be interpreted as a response to the potential unforeseen effects on the quality of neighborhoods. In this context, zoning enforcement and regulation can be seen as a neighborhood's collective response to development that poses a financial risk. Given these mechanisms, local authorities hold substantial power when it comes to shaping urban form and land-use. This collective response at the local level underscores the importance of land-use regulation and presents a challenge to urban planning and zoning reform as discussed in the following section.

1.1.4 Local Effects of Urban Adaptation

The need for zoning reform becomes clear when considering affordability and sustainability goals that cities aspire to achieve. Within the framework of sustainable development, housing development in a low carbon economy limits urban sprawl and requires densification and intensification (Intergovernmental Panel On Climate Change (Ipc), 2023b, 2023a). Cities have committed to endorse and adopt policies to promote these concepts in an effort to achieve their sustainable development goals. Several have already implemented policies to promote urban solutions, high-density development, vertical construction and

updating zoning in low-density regions (Bibri et al., 2020; Lin et al., 2021). Toronto, for instance, has directed an intensification policy primarily through residential development (Bunce, 2023).

However, changes in land-use prompted by urban planning could worsen or exacerbate the existing local conditions (Grimmond, 2007; Seto et al., 2011; Smith & Levermore, 2008). A city's urban form and morphology significantly influences its urban climate and stock of environmental amenities. Paying attention to and incorporating local urban variables within planning assessment can help to mitigate exposure to these local effects (Lenzholzer et al., 2020).

Despite the apparent conflict between NIMBY attitudes and the push for sustainable urban development- or, more broadly the resistance to local development vs. approval of densification and intensification – a common limiting factor is revealed: uncertainty on the local effects induced by local changes. As discussed in Section 1.1.1, the absence of such forward looking environmental information hampers the ability to discriminate between the cost/benefits of a proposed development, the uncertainty of the continuity of local area quality, or of an amenity's persistence, represents the underlying stressor or hazard that presupposes financial risk to property owners.

1.1.5 Local Amenities and Risk

Local amenities and the risk or changes to the quality of those amenities play a central role in the property market. Homeowner flows into and out of neighborhoods depend on the relative attractiveness of the neighborhood (Ouazad & Ranci re, 2019). Ouazad & Ranci re use an *index of trading opportunities*, defined as the difference between a home's amenity and market value, to depict the arbitrage opportunity whereby homeowners leave neighborhoods low in amenity value and high in property value. Their model describes the dynamic relationship between housing price and preferences where the variation in the trading opportunity reflect evolving preferences as well as market frictions. As discussed in sections 1.1.1-1.1.4, we can consider that among the set of possible market frictions is the asymmetry of information pertaining to the quality or

persistence of the environmental amenities. Thus, those with access to information on local urban effects could take advantage of mispricing within and across neighborhoods. Yet, quantifying such idiosyncratic risks, e.g. opportunity or vulnerability pertaining to individual properties due to impending zoning changes, has remained particularly challenging.

First, comprehensive data on environmental amenities or location-based characteristics are often limited. The limitation is less so in geographical coverage, as advances in remote sensing has enabled global scale availability of a vast array of environmental information, rather than in spatial resolution. Specifically, differences in environmental quality between neighboring buildings can only be captured via data acquired at a sufficiently high spatial resolution or approximated via physical performance modeling, which itself will be limited by resolution.

A second limitation pertains to the complexity of the property or real estate market. Defining devaluation risk in terms of change to urban attributes, requires not only data on the variables of interest but also a comprehensive set of covariates that influence the market value of the asset. These covariates include structural attributes (e.g. condition, morphology, etc), location attributes (e.g. proximity to points of interest), economic attributes (e.g. interest rates), among others.

Finally, a critical, but often understated challenge, is the identification of key relevant hazard variables. Properly selecting these factors is essential for simplifying the complexities inherent to physical performance modeling and for reducing the uncertainty of the estimated effect size within an economic sensitivity model.

Advances in computational methods and compute power present an opportunity to quantify the exposure and sensitivity to a broader spectrum of idiosyncratic risks. With the growing adoption of 3D Geographic Information Science (3D GIS) and GeoAI, these methods can now be applied to increasingly larger geographic areas, while still maintaining property-level resolution. The latter ensures that analyses remain detailed and relevant at the scale most pertinent to individual

stakeholders, thus providing an opportunity to mitigate widespread community resistance, e.g. NIMBYism .

1.2 Evaluating Environmental Risks

Spatial analytics, driven by a growing awareness of environmental risks, have increasingly influenced financial decisions (Fiedler et al., 2021). In the context of real estate, spatial modeling enables the assessment of future risks, informing property-level exposure to potential changes in urban and natural environments. Investors and homeowners pay particular attention to such exposures because of the potential for devaluation risk, or the potential decrease in the value of a property due to a given hazard or externality. As discussed in *Section 1*, by quantifying such spatial risks and attributes, homebuyers and investors can overcome information asymmetry and make informed financial decisions related to their real estate portfolio – whether to buy, sell, or develop.

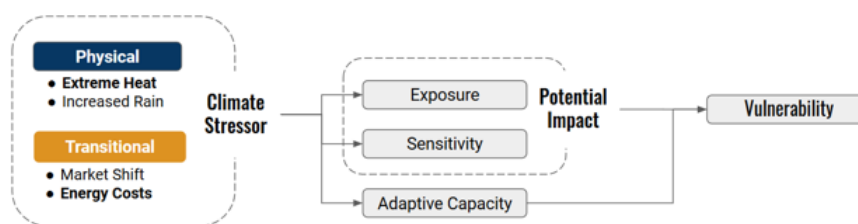


Figure 1 Abstract Definition of Environmental Risks, adapted from IPCC, EEA report

Table 1: To explore the concept of devaluation risk, this thesis adopts the following terms that define the determinates of risk (IPCC, 2023).

Term	Description
Hazard	the stressor or potential source of adverse (or beneficial) effects.
Exposure	the extent to which a property faces a particular <u>hazard</u> .
Sensitivity	the degree to which a property is affected, adversely or beneficially, by a particular <u>hazard</u> .
Potential Impact	the possible gross effect of a <u>hazard</u> that interacts with a

	property at a given <u>exposure</u> and <u>sensitivity</u> .
Adaptive Capacity	the ability of available tools to mitigate or reduce the <u>potential impact</u> of a given <u>hazard</u> .
Vulnerability	the potential for adverse (or beneficial) impacts resulting from a <u>hazard</u> considering the available <u>adaptive capacity</u> .

Using the IPCC's definitions of risk (shown in Table 1 and Figure 1), it can be reasoned that *exposure* and *sensitivity* are the fundamental elements by which to assess a particular hazard. *Exposure* can be thought of as the property-level propensity to face a particular hazard at a future time; whereas, *sensitivity* depicts the property-level consequences in the event the hazard does unfold. Prior research has largely concentrated on property depreciation resulting from large-scale natural disaster shocks, namely climate change. Another important determinant of risk is the system's *adaptive capacity*. Here, we can consider the adaptive capacity to be a property's ability to mitigate the effects, such as the financial risk transfer mechanisms described in Section 1.1.2 and 1.1.3. Quantifying the exposure and sensitivity to a hazard is often assessed through the analysis of historical financial and environmental data. Specifically, the lasting adverse effects on housing prices are demonstrated through the occurrence of natural disasters like floods (L. A. Bakkensen & Barrage, 2022; Holtermans et al., 2022; Keys & Mulder, 2020; Ortega & Taşpınar, 2018; Ouazad & Kahn, 2019) and wildfires (Issler et al., 2020). Critical to understanding the future impact of climate change on real estate is the development of detailed hazard exposure maps. For instance, detailed flood risk maps spanning from 2020 to 2050 (Bates et al., 2021) enabled subsequent studies to assess whether residential properties are overpriced relative to their exposure to flooding (Gourevitch et al., 2023). Yet, as discussed in Section 1.1.5, there remains a gap in the literature presenting methods that assess the local risks of real estate.

The challenge in assessing local real estate risks is due to its idiosyncratic nature. Local hazards, such as land-use change, can have an effect that varies from neighbor-to-neighbor, and in some cases apartment-to-apartment. Thus, it

necessitates an approach that captures effect sizes via metrics at a high-spatial resolution. To clarify, this requires an integrated or end-to-end model, producing spatially varying estimates of potential impact. To understand this process in detail, we can draw insight from the data and methods past researchers have utilized to model macro-scale natural disaster risks in real estate.

1.2.1 Modeling Physical Climate Risk

Ground and earth observation instruments acquire direct physical and biogeochemical measurements of the natural world; recorded over time, temporal change and spatial variability of this data is used as evidence for changes in the climate system (Masson-Delmotte et al., 2021). Building on available earth observation techniques and data, statistical and physical climate models are developed for spatial interpolation and forecasting of environmental phenomena (Wikle et al., 2023). First Street Foundation is an example of a group that publishes results from its climate model for a range of hazards, including flooding, wildfires, heat, and wind (First Street Foundation, 2023). Each hazard is modeled using domain specific physical models, e.g., hydraulic and hydrology models for flooding, cyclone models for wind, extreme heat models for heat, and wildfire models for wildfire propagation. The models are physics-based simulations that ingest input parameters and probabilities related to such events, representing the dynamic interactions between climate systems. Dependent on spatially varying input parameters, the model output is a prediction of hazard occurrence, commonly referred to as an exposure map. Using these structured models, researchers can simulate varying conditions or scenarios, such as the flow of carbon dioxide in the atmosphere. On the basis of exposure maps, economic impact assessment studies are possible. First Street incorporates a component-based fragility model in their Wildfire risk model, which defines the *sensitivity* of individual building characteristics. Together, the exposure maps and definitions of building components sensitivity depict the estimate of the extent and severity of potential damages, i.e. *potential impact*. To produce estimates of financial damages, First Street converts the potential physical damages from wildfires via a replacement cost curve.

Iliyasu et al use sea level rise (SLR) projection maps from *earth.org* to estimate the price effect of flooding exposure on housing prices in Lagos, Nigeria (Iliyasu et al., 2023). Similarly, FEMA projection maps have been used to reveal an overvaluation of properties in floodplains, highlighting the heightened vulnerability of communities dependent on property taxes (Gourevitch et al., 2023; Hino & Burke, 2021). Comprehensive flooding maps developed by (Bates et al., 2021) combined with available parcel data and a water depth damage curve enabled a property level economic impact assessment (Armal et al., 2020). Anderegg et al use a wildfire model developed by (Anderegg et al., 2022) along with land values and future climate projections to forecast the property value at risk due to wildfires across the continental US, identifying new vulnerable regions in the Southeast and Great Lakes (Anderegg et al., 2023)

Summarizing the studies that model the physical risks of climate change on real estate, we see that the approach is divided into distinct steps that sequentially build on top of one another. First is acquiring geospatial data that depicts parcel level attributes, and importantly the natural environment. Second is a physics-based model that describes the performance or interaction between the natural environment and hazard of interest as a function of input parameters. Often a statistical downscaling (Kumar et al., 2023) is applied to enhance the spatial resolution, alternatively, a dimensionality reduction is employed to reduce output complexity. A simulation step follows, where the performance model is iteratively computed based on updated input parameters which depict potential *future* scenarios. As a result of the performance simulation, and statistical post processing, we obtain an exposure map. The exposure map indicates the extent to which a property is affected by the hazard of interest. Third, a sensitivity function is developed capable of translating the exposure into economic terms. This is typically done using a statistical model that applies a fitted damage (or replacement cost) estimate as a function of the exposure. Lastly, by combining the sensitivity and exposure measures, we obtain a property-level economic impact assessment with respect to a given hazard.

1.3 Modeling Local Area Risk

1.3.1 Land Use Change as a Hazard to Property Valuations

With a procedural framework for how to structure our risk modeling approach (Section 1.2.1), let's turn the attention to selecting the hazard or stressor. Given the sequential steps involved in environmental risk modeling, it becomes evident that identifying the hazard of interest is of important consequence and dictates the necessary spatial data and modeling choices. An overly broad hazard increases the complexity of information required to capture it.

So far, Sections 1.1.3 had indicated that of the risks to property owners, a particular uninsurable concern is the devaluation due to nearby changes, also referred to as Land Use Change. Section 1.1.4 demonstrates that Land Use Change, defined as the functional use of an altered parcel, could worsen the urban condition, despite its importance for densification strategies that mitigate housing affordability and improve sustainable development. Section 1.1.5 reveals that Land Use Change ultimately disturbs the specific urban attributes and amenities, that are of value to individual stakeholders and that are capitalized into property valuations. Therefore, land use change has implications for nearby property valuation through disturbances to valuable amenities.

Indeed, developers or urban planners are interested in evaluating trade-offs between alternative design decisions in order to optimize the building design with respect to a set of criteria. Among the 'amenity' factors typically considered is a class of metrics describing the micro-climate also known as *Urban Environmental Quality* (UEQ). UEQ comprises metrics describing the local environmental condition that directly affect the quality of life in an urban setting. UEQ factors include air quality (C. Lee, 2019), noise pollution (Morillas et al., 2018), daylighting (Chinazzo et al., 2019), thermal comfort (Vellei et al., 2021), and visual quality (Ko et al., 2022); and play an increasingly important role in urban planning and real estate development, particularly so in the transition towards sustainable development— see *Section 1.1.4*, as well as defining the acceptability of a proposed design – see *Section 1.1.5 and 1.1.3*. Thus, changes in UEQ metrics can be used to

depict the effect, either gained benefits or damages, as a result of land-use change. Leveraging spatial modeling methods to simulate proposed land-use changes or proposed development projects, and to generate local exposure maps of, as well as estimate sensitivity to, change in UEQ could help to assess the localized impact to changes to the persistence of UEQ on property values.

1.3.2 Addressing the Challenges with 3D GIS and the View Metrics

Section 1.1.5 described the challenges to modeling local risks to devaluation, most of which centered around the availability of data at a high spatial resolution and the choice of variable of interest. To address these, this thesis exploits the inherent advantage of 3D GIS over other data types common to urban analytics.

Urban Analytics employs computational and statistical methods to study the built environment, covering a range from the heat island effect and vegetation to urban sprawl and aspects as abstract as visual quality. Table 2 illustrates the characteristics and advantages of various data types commonly used in research based on Urban Analytics. At the heart of these methods is the input data. The majority of studies in this field utilize high-resolution imagery, with satellite and street view images being the most common. However, a closer examination reveals a significant opportunity for 3D GIS and Computer-Aided Design (CAD) data. The biggest differentiator is, of course, 'mutability.'

Table 2 Data Types common to Urban Analytics

	Coverage	Degrees of Freedom	Fidelity	Mutability
Satellite Remote Sensing	✓		✓	
Drone Sensing		✓	✓	
Street-View Imagery	✓		✓	
Photogrammetry/Laser		✓	✓	
3D CAD	✓ *	✓		✓

Unlike images, CAD data can be systematically altered, allowing for the creation of new design scenarios and their programmatic comparison. This mutability characteristic is the primary driver behind the computational design or generative design field (Caetano et al., 2020; F. Jiang et al., 2023). 3D GIS is often limited in coverage, with low levels of design detail or availability in certain regions only. In Switzerland, however, thanks to significant investment in GIS and geospatial infrastructure, country-wide 3D CAD models of Switzerland's entire territory are available. The downside of using CAD data is its fidelity, or how realistically the data reflects actual urban settings. However, considering that many machine learning algorithms processing satellite imagery, namely Convolutional Neural Networks (CNN), compress images and segment the image into an embedding, this information loss may represent an acceptable tradeoff given its advantage of mutability. In essence, is the information loss due to compression greater than the information variance across simulated design permutations? This thesis explores this hypothesis and introduces an approach to model the risks of property devaluation due to local changes in the built environment by leveraging the mutability of 3D CAD data.

The second challenge, outlined in Section 1.1.5, highlights the importance of selecting a variable that can simplify the complexity of the design study. As discussed in Section 1.3.1, changes in Urban Environmental Quality (UEQ) metrics can illustrate the effects, whether they are benefits gained or damages incurred, as a result of land-use change. Among the common UEQ metrics of interest to many generative designs or building performance simulations, visual quality, or the view from windows, is widely regarded as having the highest price-amenity gradient, i.e., the greatest willingness to pay, and thus the greatest potential to result in devaluation in case of amenity loss. While other UEQ metrics, such as daylight and noise pollution, do contribute to explaining variability in prices, high-quality views are commonly seen as determinants of housing prices and are often considered a luxury good. Thus, visual landscape quality and a property's risk of visual obstruction represent ideal variables of interest in assessing devaluation due to changes in the local urban context.

1.4 Motivation

Despite the noted shortcoming in research on building-specific assessments of local area risk, there is a growing body of research on evaluating the economic value of urban systems and ecosystem services to draw from. Furthermore, the availability of city CAD models and GIS has enabled researchers to blend topics such as design, finance, and ecology, experimenting with new approaches to financially evaluate the physical capabilities of a broad range of aspects of the natural and built environment. This thesis is motivated by the goal to investigate ways to enhance our capacity for understanding uncertainties in real estate valuation using spatial data, with a particular focus on local vulnerabilities to the persistence of urban amenities, such as the view. While much work remains, this thesis represents a step forward in integrating the value of design, environment, and similar non-market goods into the site selection toolkit. Importantly, as more cities digitize their building stock, the approach described here can serve as a blueprint for future assessments of environmental preferences within the design-decision-making process of the built environment

Past research employing 3D city models and digital twins has faced criticism for its failure to incorporate human and economic complexities. Advocates, such as (Fotheringham, 2023), have called for a shift towards research that is more functionally useful and attentive to these aspects. In other words, many studies fall short of applying learned environmental parameter estimates to guide design decisions in the built environment. This thesis, along with the studies that comprise it, introduces a methodology that bridges economics and spatial modeling techniques, aiming to address these concerns.

The remainder of this thesis will detail the completed work on modeling local area risk, which can be summarized into four distinct parts, initially identified in Section 1.2.1: (1) Simulation, (2) Evaluating Performance, (3) Price of Performance, and (4) Impact Assessment. To address the challenges outlined in Section 1.3.2, this thesis emphasizes localized risk estimation by focusing on building-level visual impact because views (1) are widely acknowledged to play an

important role in property valuations and (2) have remained challenging to quantify. In the following section, I will provide an overview of each of these four parts of local area risk estimation and itemize the unique challenges within visual impact assessment that this thesis aims to address.

1.4.1 Background on Design Simulations

Design simulation is commonly described as a mathematical modeling approach used to quantify the dynamic properties of a given design. Computational Fluid Dynamics (CFD) is among the most computationally intensive applications of simulation. For example, when applied to wind simulations, CFD helps mechanical engineers test the air drag performance of a design.

Design simulation applied to building computer-aided design, or CAD models, is referred to as building performance simulations or the computer-based evaluation of architectural building models. There is substantial literature covering various applications and approaches to quantifying the dynamic behavior and properties of building designs. Building performance simulation is particularly useful when integrated with parametric computing in the building concept phase (Wortmann et al., 2022). In this phase, building simulation helps to optimize architectural plans with respect to their set of objective functions. For example, a recent and growing application of simulation-based optimization is to promote the integration of digital fabrication as a co-designer in the architectural design process (Skoury et al., 2024). In the urban context, CAD-based simulations help to quantify the condition of the surrounding city and urban context and are most commonly used for 'energy-driven' generative design (Natanian & Wortmann, 2021; Shi et al., 2017; Sonta et al., 2021).

Building performance simulation itself comprises a set of mathematical functions that describe the urban condition; also referred to as Micro-Climate, Urban Environmental Quality. Common attributes of UEQ that environmental simulations methods attempt to capture include air quality, daylighting, noise pollution, thermal comfort, and visual quality. Among the readily available tools (Ameen et al., 2015), the most popular is Energy Plus (NREL, 2017) which has

served as the back bone for energy simulation literature and utilized for such energy-driven design optimizations. A recent tool to generate noise maps is sonAIR, which models the effects of aircraft noise (Wunderli et al., 2018). Similarly, sonROAD models traffic noise (FOEN, 2023), and sonRAIL models transit and train noise (Wunderli, 2012). Each of these tools introduce a physical model of propagation and summarize the urban performance on urban maps.

Despite advances in several UEQ domains, methods to quantify visual landscape quality vary widely, and those that develop view metrics largely utilize satellite imagery. However, as the remainder of the thesis will discuss, this approach does not translate well to 3D applications. As noted in section 1.1.5, without local scale simulations, the development of measures of the view from the perspective of a building, or building-level view metrics, has lagged behind.

1.4.2 Background on Building Performance Evaluation

Building simulations, as introduced in Section 1.4.1, help to capture the spatial properties pertaining to a 3D geometry, or more specifically, a building's CAD design. Evaluating the spatial statistics characterizes the select building or the conditions to which the building is exposed.

Urban Environmental Quality (UEQ) indicators are characteristics of the built environment that are broadly considered as indicators of a region's capacity to sustain its resident population. The limits of such capacity are most evident in regions experiencing rapid urbanization or increasing rates of resource consumption, where a range of environmental and urban challenges arise. These challenges include, for instance, the contamination of air and water, or elevated levels of traffic noise, and heat stress.

In section 6.1, I illustrate the usefulness of building level urban environmental performance or micro-climate metrics by developing small case-studies showing the relationship to Urban Health and Energy Consumption. The methods in these case studies are not novel in and of themselves, however, it is applied in a novel

context. A large portion of the urban informatics literature utilizes similar methods and environmental performance metrics and study covariates of interest.

Evidence shows prolonged exposure to poor environmental quality, whether daylighting, noise pollution, thermal comfort, air quality, or visual quality, can have a profound impact on the public's health as well as the overall perception of quality of life.

Daylighting literature underscores the point that building occupants' preference for natural daylighting is linked to both physiological and psychological reasons (Cho et al., 2023a; Karmann et al., 2023; Ko et al., 2022; Münch et al., 2020; Turan et al., 2020a). In the specific context of indoor office work, the number of hours and availability daylight has been linked to higher productivity (Ander, 2003) as well as lower levels of sick leave (Elzeyadi, 2011). The number of daylight hours, whether indoors or at street level, directly depends on the urban form, more specifically, a point's orientation towards and direct obstructions to the sun. Further, daylight hours can be viewed as the cumulative exposure to direct sunlight, thus it is common to treat the aggregated solar irradiation as a proxy for daylighting (see Section 6.1).

Noise pollution, similar to air quality though rarely studied in parallel, largely results from traffic noise. Excessive exposure to traffic infrastructure, such as highways and airports, poses adverse health effects (Khan et al., 2018; Roswall et al., 2015). Additionally, the hedonic pricing literature indicates that homes exposed to high levels of road noise typically sell as a discount, revealing the preference for low to no level of direct noise pollution (Baranzini et al., 2006; Y. Wang et al., 2023).

Air Quality is described as one of the largest environmental risks, with countless studies reflecting the health consequences of exposure to air pollution (EEA, 2015). Historical air pollution from coal use has even been linked to persistent neighborhood-level segregation decades later (Heblich et al., 2021). Although various industrial air pollutants exist and vary by region, the World Health Organization's air quality framework (World Health Organization, 2021) provides

guidelines for a set of five pollutants: PM_{2.5}, PM₁₀, ozone, nitrogen dioxide, sulfur dioxide, and carbon monoxide, which are now the focus of most air quality monitoring efforts. Beyond direct health effects, economists have investigated "non-health" links, including labor productivity, cognitive performance, and decision-making (Turner, 2016).

Visual Quality, though difficult to quantify, and visual aesthetics are widely recognized as playing a significant role in how individuals perceive landscapes and their environments (Wartmann et al., 2021). Often it is studied alongside daylighting (Cho et al., 2023a; Elzeyadi, 2011; Jain et al., 2023; Ko et al., 2022; Sruthi Krishnan & Mohammed Firoz, 2020; Vardoulakis et al., 2016). Real estate literature has long highlighted the revealed preference for high-quality window views (Benson et al., 1998; Turan et al., 2021; Ye & Becker, 2018). Evidence from indoor office research suggests that a visual window view improves workers' mental state, including sleep quality, stress reduction, and creativity (Aries et al., 2010; Farley & Veitch, 2001; Tennessen & Cimprich, 1995). The most common method to represent a view is with a binary indication of a visible point of interest from an observation point. However, more comprehensive works in landscape quality assessment reveal that high-quality and preferred landscape views are characterized by, but not limited to, visual complexity and open panoramic scenes. More recently, Cho et al point out that motion is fundamental attribute of visual quality often overlooked, and calls for methods to capture the dynamic properties of a view (Cho et al., 2023b). Similarly, neuroscience research emphasizes the unconscious influence of fractal patterns and biophilic factors on visual perception, describing an optimal band of fractal dimensions that significantly reduces stress and triggers the release of powerful endorphins (Briemann et al., 2022).

This literature illustrates a substantial connection between environmental quality, public health, and economic preferences. Furthermore, we understand that this relationship extends to the scale of buildings or neighborhoods and is identifiable through location decisions in the form of urban amenities – as discussed in Section 1.1.5. Yet, of the range of UEQ factors, Visual Quality stands out. Section 1.4.1 illustrated the challenges and proposed a method for capturing

the spatial characteristics of the view from the building. Additionally, a lack of methods for evaluating visibility simulation hinders the development of a standardized metric for visual landscape quality.

1.4.3 Background on Environmental Valuation

Unlike tangible economic goods that can be directly traded, environmental goods lack a straightforward method for valuation. However, it is widely accepted in real estate analysis that properties featuring certain environmental and urban amenities tend to command higher market prices. By utilizing hedonic regression analysis, a technique well-documented in real estate literature (Sirmans et al., 2005), researchers can quantify the marginal impact of various characteristics or amenities on housing prices. This approach reveals the premium that buyers are willing to pay for specific features, effectively capitalizing on 'non-market' environmental goods, such as micro-climate factors and visual landscape amenities, into property values.

Visual amenities, in particular, have garnered significant attention within hedonic valuation studies, despite the challenge of their qualitative nature and lack of standardized measurement units. This variability complicates comparisons across different studies, which often focus on localized regions. A comprehensive review of hedonic valuations highlights the diversity of research in this field (Bourassa et al., 2004). For instance, studies have found that visual accessibility can lead to a price premium of 3.2% in Worcester, Massachusetts (Mittal & Byahut, 2019), while views of residential gardens in Shenzhen Bay Area command a 17.2% premium (W. Y. Chen & Jim, 2010). Water views exhibit particularly variable premiums, with studies showing an 89% increase for lake views (Benson et al., 1998), a 3.8% premium for ocean views in Oslo (Osland et al., 2022), and a 59% premium in Auckland, Australia (Bourassa et al., 2004). These findings underscore that although the direction of price gradients for visual amenities is consistently positive, the magnitude of these premiums varies significantly (Boyle & Kiel, 2001).

Incorporating variables from large-scale building performance simulations into hedonic regression models enables the estimation of the financial value of specific environmental amenities, going beyond the traditional locational, structural, and economic factors. As introduced in Section 1.1.5 and further detailed in Supplement Section 6.2, this methodology has been applied to estimate the marginal price effect of two significant view metrics: the maximum visual share of water bodies and views of distant elements, as well as a composite metric of visual landscape quality. This approach broadens the understanding of how views contribute to well-being and property value, offering a nuanced perspective on environmental valuation in urban real estate markets.

1.4.4 Background on Design Impact Assessment

Design impact refers to the direct and indirect effects exerted by a particular building or urban form. For instance, Rong et al. demonstrate that the form of a building can positively influence the property's direct value – for example, diagonality (+12.4 percentage points) and podiums (+9.7 percentage points). Furthermore, as outlined in Section 1.1.4, the design of urban spaces significantly affects local climate conditions and environmental amenities. Awareness and consideration of local urban climate variables can assist in mitigating adverse effects (Lenzholzer et al., 2020). Yet, despite the available methods to determine real estate valuation (see Section 1.4.3), the disconnect between real estate valuation and building design results in suboptimal design and economic outcomes (Rong et al., 2020). This thesis posits that leveraging spatial analytics to measure local exposure effects, particularly in financially sensitive neighborhoods, can unveil the potential impact of design.

In architectural design optimization, economic performance indicators quantify the financial implications of architectural or design decisions. A number of startups in the Architectural Engineering and Construction space, also known as aec-tech, are leading this effort (Allegrini et al., 2015; Ameen et al., 2015). For instance, Cove-tools (Cove.Tools, 2024) is a spatial analytics platform designed for single building designs, generating building and urban quality indices based on a

3D building design. Additionally, platforms such as Autodesk Forma, Google Delve (Delve, 2024), and Giraffee (Giraffee, 2024) are integrating spatial analytics with generative design. They employ parametric engines to simulate and evaluate multiple design iterations based on environmental criteria like sunlight exposure, energy efficiency, and material use. These tools not only demonstrate the applicability of such technologies for developers and urban planners but also highlight the largely unexplored area of assessing design's indirect effects on surrounding neighborhoods. By combining spatial analysis and parametric design, there is an opportunity to examine both the direct and indirect impacts of architectural decisions, thus offering a comprehensive view of a design's potential benefits and its influence on nearby developments.

These platforms and wider literature, however, utilize cost-based economic performance metrics and do not consider the financial risk. Nagy et al.'s approach, which involves using predefined values for selling prices and project costs to generate profit-optimized designs that consider environmental quality and sunlight, illustrates one method. While this approach effectively addresses key considerations by adopting a fixed sale price, it overlooks the unique spatial attributes of a building design, along with both its direct and spillover effects onto sales price (see Section 3.2.1).

Section 3 of this thesis aims to bridge these identified gaps by proposing methodologies that account for both the direct and indirect local urban effects of design changes and by exploring how economic valuation metrics can be applied to assess design-related financial risks. Furthermore, Section 5 will delve into the potential future applications of these methodologies in architectural design optimization and generative design, highlighting their significance in advancing the field.

2 Visual Capital: Evaluating Building Level Visual Quality at Scale

Adam R. Swietek ^{a,*}, Marius Zumwald ^b

^a Laboratory of Environmental and Urban Economics (LEURE), École Polytechnique Fédérale de Lausanne (EPFL), Lausanne, Switzerland

^b Wüest Partner, Zürich, Switzerland

* Corresponding author: adam.swietek@epfl.ch

Original Publication in Landscape and Urban Planning

Swietek, Adam R.*, and Marius Zumwald. "Visual Capital: Evaluating building-level visual landscape quality at scale." *Landscape and Urban Planning* 240 (2023): doi:10.1016/j.landurbplan.2023.104880

Abstract

Evaluating visual landscape quality provides valuable information for urban development and spatial planning. In practice however, obtaining high resolution view-metrics and outcome data with sufficient geographic coverage has remained challenging. To overcome this limitation, we construct a scalable measure of visual landscape quality by first defining building-level view-metrics derived from a large-scale 3D representation of Switzerland's building stock. Leveraging the principle of income-sorting, we estimate visual preferences by calibrating the building level view-metrics with commune-level incomes (CLI). The learned model captures common intuition on visual preferences, i.e. attributing positive weight to lake-views, and identifies context-dependent relationships between view metrics. To contextualize the derived quantitative measure, we refer to the preference for a building's portfolio of viewpoints as a building's visual capital (VC). By assessing the supply of VC across Switzerland's entire building stock, we uncover an association between VC and the urban and natural form, where urban density and landscape topology explain the strength of view-driven-income sorting across agglomerations. We demonstrate that spatial clustering of VC varies across cities and frequently crosses administrative boundaries. Finally, we release a privacy protected version of VC at www.visualcapital.xyz, which we expect to promote future interdisciplinary studies focused on correlates of visual landscape quality (whether financial, social, environmental or physiological).

Keywords:

3D spatial metrics, Preference, Natural *capital*, *GeoAI*, *Spatial* analysis, Urban economics

2.1 Introduction

To estimate the revealed preference for housing views and visual landscape, defined as the geographic areas visible as perceived by an observer from one or more viewpoints (Inglis et al., 2022a), it is common to use the hedonic pricing model to calculate the marginal effect of a derived view indicator on real estate transaction prices (Baranzini & Schaerer, 2011; M. Chen et al., 2022; Law et al., 2019; Turan et al., 2021; Yamagata et al., 2016). However, limiting its wider use, sales transaction data and view-relevant details are not always (publicly) available, are often limited in geographic coverage, or focus on rare, yet easily extractable view attributes, such as ocean-views (Yamagata et al., 2016). This lack of large scale spatial data hampers efforts to assess the factors that influence visual quality at the building-level, with most studies focusing on a single city or region with sample sizes of typically less than 10,000 observations (Yamagata et al., 2016).

In place of transaction data, income data may be used as a proxy for high quality amenities by modeling income-sorting. Income-sorting can be described as the tendency of higher-income earners to settle in regions with better and higher quality amenities (Couture et al., 2023). Lee & Lin 2018 formally extended this theory to natural amenities, presenting evidence that geographic features shape the spatial distribution of incomes. Similarly, Bosker & Buringh, 2017 use geographic attributes to explain initial location choice for European cities, and Burchfield, Overman, Puga, & Turner, 2006 and Saiz, 2010 find geography plays a causal role in a city's continued urban growth and development. Beyond obvious factors, such as waterbodies, other amenities, such as climate and seasonal temperatures have also been found to play an important role in household income sorting (Sinha et al., 2021). Importantly, terrain hilliness contributes to income-segregation, where the view – as a 'housing luxury good' – likely plays an important, yet difficult to assess role (Ye & Becker, 2018). Despite recent progress, leveraging income sorting to reveal location preference for building-level views remains challenging for different reasons. Although income statistics are typically widely available, they are reported on aggregate as commune, zip-code, or district-

level averages. For small scale studies, this leads to an insufficient number of observations for inference. As a result, view attributes can only be assessed if they are either aggregated (based on landscape or urban features rather than building-level information) or they are extracted on a large scale.

To overcome these challenges, we present a large-scale approach aimed at establishing a building-level metric for visual landscape quality. The methodology combines income with quantitative view data on a national scale. Based on previous findings that high-quality views are economic determinants of property valuation and of an individual's judgement, attention, and decisions (Ko et al., 2022), we hypothesize that a building's visual landscape quality plays an important role in residential income-sorting. Consequently, average communal income levels should reflect visual preferences. Leveraging this relationship, we characterize the preference for a building's visual landscape by the observed relationship between building-level view metrics and regional income level. To do so, we first derive building-level view-metrics from a 3D digital model of the Swiss building stock, including topography and land use. Next, we model commune-level income as a function of a building's view-metrics using machine learning. Calibrating building-level view metrics with average incomes allows us to derive a single composite measure for each building, namely its visual capital (VC), which can be understood as the scaled predicted income of a household residing in a building with a given portfolio of viewpoints. Large geographic-coverage analysis of VC allows us to reveal spatial patterns of visual inequality, and to define new urban boundaries of similarly ranked visual landscapes. These *de novo* boundaries of high or low VC could enable future studies interested in socio-economic covariates, such as urban health, within and across income levels. Importantly, we can infer the relative strength of view-driven income-sorting for a given region and relate it to differences in natural and urban form.

2.2 Literature Review

2.2.1 Spatial Feature Extraction

The availability of satellite and street-view images has enabled a range of methods to quantify visual attributes of urban areas (Biljecki & Ito, 2021). Although informative on a neighborhood level, such image-based feature-extraction and evaluation methods do not generalize well to views from an individual building (i.e. street-view images can be a proxy for neighborhood appeal, but not for visual landscape differences across neighboring buildings).

To investigate a building's visual landscape, Digital Twins, or simulated 3D urban environments are a common alternative to satellite and street-view imagery. Although qualitatively not as detailed as an image, they capture 3D information from an elevation- and orientation-specific vantage point, thus enabling a more comprehensive and quantitative definition of a view. Information with respect to elevation and orientation provides a greater spatial resolution for viewshed and visibility analysis; as well as for noise, solar and similar environmental simulation common to urban informatics (Biljecki et al., 2015). Further, due to crowdsourcing and federal open data initiatives, 3D urban data have become widely available, enabling urban informatic applications at a large geographic coverage. Highlighting the scalability of 3D data, Milojevic-Dupont et al., 2023 harmonized disparate databases covering the European building stock, and Biljecki & Chow, 2022 consolidated common building morphology metrics and developed a global database. Despite these advantages, country scale studies focusing on building-level environmental performance have been limited to heat demand (Buffat et al., 2017), and roof top solar potential (Assouline et al., 2017; Walch et al., 2020). To our knowledge, there are no previous studies that have quantified visual landscapes from the perspective of individual buildings on a national scale.

This gap in research is in part due to the abstract nature of the view. Unlike other environmental quality attributes such as solar and noise, the extent of possible metrics to describe view quality is considerably broader, making consensus on measurement difficult. As a result, scaling and evaluating the view quality

demands greater computational effort. Broadly, we find that 3D-view based metrics define a visual landscape quality by the elements it contains – mountains, greenery, historical buildings, agriculture and similar land use categories (Baranzini & Schaerer, 2011; Yamagata et al., 2016, 2016; Yu et al., 2016), or by the spatial arrangement of elements unique to the observer’s perspective – access, distance, sky-openness & diversity (Turan et al., 2020b, 2021; Yu et al., 2020). Although there are many more possible ways to describe the view-metrics, the categorization given above is in line with the approaches previously utilized in spatial statistics and spatial pattern comparison (Long & Robertson, 2018), namely those that measure the spatial patterns that relate the abundance and arrangement of values. It is thus feasible to characterize a building’s visual landscape based on the composition and configuration of elements visible from the set of façade viewpoints associated with the building. Put another way, composition metrics define the aspatial properties of each element within a visual landscape (e.g. view of a lake, sky-view-factor, proportion of views onto greenery), whereas configuration metrics define the spatial properties of elements within the visual landscape (e.g. balance of all elements, total elements in far distance). The required computation efforts to apply such structured approaches, however, has thus far limited studies to single cities or smaller geographic area, which in turn inhibits a wider adoption and reach across disciplinary boundaries (Inglis et al., 2022a; Kang & Liu, 2022; Yamagata et al., 2016)

2.2.2 Evaluation of view-metrics

Substantial effort has been devoted to determining and correctly quantifying attributes of a ‘good view’ from an urban and building-level perspective. Yet, there are few empirical studies on landscape preference, and the methods to weigh the importance of visual attributes remain disparate (Inglis et al., 2022a; Kang & Liu, 2022). A likely confounder is that what constitutes a ‘good view’ is complex and driven by both individual and societal preferences. This complexity may not simply be described by the sum of individual elements, but rather by a nonlinear weighting of elements according to their arrangement, proportion, scarcity, cultural importance, and overall context.

Interestingly, although no standardized measure of a building's visual landscape quality exists, window-views and visual quality are commonly understood to play an important role in how individuals perceive landscapes and make decisions (Ko et al., 2022; Schutte & Malouff, 1986; Ulrich, 1977, 1981, 1986). Accounting for visual quality and an individual's preference thereof is thus an important consideration when it comes to financial and urban planning decisions in the context of the built environment. For instance, it is known that visual landscape quality influences public opinion in Switzerland, and increases the economic value of a building (Lindenthal, 2020; Lindenthal & Johnson, 2021; Turan et al., 2021), and changes to the visual landscape have a measurable impact on public perception (Ögçe et al., 2020; Oh, 1998). Yet the methods to support these findings rely on disparate sets of spatial metrics that are difficult to compare. Therefore, the creation of a unifying, quantitative measure to represent a building's visual landscape quality would represent an important step forward, facilitating cross disciplinary adaptation (Inglis et al., 2022a; Kang & Liu, 2022).

In perhaps the closest adaptation of such goals, Walz et al and Roth et al have introduced methodologies for a country-scale scenic landscape assessment. However, since they had to rely on stated-preference surveys and 2D imagery, the resolution of the produced estimates remained restricted to 1 to 5km.(Roth et al., 2018; Walz & Stein, 2018)

To our knowledge, a structured approach by which to evaluate the weighted importance of elements in the visual landscape of buildings has yet to be developed. Only then can building-specific estimates of visual landscape quality be assessed at a national scale.

2.3 Data & Methods

In the following section we outline the steps to develop a large-scale accounting of Switzerland's building-level visual landscapes and to investigate its variability across urban agglomerations and topology.

2.3.1 Viewpoint Visual Share Data

Our approach leverages a precomputed dataset containing point-of-view results from a viewshed visibility simulation based on open-access 3D databases, and presents a systematic and automated method to develop building-level view-indicators. Specifically, the large-scale viewpoint visibility analysis and resulting visual share dataset, provided by n-Sphere and Wüest Partner, was computed using a ray-tracing approach, whereby the proportion of rays cast outward, in a 120-degree cone orthogonal to the façade surface (**Figure 2**) from a single façade viewpoint, that intersect a select visible element represents the visual share of that element. Visual shares are expressed as a percentage ranging from 0-100%, and the total visual share proportions for a single façade viewpoint sum to 100%. A single façade viewpoint observation containing visual share data can be thought of as an image taken from a window. In **Figure 2**, we illustrate the data sources and how this procedure was applied to a generated 3D urban environment. Origin viewpoints were computed for all facades and floors within a building, and viewpoint target intersection information, distances between origin and target points, as well as obstructions and landscape elements in line of sight were recorded. **Table 3** describes the landscape elements, obstructions, and distances contained within the provided database. The selection of landscape elements is limited to the elements provided in the landcover maps (Federal Office of Topography swisstopo, 2018c) that the view database is derived from.

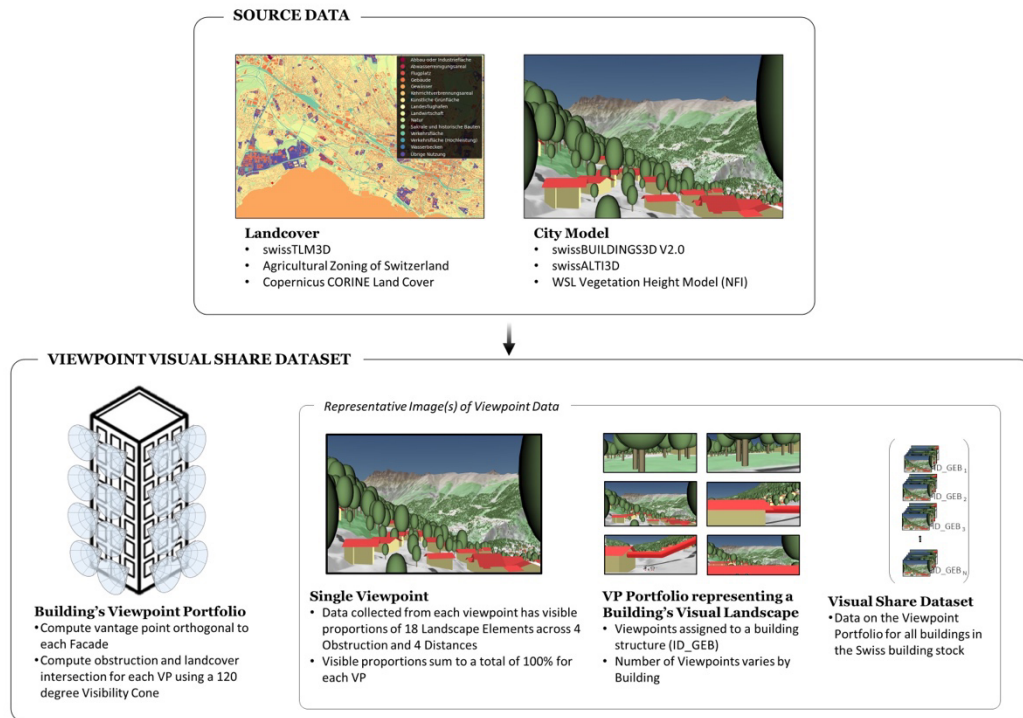


Figure 2 Schematic summarizing the visual share dataset. Data collected from each Viewpoint (VP) is illustrated with a representative Viewpoint Image. The actual database contains values representing the proportion of each landscape element visible from a single VP.

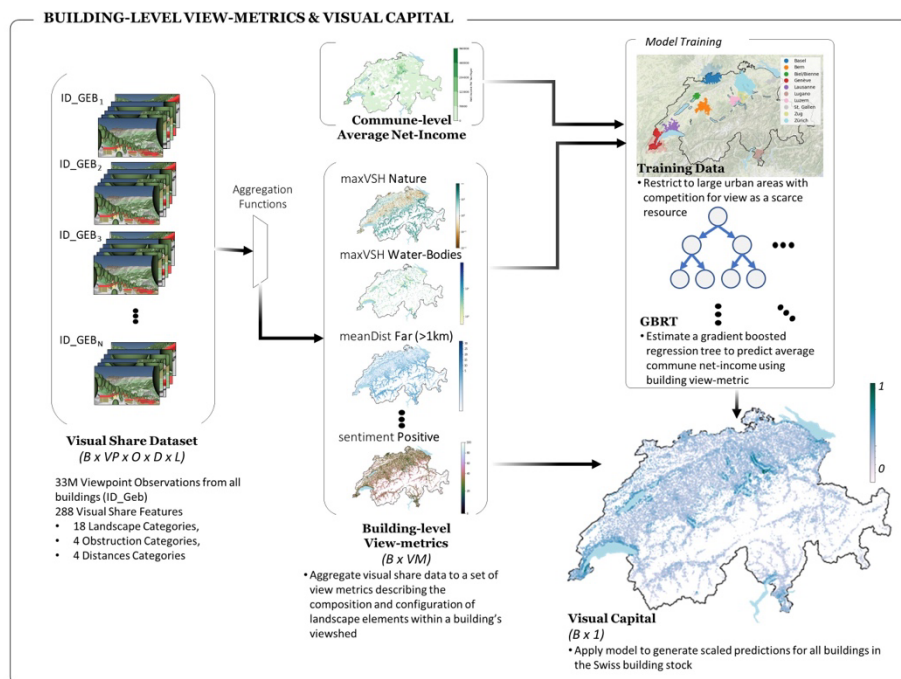


Figure 3 Schematic summarizing the developed methodology

Table 3 Landscape Elements and Distance Considered

Visual Element		Distance
Mining and Industrial	National Airport	Near (< 100m)
Waste-Water Treatment	Agriculture	Mid (100m – 1km)
Roof Obstruction	Nature	Far (1km – 50km)
Facade Obstruction	Sacred/Historic Buildings	Infinite (> 50km)
Airfield	Other	
Buildings	Vegetation Obstruction	
Water Bodies	Traffic area	
Heliport	High-performing Traffic area	
Waste Incineration	Water Basin	
Artificial Green	Sky	

2.3.2 Developing Building-Level View-Metrics

As a result of the viewpoint spacing approach used to develop the visual share dataset, the number of viewpoint observations collected per building varies with the size of the building, i.e. the larger the façade surface area, the more viewpoints. Since we are primarily interested in comparing the view quality of one building vs. another, we first generated building-level indicators from the viewpoint visual share data. Specifically, we compute two sets of building-level summary statistics. They characterize the view based on the abundance (composition) and arrangement (configuration) of visible elements, which from hereon are referred to as *visual composition* and *visual configuration*. Building level metrics used in this study are listed in **Table 3** with examples for further clarification. Together, the 57 developed visual composition and configuration metrics (see summary statistics in **Table 5** and **Table 6**) quantify the quality of the visual landscape. In **Figure 3**, we illustrate the main steps in our methodology.

Table 4 Definitions for Visual Composition and Configuration Metrics

Visual Composition

ID	View-Metric	Description of Calculation
maxVSH	maximum visual share	The maximum visible share of a select element from the set of a building's viewpoints. e.g. out of all visual shares of the lake, the maxVSH for a building may be 5%.
VA	visual access	The fraction of a building's viewpoints that have a visible share that meets a minimum threshold of 1%. e.g. a 1% view of the lake is visible from 10% of a building's viewpoints.

Visual Configuration

ID	View-Metric	Description of Calculation
richness	element richness	The total number of unique visual elements from a single viewpoint. E.g. 5 landscape elements are visible from a given point.
balance/gini	element balance	The statistical dispersion of the visual shares of unique elements from a single viewpoint. E.g. 5 unique landscape elements each with a 20% visual share, would produce a perfect equality balance score of 0.
pano	panorama	The total visual share of elements (excluding sky) located in the far and infinite distance, i.e. >1km away.
refuge	refuge	The ratio between the total visible share of elements in far distance and the near distance. E.g. the visible share of far elements in the distance is 10% that of elements in the near distance.
snt	visual sentiment	The total visual share of positive, negative, or neutral elements from a single viewpoint. E.g. 20% of the visual landscape is attributable to positively labeled elements (vegetation, water, nature, etc.).
dist	visual distance	The total visual share of elements located at a particular distance: Near, Mid, Far, and Infinite distance. 25% of the visual share is of elements in the near distance.

Table 5 - Summary Statistic for Visual Composition Indicators for 33 million viewpoints.

ID	Visual Element	Visual Composition					
		Max Visual Share (maxVSH)		Mean Visual Share (mnVSH)		Visual Access (VA)	
		mean	std	mean	std	mean	std
Abb7	Mining and Industrial	0.27	2.63	0.09	1.31	6.26	17.19
Abw14	Waste-Water Treatment	0.05	1.36	0.03	0.82	0.40	4.71
Dac1	Roof Obstruction	6.88	11.47	1.85	3.50	80.84	27.27
Fas2	Facade Obstruction	26.33	21.86	12.99	11.57	91.77	20.08
Flu18	Airfield	0.01	0.66	0.01	0.42	0.49	5.03
Geb12	Buildings	11.94	10.53	3.85	4.04	88.35	20.24
Gew1	Water Bodies	0.34	2.52	0.13	1.20	9.56	21.57
Hel19	Heliport	-	0.19	-	0.12	0.01	0.69
Keh15	Waste Incineration	0.01	0.45	-	0.23	0.06	1.69
Kue8	Artificial Green	33.64	16.88	22.75	12.67	89.21	26.73
Lan10	National Airport	5.19	12.34	3.02	8.75	52.39	39.09
Lan17	Agriculture	0.01	0.69	0.01	0.40	0.38	4.40
Nat3	Nature	7.54	14.12	4.81	10.74	76.19	29.69
Sak13	Sacred/Historic Buildings	0.10	1.57	0.03	0.58	1.38	7.78
Ueb5	Other	0.60	4.59	0.29	2.62	7.00	18.19

Veg3	Vegetation Obstruction	22.42	16.93	12.62	10.61	97.22	10.62
Ver6	Traffic area	0.16	1.91	0.04	0.60	5.01	15.01
Ver11	High-performing Traffic area	9.68	11.34	3.31	4.47	76.29	28.88
Was16	Water Basin	0.12	1.37	0.03	0.40	2.12	9.37
Sky	Sky	40.94	6.59	34.14	7.19	99.62	3.89

Table 6 Summary Statistics for Visual Configuration Indicators

ID	View-Metric	Visual Configuration						
		mean	std	min	0.25	0.50	0.75	max
cmpx_rh	Element Richness	9.42	1.73	1.00	9.00	9.00	10.00	19.00
cmpx_shanon	Element Balance - shanon	1.48	0.18	0.00	1.39	1.50	1.60	2.14
cmpx_gini	Element Balance - gini	0.83	0.03	0.67	0.82	0.83	0.85	0.95
snt_0	Neutral Sentiment	46.94	6.53	0.00	43.25	47.80	50.62	100.0
snt_Neg	Negative Sentiment	3.78	5.42	0.00	0.18	1.69	5.37	91.50
snt_Pos	Positive Sentiment	30.76	10.04	0.00	25.10	31.53	37.30	100.0
rh_snt_0	Neutral Sentiment Richness	7.33	1.82	0.00	6.00	8.00	9.00	12.00
dist_gini	Distance Balance - gini	0.54	0.06	0.07	0.51	0.54	0.57	0.75
pano_sum	Panoramic Share	3.61	4.13	0.00	0.78	2.09	4.97	51.30
pano_rh	Panoramic Richness	22.24	9.94	0.00	15.00	23.00	29.00	85.00
refuge	Refuge	0.64	0.22	0.00	0.50	0.64	0.76	47.66
ShNah1	Share of Elements in Near Distance	62.24	8.49	2.06	56.78	61.10	66.60	100.0
ShMit2	Share of Elements in Mid Distance	2.11	2.61	0.00	0.47	1.22	2.74	46.84
ShFer3	Share of Elements in Far Distance	1.50	2.36	0.00	0.09	0.46	1.87	37.22
ShUne4	Share of Elements in Inf Distance	0.01	0.02	0.00	0.00	0.00	0.00	1.33
ShSky	Share of Sky	34.14	7.19	0.00	30.42	35.38	39.25	50.62

2.3.2.1 Defining Visual Composition

Visual composition, defines the visual landscape in terms of individual elements or points of interest. We propose maximum visual share (*maxVSH*) and visual access (*VA*) to represent aggregate values of a single element within a select building (see **Table 4**).

The first visual composition metric, *maxVSH*, describes the maximum visual share of a selected target element (e.g. Nature) from a select building's set of viewpoints. Using the maxima helps to preserve variance across the national sample and, importantly, is robust to the shape and size of a building's footprint and surface. The second, *VA*, describes the proportion of a building's viewpoints that a select element is visible from. Put another way, the *VA* quantifies the potential exposure a select building has to a select visible element.

2.3.2.2 Defining Visual Configuration

Visual configuration, the second approach to define view-metrics, defines the visual landscape in terms of the spatial arrangement of these visible elements from a particular viewpoint. In this paper, we apply the commonly used metrics: richness, balance, panorama, refuge, distance, and sentiment (see **Table 4** for definitions and examples). A few of these offer a relative measure of the average visual shares (as a %) across all viewpoints within a building, for all cardinal directions (richness, balance, and refuge). The remainder describes a building's average exposure level in terms of distance or sentiment: such as the average sky exposure, or the average exposure to positive elements. Combining these metrics could be particularly useful when comparing the visual landscape from buildings across regions, as each of these measures highlights the spatial structure of elements as opposed to the elements themselves. For instance, element balance informs the degree to which the visual scenery is dominated by a single element or whether an even distribution is present. Similarly, this metric can be repeated to measure the balance of elements grouped by distance. Visual balance as a function of distance could help to characterize the natural topography (e.g. terrain slope) and the urban form, e.g. dense urban core, suburban periphery, or rural outskirts

2.3.3 Measuring Visual Capital

To perform a national-scale evaluation and accounting of visual landscapes and of window-views, we develop a framework to measure VC. The measurement framework consists of our 57-view metrics and our target variable, commune-level income (CLI). CLI is assigned using the 2018 average net-income per taxpayer for a given commune (Federal Statistical Office, 2022). We apply a machine learning model that learns the relationship between the two at the building level, granting us a method to directly estimate income from view-data. Specifically, we estimate a gradient-boosted regression tree, eXtreme Gradient Boosting (T. Chen & Guestrin, 2016). Despite the CLI not varying at the commune level, the large amount of data allows us to extract intra-communal variation across communal building stocks, which enables building-level predictions of CLI, that can solely be attributed to visual characteristics. Hence, while the response variable CLI is uniform across buildings within a commune, the model predictions are individualized. We define the rescaled predictions of a building’s ‘income’ derived directly from the building’s view metrics as visual capital (VC).

VC is thus a weighted combination of the visual composition and visual configuration view-metrics that were extracted directly from 3D data of the building itself and its surrounding landscape. Following our assumption that buildings found in high-income neighborhoods have, on average, desirable, high-quality views, our model thus finds the combination of these view-metrics that best predicts CLI. Considering the likely nonlinear nature of visual preference, we use a gradient boosted decision-tree algorithm, which is well suited and has been deployed in similar frameworks, such as predicting an individual’s economic success (income) based on friendship network attributes (Chetty et al., 2022). To ensure a high degree of income-sorting (competition for housing), which is generally the case in urban areas, we compile a training sample of buildings located within the top 10 agglomerations (for information on selected agglomerations, see **Table 7**); located in communes with at least 100 taxpayers; and which have a maximum of five stories. Limiting building height reduces the model’s propensity to overfit to inner-city urban areas and minimizes biases that

arise due to the underlying correlation of building height and visual composition (e.g. the size of a lake view increases the higher up you are in the same building). The focus of this study is thus on individual and single-family homes, which are typically the main focus of real estate valuation approaches. Our final training sample consists of 781,220 buildings from 365 communes.

Table 7- Summary of Commune-Level Income Statistics for Agglomerations Used in Training Sample

Agglomeration	No. Communes	No. Buildings	Commune Average Net-income Per Taxpayer (2018, CHF 1'000)					Commune Average Taxable Income Per Tax Payer (2018, CHF 1'000)				
			mean	std	min	median	max	mean	std	min	median	max
			Basel	44	92,789	95	16	71	91	135	86	15
Bern	28	62,172	83	10	70	80	121	76	10	64	73	113
Biel/Bienne	11	14,791	75	12	67	69	111	68	11	61	63	102
Geneva	46	62,246	137	62	75	119	480	128	62	67	108	468
Lausanne	35	41,750	99	21	68	92	142	90	20	60	83	133
Lugano	36	43,809	91	16	61	94	146	84	16	56	84	138
Luzern	15	33,411	96	29	67	80	170	88	29	60	74	163
St. Gallen	12	36,025	81	14	70	73	122	74	14	64	67	111
Zug	13	22,952	134	31	78	116	196	126	31	70	108	188
Zurich	106	214,258	108	43	69	92	300	99	43	61	86	292

2.3.3.1 Machine learning setup and evaluation

To assess model robustness, we ran 100 iterations of 10-fold spatial cross-validation (see illustration in **Supplement 6.3 Fig S1A**). Each round consists of the following 4 steps: (1) Randomize the order of communes and partition into 10-groups, (2) Train the model on buildings located within communes of 9 groups, (3) Evaluate the model on buildings in the excluded group, assign R^2 -score, and (4) Repeat until all 10 groups are excluded. R^2 -scores are derived from comparing the average building-level prediction within a commune to that of the average commune-level net income. As a result of the 100 iterations of the 10-fold spatial cross validation, we obtain 1000 models, where each commune has exactly 100 associated R^2 -scores. The distribution of model performance provides an assessment and range of how well the model performs and allows us to explore communes associated with under/over performing models. After validating model robustness, a final model was fit on the entire training dataset. In section 2.5 we

further validate our approach by using a separate data-set that provides a high-income label for each commune from the year 2000 (Federal Statistical Office, 2000).

To further assess prediction sensitivity, we compared the results across 7 machine learning regression models: Linear, Penalized Linear Regression (Lasso), Generalized Linear Model (GLM), Light Gradient Boost Model (LightGBM), Neural Network (NN100), Random Forest (RF), and, our chosen model, eXtreme Gradient Boosting (XGB) (Breiman, 2001; T. Chen & Guestrin, 2016; Ke et al., 2017). In addition to comparing model accuracy on a common test-set, we visually compare the spatial distribution of fitted valuation for lake-shore communes with 3 different CLIs: Morges (CHF 79K), Prévèrenge (CHF 96k), and St.Sulpice (CHF 134k). This helps to visually determine whether the model is simply learning administrative boundaries or rather important visual characteristic. Lastly, we compare the correlation of the fitted values to the individual view-metrics as well as a subset of relevant non-view metrics, to gauge variability of the association between metrics and model predictions. The subset of used non-view metrics define building attributes (including year of construction, volume, land area, condition, free-standing, number of rooms, sun exposure, street noise), distances to regional amenities (including main street, train station, atomic power plant, city center, shopping, nature, lake, river, and public transport) and location attributes (including lake access, and public transport quality).

To better interpret the influence of a select view-metric, we implement the SHAP algorithm, which quantifies the optimal credit allocation across all model features (Lundberg & Lee, 2017) and computes a proxy value characterizing the marginal contribution of each feature towards one additional unit of VC. The SHAP algorithm provides greater model explainability, and as a result has become common place in spatial modeling methodologies. For example, a recent study (Zekar et al., 2023) used the method to measure the effect of urban form features on temperature changes. Additionally, SHAP allows us to explore the context-dependence of view-metrics. After training the final model, we rescale the fitted values to derive the normalized $[0,1]$ measure of VC across the entire building

stock sample. For spatial analysis, we can further standardize these values, centering the mean at 0, to visually identify regions that tend to be above or below average.

2.3.4 Measuring Regional Difference of Visual Capital

Building level indicators at a national-scale enable a quantitative assessment of inter- and intra-regional differences. In this study we summarize a region by the median building value or the proportion of buildings with a select value; for instance, the percentage of buildings in a commune with a *maxVSH* greater than 1%. When directly comparing the distributions of building-level values across regions or agglomerations, we additionally account for spatial concentrations of buildings. To do so, we can group buildings into 1-km² regions, called hexbins. Such standardized hexbin regions control for the spatial dispersion of buildings and allow to directly compare the spatial distribution of a value across an agglomeration. When comparing landscape topology differences across regions, utilizing administrative boundaries such as communes can complicate the analysis, since communes can vary in both size and shape and hence obscure intra-commune variability of the urban and natural form. Thus, in this study, we also calculate a 100m buffer area for each building and compute the building density (e.g. the number of buildings) and the terrain slope (e.g. the average terrain slope). These buffer areas represent the respective urban and natural forms each building is exposed to. Terrain slope was calculated utilizing readily available digital elevation models of Switzerland (Federal Office of Topography swisstopo, 2018a).

2.3.5 Drawing New Geographic Boundaries of High Visual Capital

To validate and show the usefulness of a building-level measure of VC, we define new geographic boundaries of high-VC as a case-study. Specifically, we adopt the LISA (local indicator of spatial association) method (Anselin, 1995) to isolate buildings that have a spatial association with high values of VC, and partition these buildings into distinct clusters to draw new urban boundaries.

Following the LISA method, we compare the VC of a select building to that of its 100 closest spatially lagged neighbors. To test for the spatial dependence between a building's VC and that of its neighbor, we compute the Local Moran statistic for the observed data and compare it to the Local Moran of a randomly generated set of neighbors. After correcting for multiple hypothesis testing, we retain only the buildings with a significant Local Moran statistic, a high-VC and high spatially lagged-VC. We then group the location (coordinates) of these buildings into distinct clusters using an unsupervised hierarchical density-based clustering method, (HDBscan) (McInnes et al., 2017). Buildings that are either isolated or in low density areas are considered noise and thus removed. Next, we generate geographic boundaries by calculating the alpha shape for each cluster's set of buildings using an alpha parameter of .01. The newly generated shape boundaries are considered regions of high-VC. Note, this process can also be used to identify geographic boundaries of low-visual capital clusters. Importantly, these newly defined boundaries of high VC can be compared against a validation dataset of high-income communes held out of the training sample.

2.4 Results

2.4.1 Distribution of building-level view-metrics across the Swiss building stock

We find that the 20 visual elements considered in this study vary in abundance. **Figure 4** shows that only about 15% of the building stock has any view of Water Bodies. Visually abundant elements, such as Nature, Sky and Agriculture, are seen by at least 50% of the building stock (we consider $> 0\%$ *maxVSH* as the cutoff for being seen).

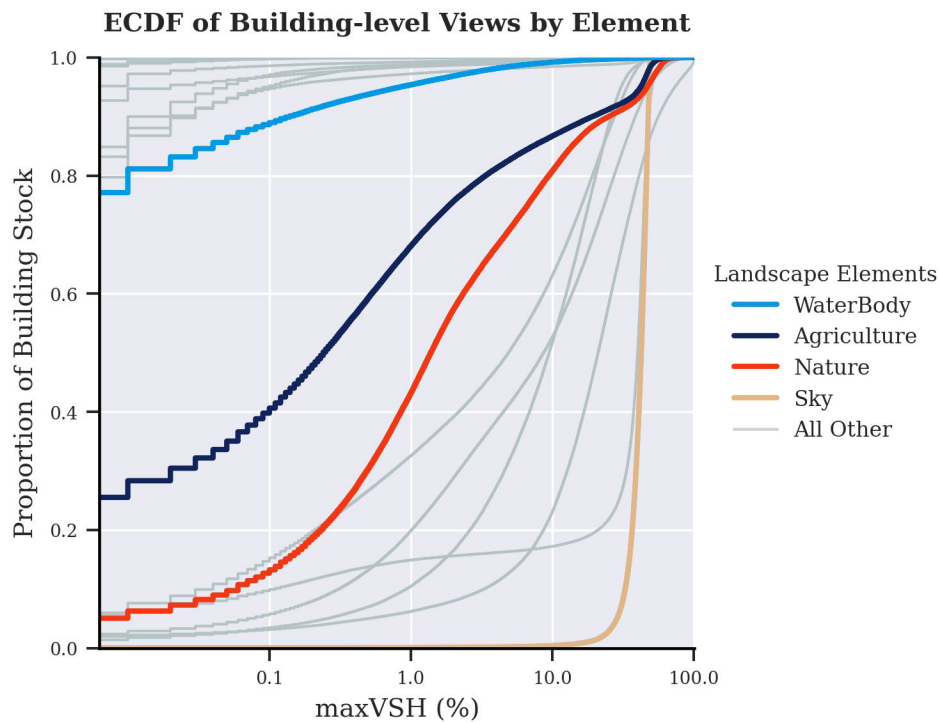


Figure 4 ECDF of maxVSH elements across the Swiss building stock. Figure indicates that building-level views of elements vary in abundance, where abundant elements are seen ($\text{maxvsh} > 0\%$) by more than half of the building stock and scarce elements are visible in less than half.

While visually-abundant elements exist in similar quantities from region to region, we identify a few exceptions. Buildings in rural regions have about ten times larger view-shares of nature – where a 75th percentile-ranked building in the rural region will have a 10% *maxVSH* of nature, whereas an equally ranked building found in any major agglomeration will have less than a 1% *maxVSH*. For views of vegetation, Geneva ranks highest among Swiss agglomerations, where the median building has a 5 – 10% greater share. See **Supplementary 6.3 Fig S2,S3,S4** for information on the visually-abundant elements.

Upon inspecting the visually scarce elements, i.e. seen by less than 50% of the building stock, we find much greater variety across the major agglomerations of Switzerland (see **Supplementary Fig S2**). Buildings in Lausanne are more likely to have a view onto a body of water, with 40% of buildings having a water-view of some quantity; approximately 15% more than in Zurich and 30% more than in Bern and Basel (river-cities). We find substantial differences in visual configuration across urban and landscape typology classification (see

Supplementary Fig. S3, S4). For example, visual landscape for urban areas is dominated by elements in the near distance, whereas the Alpine region boasts more balanced views and has the largest panoramic views, namely 4 to 8-fold larger than other terrain typologies.

2.4.2 Model

2.4.2.1 Model results

We assess the performance of the full XGB model, trained on the full training dataset (i.e. all buildings located within the top 10 agglomerations), by comparing the average model prediction across all buildings within a commune to the commune's actual average net-income per taxpayer – the CLI. We find that the residuals for average commune predictions are normally distributed for communes with a CLI of less than or equal to CHF 100k, whereas for communes above this threshold the residuals are skewed and the 95% percentile ranked prediction is a better predictor of CLI than the mean predicted value (

Figure 5).

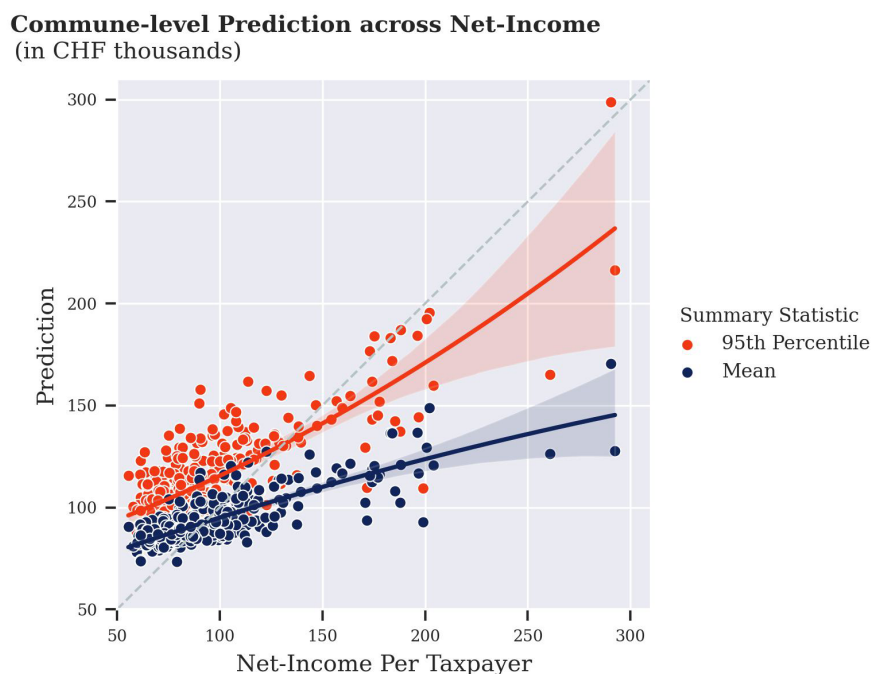


Figure 5 Scatterplot of commune-level predictions against commune-level net-income. Plot illustrates the dispersion of commune-level prediction increases against net-income, where the 95th percentile and Mean score are shown in Red and Blue.

The k-fold spatial cross validation procedure (section 2.4) confirms the robustness of the chosen XGB methodology, with a normally distributed model performance (mean of R^2 -score = .32, standard deviation = .09) consistent across agglomerations (see **Supplementary Fig S1**). The final model achieved an R^2 -score of .47, which falls within the upper decile of the cross-validation performance range (see **Supplement Fig S1**).

We find model estimates are robust to other tested regression architectures: Linear, Lasso, GLM, LightGBM, NN100, XGBoost, and RF regression models (see **Supplementary Fig. S5**). Specifically, the individual correlation of each model's prediction against individual view-metrics is consistent across all models (see **Supplementary Fig. S5A**). While correlations between model predictions and the subsets of non-view metrics are equally consistent; values for non-linear model architectures (LGBM, XGB, NN100, and RF) are more similar than for linear architectures (Linear, Lasso, GLM) (see **Supplementary Fig. S5B**). While the Random Forest model maintained similar prediction accuracy compared to the two gradient boosted regression tree models (i.e. LGBM and XGB), it was prone to overfit to the training data and the compute time was orders of magnitudes larger (see **Supplementary Fig S6**) than the XGB model, chosen in this study.

2.4.2.2 Understanding the factors that determine Visual Capital

We find that a handful of metrics have a particularly strong positive impact on the model prediction (**Figure 6A and Supplementary Fig S7**). Greater visible proportions (i.e. *maxVSH*) of water-bodies, sky and far-distance views contribute positively while agriculture views are inversely predictive of high CLI and indicate distinct non-linear effects. Importantly, we find the influence of most landscape elements on model prediction is context-dependent, i.e., conditional on the other elements within the same visual landscape (**Figure 6B-E**). For example, the influence of a nature view varies with the visual access to waterbodies (**Figure 5B**), and large (50% or greater *maxVSH*) views of vegetation are amplified in the context of an imbalanced share of elements and a balanced proportion of the visible distances; i.e. elements in the near, mid, far, infinite distance (**Figure 6E**). Views of waterbodies have a substantial influence on the prediction, and can amplify the

influence of views of elements in the far distance (**Figure 6D**). Interestingly, sky exposure has a persistent influence on the predictive capacity of all other attributes. For instance, within the context of limited sky exposure, views of buildings have a negative impact on predictions. Conversely, views of buildings with high sky exposure positively influence the predictions (**Figure 6C**).

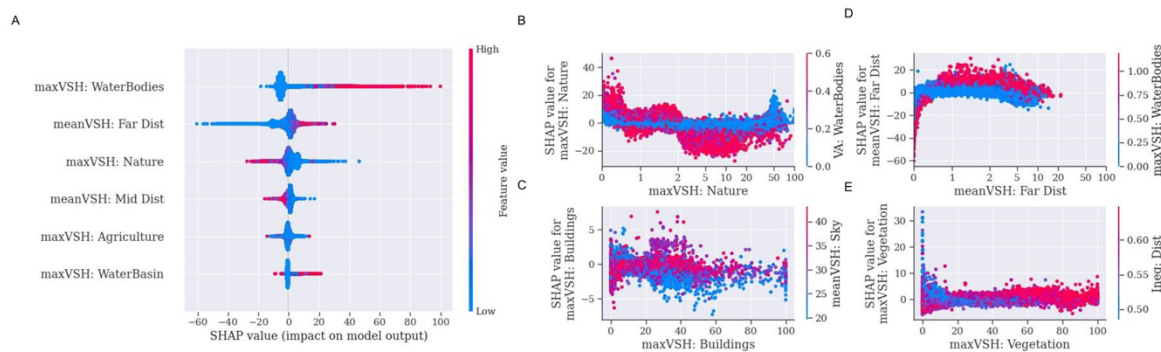


Figure 6 Impact of view-metrics on a single building's prediction. (A) Summary plot illustrates the SHAP value of a single instance and directionality of impact of the view-metric, where high and low feature values are shown in Red and Blue. The impact of the top 6 features are shown, the remaining, less influential metrics (by absolute mean) can be found in the Supplementary material Fig S7. Interaction plots show that prediction influence of (B) nature views vary across visual access to water, (C) views of buildings vary against sky exposure, (D) larger views of a waterbodies in the same scenery, as well as views of far-distance, have larger predictions than smaller views of waterbodies, and (E) vegetation varies across distance inequality.

2.4.3 Visual Capital

In the following section, we present Visual Capital (VC), the rescaled fitted values representing the building-level visual landscape quality preference across the entire swiss building stock. We directly compare the VC of cities and communes and present evidence illustrating (1) the extent to which visual quality contributes to income sorting within and across agglomerations, (2) VC's association to the urban and natural form, and (3) a validation case-study that correctly identifies held-out high-income regions.

2.4.3.1 Regional Difference in Visual Capital

Generally, we find that averaging all building level VC predictions per commune correlates well with the CLI of the respective commune, however, in some Swiss cities this relationship is stronger than in others. Comparing Lausanne and Basel, which are two cities with a similar CLI range, we find that view metrics are more

predictive of CLI in Lausanne than Basel, suggesting that view-based income sorting is stronger in Lausanne, whereas in Basel other socio-economic factors may play a more important role (**Figure 7**). Comparing the slopes across the top ten agglomerations, we can identify Zug and Lausanne as the cities with the strongest slope, i.e. VC to CLI association.

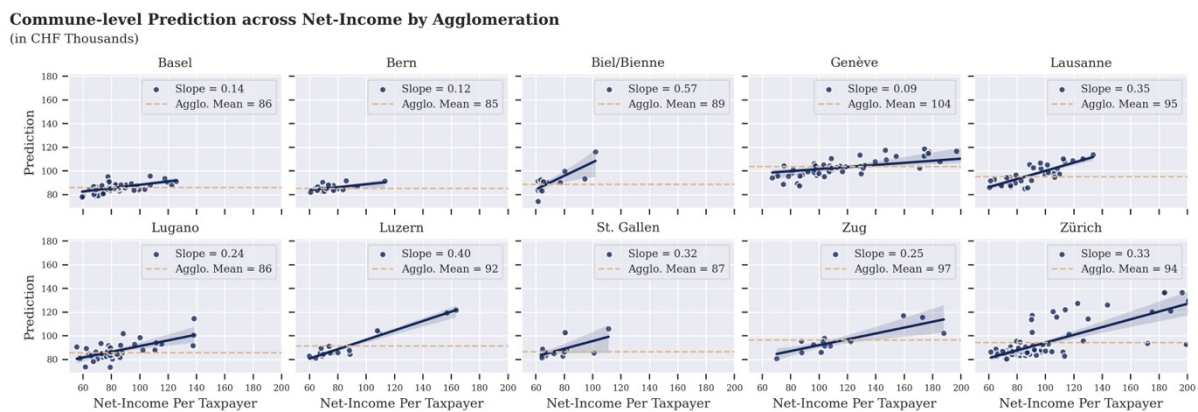


Figure 7 Scatterplot of Commune-level prediction for the 10 largest Swiss urban agglomerations. A fitted line, and its slope shown in blue and the agglomeration's mean prediction is shown in orange. The plot and computed slope describe the degree to which income sorting can explain residential sorting variations across Switzerland. A steeper slope, e.g. Lausanne, implies that the visual environment can describe the difference between low- and high-income communes; whereas in Bern smaller differences in visual capital between the high- and low- income communes, i.e. flatter slopes, suggests visual landscape to be less important to the residential income sorting process.

Another indicator we can compare across agglomerations is average predicted VC. Conceptually this can be understood as the expected view when choosing a building at random. We find that Geneva and Lausanne achieve the highest average VC. Importantly this is true even in the lowest CLI bins, indicated by a higher intercept for the agglomeration-specific fitted line in **Figure 7**. Zurich, although situated by a lake, barely ranks higher than river-cities like Basel and Bern. Beyond average expectations, the variability in building-level predictions of VC for a given income bin allows us to investigate “view-inequality” both at a global and local scale .

2.4.3.2 Generalizing the Regional Difference in Visual Capital

To investigate what drives the differences in the average and the variability of VC across different agglomerations, we analyzed the spatial distribution of VC across agglomerations. We observe a similar spatial dispersion of VC in Lausanne and

Geneva; whereas Zug and Zurich exhibit heavily skewed values. Specifically, the first 60% of Zurich's building-level VC values and land-level values (i.e. using hexbin aggregation to control for spatial dispersion) are substantially lower than that of cities along Lake Geneva (see **Supplementary Fig S8**). Further, we observe a spatial concentration of high VC along the East and South-Coast of lake Zurich; whereas in Lausanne VC is evenly distributed across the city boundaries. **Figure 8** illustrates the spatial distribution of above average VC and highlights the importance of distance to lakes for all cities. Intriguingly, the spatial distribution of VC across the two cities Zurich and Lausanne appears to not only reflect distance to the body of water (see **Supplementary Fig S9**), but also differences in natural topography. For instance, Lausanne sits on a hill, however, its downtown lies in an area of depression, which is reflected by lower VC values for buildings in this area (**Figure 8**). Similar holds true for the nine other agglomerations. This indicates that our measure of VC can accurately capture natural form.

Spatial Dispersion of VC (Standardized Values)

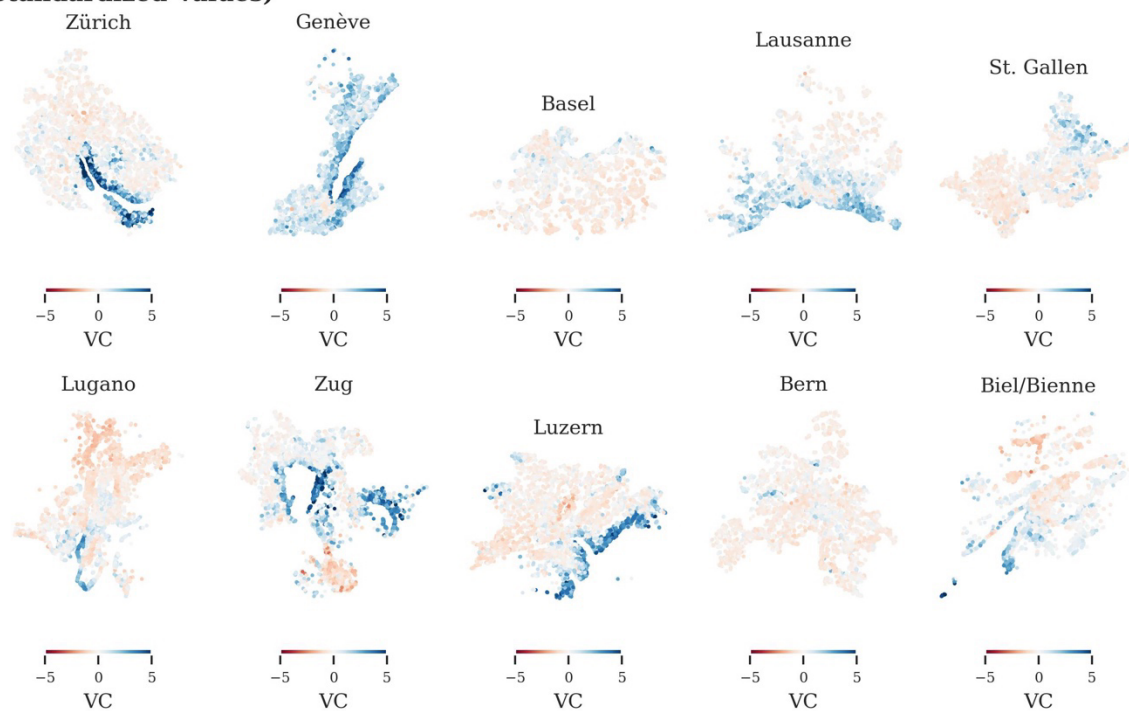


Figure 8 Spatial Distribution of Visual Capital across Swiss agglomerations. Standardized VC values are used to illustrate the spatial dispersion of above and below average within and across agglomerations.

2.4.3.3 Visual Capital and the Urban Natural Form

At the national scale, we observe that buildings with high visual-capital tend to be located near lakes and on the foothills of the Alps (**Figure 9**). As such, our building-level view scores confirm what one might expect, that rural-like views are most sought after when buildings are located within urban centers. The concentration of popular urban view-preferences at the foothill of the Alps further suggests that there may be a direct link between VC and landscape topography such as hilly/mountainous terrains. Supporting this notion, intra-communal variation in VC still display spatial patterns, with similar VC values forming localized clusters (**Figure 9**).

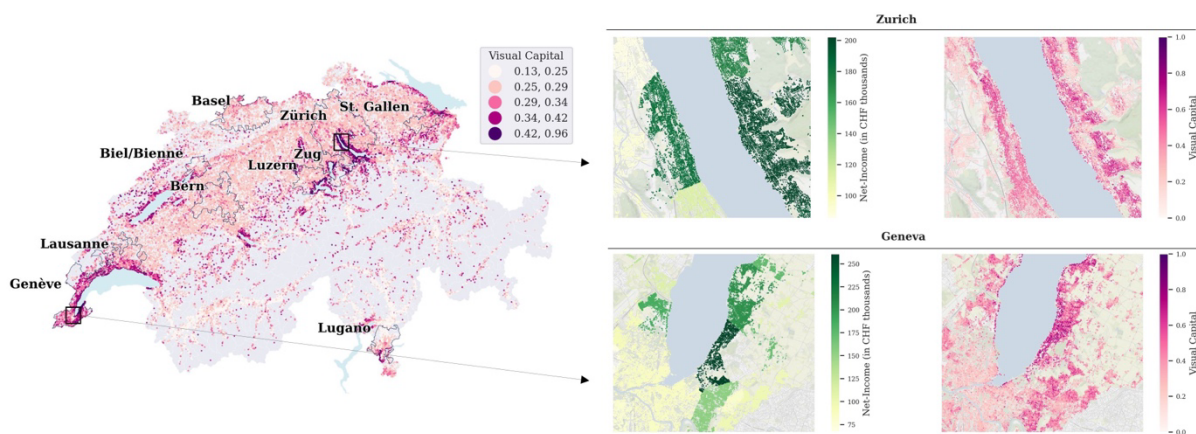


Figure 9 Choropleth depicting visual capital of the Swiss building stock shows higher levels of visual capital are found nearby lakes and on the foothills of the Alps. Comparison of the distribution of building-level average net-income and Visual Capital values for Zurich and Geneva reveals that VC captures intra-communal differences in building-level view quality.

When we stratify VC by landscape attributes (the slope of the land the buildings are located on) and the urban form (using building density within 100m as a representation), a non-linear pattern emerges. It recapitulates the intuition one might have on the relationship across terrain slope, building density and views: the average VC of dense urban areas increases with the slope of the terrain, as steeper slopes make it more likely that the view of a given building is not obstructed by another one (**Figure 10**). Unlike income, the optimal VC trendline cannot be defined to a single best slope, as lower density areas can achieve similarly good or better views with minimal elevation gain. Moreover, the likelihood of a good view decreases once the slope of the terrain passes 20%, which

may indicate distance from other important urban view indicators, such as view complexity. Further, investigating the VC variance within a given urban and natural form bin, confirms that VC scores reflect our intuitive understanding of the relationship between view and the urban form: For low-density urban environments, the skewness of visual capital remains low across terrain slopes, as buildings are spread out making it less likely that one building's view is influenced by another; on the contrary, skewness increases for dense regions as a function of terrain slope, with a hotspot of high-VC skewness within dense urban areas with a moderately steep elevation gain, indicative of visual obstruction due to neighboring buildings as a driver for view inequality (**Figure 10**). This presents strong evidence that our model of building-level VC accurately reflects important view characteristics, such as the intricate interplay between typology, terrain, and building-specific viewpoints that cannot be captured by a simple measure such as CLI (**Supplementary Fig S10**).

Visual Capital Stratified by Building Density and Terrain Slope

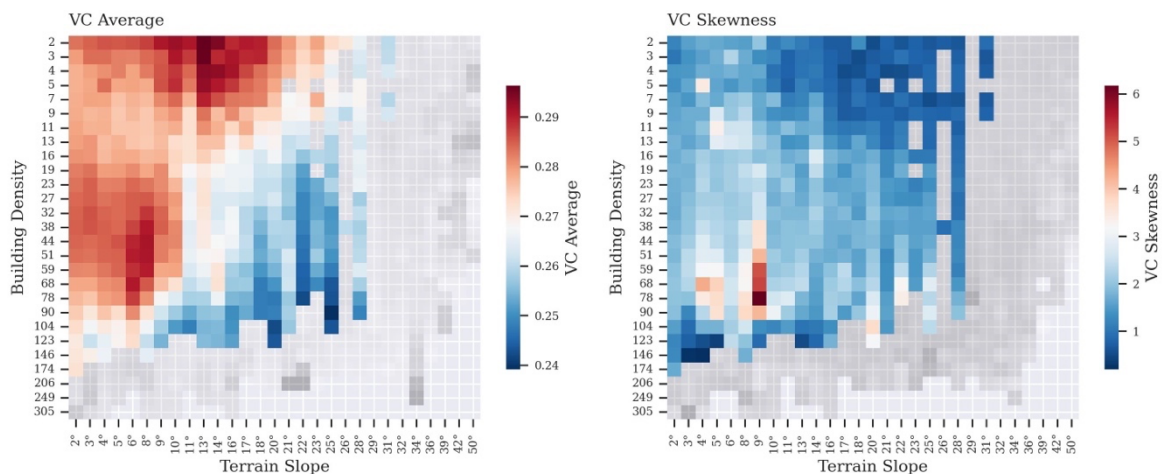


Figure 10 Heatmap depicts the average VC (left) and skewness of VC (right) when stratified by urban and natural form; i.e. building density (100 m radius) and terrain slope (1 km area). Urban/Natural form conditions with less than 1000 buildings are excluded (greyed).

2.4.3.4 Drawing Geographic Boundaries of High Visual-Capital

Here we present the result from our methodology to generate micro-location visual quality indicators for our validation case study in Lausanne. We group buildings

based on their VC similarity and identify natural boundaries of shared visual quality.

Our spatial clustering analysis of Lausanne identifies a number of high-VC clusters (**Figure 11**). The generated regions overlap, to a large extent, with both administrative boundaries of high-income communes used during the model training, as well as those held-out for testing. However, our newly defined regions often extend past these predefined administrative bounds. This spill-over effect tends to track with terrain and urban form, confirming our previous findings. For example, **Figure 11** shows the largest identified cluster encompasses the majority of the commune Pully, which has an average CLI of CHF 119k, however, the natural view boundaries spill over into the neighboring commune of Lausanne center, whose CLI is a comparatively meager CHF 79k. We identify high VC spill-over in several other high-income communes, such as Saint-Sulpice, Buchillon, and Saint-Prex. Notably, despite being surrounded by lower-income communes, a cluster of high VC is found within the boundary of Jouxens-Mezery, whose net-income per taxpayer information was not publicly available, however gross net-income data from 2018 and tax data from the year 2000 labeled this commune as high-income (**Figure 11**). Furthermore, we identify several smaller clusters of high VC that are not labeled as high income, either because of missing data or because they are located in lower income communes. These findings indicate that spatial clustering of VC can serve as a local indicator of areas with similar, and particularly highly valued views. This analysis may be extended to locate clusters of low-VC regions, or be applied to other cities and regions.

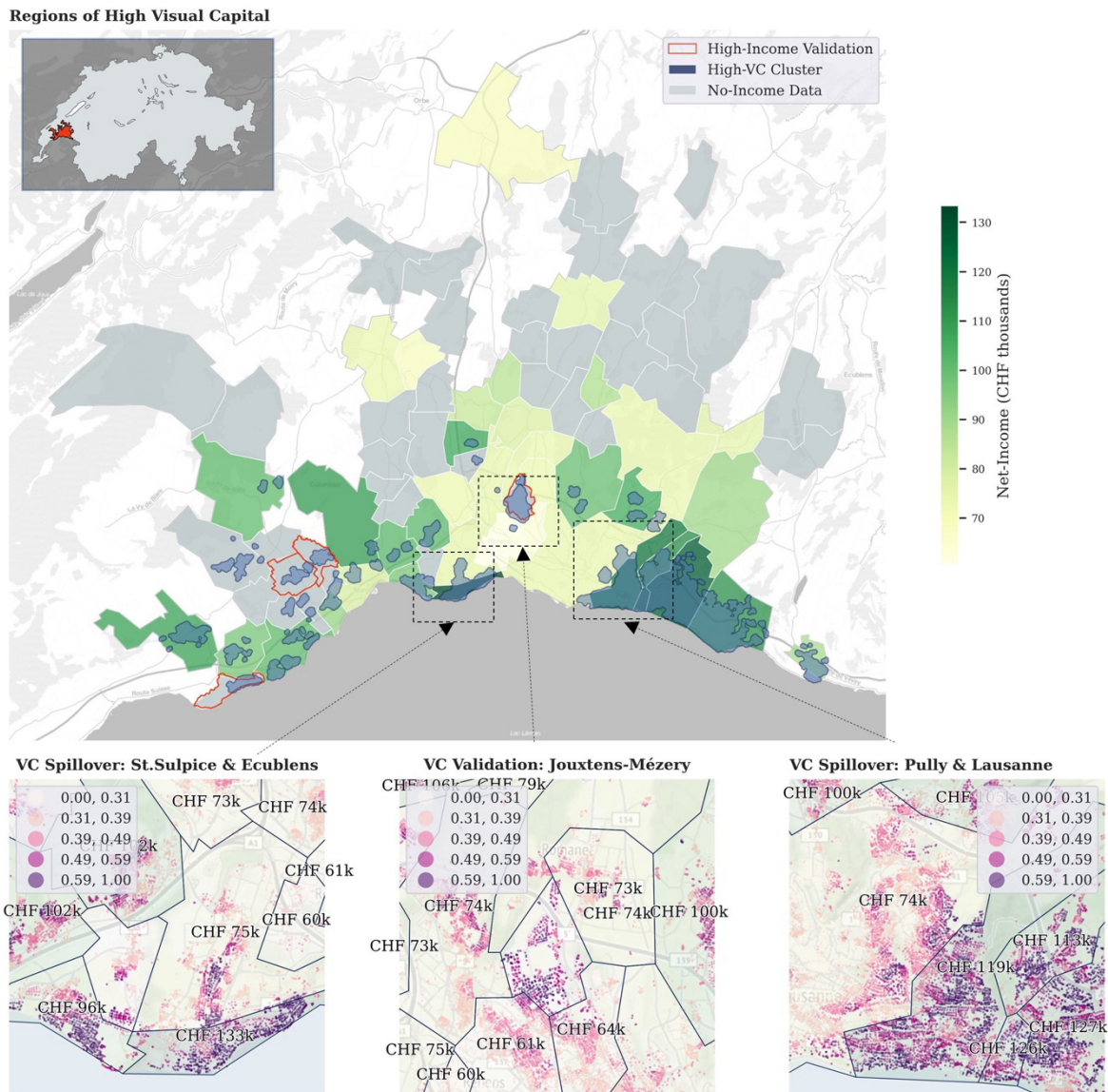


Figure 11 Computed boundaries of high visual capital (HVC) are shown in blue. Communes with darker shades of green indicate higher income levels, grey communes were excluded from the training-sample because no income data was readily available, and the red border indicates high-income communes as labeled by a secondary data source. HVC appears in all held-out validation samples; including Jouxten-Mezery. HVC spills past administrative boundaries of high-income neighborhood, including St.Sulpice and Pully.

2.5 Discussion

Determining the value of visual landscapes is challenging in part due to the difficulty of how to best quantify the view itself. Viewpoint data from 3D GIS and Digital Twins, in combination with spatial machine-learning techniques, offer an opportunity to both develop comprehensive view-metrics and uncover the context

of visual landscape preferences. We leverage commune-level income (CLI) statistics to generate a composite measure of building-level visual landscape quality, which we term visual capital (VC). Visual capital is derived by extracting visual composition and configuration metrics directly from a building's 3D configuration and that of its surrounding environment. Hence, we extend the existing literature in two ways: First, we provide an accounting of the visual landscape of the entire Swiss building stock and, second, we provide a building-level visual landscape ranking in the form of VC, which can be understood as the view-based, individualized 'income' of each building. Furthermore, we show that VC captures non-linear relationships of individual view metrics, urban density and natural form, thus providing an accessible summary indicator of a building's visual environment. Such assessments have remained challenging in the past, due to either a lack of large-scale data or accessible response variables.

Our model relies on the assumption of view-based income sorting, and thus relies on competition for the scarce resource 'good view'. In contrast to previous studies (Inglis et al., 2022a), we are not bound by a limited number of observations, thus allowing us to benchmark landscape-based preferences at the resolution of individual buildings. By restricting the trained model to the ten most populous agglomerations, we maximize amenity-driven income sorting effects, providing a more accurate depiction of building-level view preferences. Supporting this notion, view-based income sorting is strongest in agglomerations with access to high-quality views, as typically found in lake-regions. Individualizing view preferences at the building-level in this manner, allows us to quantify and compare how good of a view an average citizen of a select city can expect and what income is required to obtain it.

An important aspect of our approach is the applicability of the learned visual preferences to the entire national building stock, including rural regions. The positive correlation between the variability in inter-commune VC and CLI suggests that communes attracting higher income individuals have larger visual inequality, with only a portion of buildings (20-40%) attaining desirable and differentiable visual landscapes, whereas the VC of the remaining stock resembles

that of lower-income communes. Further, we can use the global predictions of VC to assess how the visual landscape quality of Switzerland is associated with both urban and natural form factors. For example, we can confirm the intuitive assertion that, on average, income-sorting tends to favor either elevated or less-dense areas within an agglomeration. Unlike previous studies that lacked building-level information, our methodology reveals a more complex relationship between slope and building-density. The high overall high skewness of VC within dense communes supports that view preferences are well-captured as, unavoidably, there will be buildings whose view remains blocked by others. It further indicates that proximity-metrics (such as distance to the lake) or simple neighborhood-scale attributes, i.e. net-income, may not be sufficient to capture a 'good view' for individual buildings, as it discounts important 3D differentiators such as natural and urban form.

Since the resulting predictions of VC are individualized and thus no longer bound by communal statistics, we can de novo assign 'view-boundaries' that indicate local clusters of buildings with similar VC. These newly defined regions of shared VC may thus provide a basis for view-based micro-location indicators, as commonly used in housing price evaluation studies: comparing clusters of shared VC could highlight buildings or neighborhoods that are over/undervalued with respect to their visual quality. Such assessment could prove valuable to developers looking for properties in economically undervalued, but perhaps visually appealing areas, as well as urban planners interested in quantifying the visual impact of a proposed new development.

A single quantitative measure for building-level VC may provide further benefits: automated real estate valuation and mass-appraisal methods can particularly benefit from building-level differentiation of visual quality. Previous studies have highlighted that iBuyers, who use automated valuation models, are challenged by adverse selection (Buchak et al., 2020), which may partly reflect a lack of data on 'hard-to-measure' qualities such as the view. Including VC into valuation models may thus improve the predictive performance of a statistical model. In this context, extending our analysis to individual floors, sides, or even units within a

select building, may allow modeling view-based price variation within large multifamily buildings. Further, extending the analysis to focus on other urban form typologies, i.e. tourist communities, may yield interesting insight into the factors that predict visual capital in specific regions or contexts. Pricing studies incorporating sales, rental or hotel prices, while controlling for other important building and local attributes, could further validate the importance of this metric. In addition to determining the willingness to pay with hedonic pricing, studies can utilize mixed-effects models and spatially varying coefficient models (Dambon et al., 2021) to assess whether the marginal effect of visual capital on home prices varies across space (e.g. coordinates or urban typologies), and income (i.e. as a luxury or inferior good).

Although our building-level VC metric captures many intuitive concepts on how individual view metrics, as well as urban and natural forms, should interact to create a preferential visual landscape, there are several limitations of our automated assessment tool. While it could be reasonable to assume that visual landscape preferences do not significantly change from year to year, our approach only considers income from a single year and thus may not fully represent changes in visual preferences over time. Despite defining view-metrics at nation-wide resolution, the view-metrics used in this study cannot fully capture the aesthetic quality of a particular view. For example, we currently cannot differentiate the view towards a facade with damaged and unmaintained cladding from one with architectural sculptures and intricate stonework. Thus visual capital may struggle to explain income sorting for building stocks with undifferentiable visual landscapes or with variability arising from a more abstract level of detail, such as specific building components. Future approaches may thus benefit from incorporating aesthetic aspects, i.e. as learned from street view images.

Lastly, our approach is restricted to buildings for which 3D GIS models are available. With more regions and countries digitizing their building stock, and given the standardized approach to generate view metrics, it should however become feasible to extend our analysis and compare differences in view preferences across a more diverse building stock. Comparing results from two or

more regions with differing source 3D data may require additional data engineering to ensure reliability of results and consistency of labeling.

2.6 Conclusion

Evaluating visual landscape quality at large-scale has remained challenging. In this paper we have introduced a spatial machine learning approach to generate an income-derived building-specific measure of Visual Capital.

We identify that waterbodies, elements in the distance (>1km), and sky exposure are the strongest individual predictors of high-income. We further show a context-dependency of individual view metrics, with certain features gaining importance only in the presence of another.

We demonstrate the utility of this approach by estimating Visual Capital values for the entire Swiss building stock and investigating the inter- and intra-regional distribution in building-level Visual Capital, including view equity, and the agglomeration-specific degree to which view contributes to income-sorting. We further show that our composite measure of Visual Capital captures urban and natural form attributes, such as a non-linear relationship of view quality with terrain slope and building density. Lastly, we validate our work with a case-study. By clustering our building-level prediction of Visual Capital directly, we generate view-based boundaries that capture groupings of buildings with similar visual landscapes unbound by administrative boundaries.

Visual landscape quality, and changes to it, have a direct influence on urban planning, policy decisions and individual preferences. Yet, assessing and quantifying visual quality on a large scale remains a challenge. Overcoming this limitation, visual capital provides an easily accessible indicator of a building's visual landscape quality. It thus enables studies that aim to identify correlates with a 'good' view; improve automated real estate valuation models, or quantify the visual impacts of new landscape and urban development projects.

3 Automated Design Appraisal: Estimating Real Estate Price Growth and Value at Risk due to Local Development

Adam R. Swietek^{a,*}

^a Laboratory of Environmental and Urban Economics (LEURE), École Polytechnique Fédérale de Lausanne (EPFL), Lausanne, Switzerland

* Corresponding author: adam.swietek@epfl.ch

In Review at Sustainable Cities and Society

Swietek, A. R.*. “Automated Design Appraisal: Estimating Real Estate Price Growth and Value at Risk due to Local Development.” (2023) *arXiv preprint arXiv:2401.08645*

Abstract

Financial criteria in architectural design evaluation are limited to cost performance. Here, I introduce a method – Automated Design Appraisal (ADA) – to predict the market price of a generated building design concept within a local urban context. Integrating ADA with 3D building performance simulations enables financial impact assessment that exceeds the spatial resolution of previous work. Within an integrated impact assessment, ADA measures the direct and localized effect of urban development. To demonstrate its practical utility, I study local devaluation risk due to nearby development associated with changes to visual landscape quality. The results shed light on the relationship between amenities and property value, identifying clusters of properties physically exposed or financially sensitive to local land-use change. Beyond its application as a financial sensitivity tool, ADA serves as a blueprint for architectural design optimization procedures, in which economic performance is evaluated based on learned preferences derived from financial market data.

Keywords:

GeoAI, building performance simulation, design optimization, real estate price, machine learning

3.1 Introduction

In architectural design optimization, computer generated designs are iteratively evaluated with respect to building performance criteria. While building design concepts are commonly assessed for engineering performance, including structural resilience (Mayencourt & Mueller, 2019), environmental quality (Gagne & Andersen, 2012; Natanian & Auer, 2020) and energy performance (Natanian & Wortmann, 2021; Shi et al., 2017), as well as for cost performance, including material usage (Weber et al., 2022) and sustainability goals (Ameen et al., 2015; Elshani, 2021), current approaches have stopped short of considering the financial value of a given design directly, or more broadly speaking the preference thereof. The limited feedback between building design and real estate valuation models can be attributed to a lack of availability of simulations and pricing models with similarly specified attributes and parameters, in part due to the traditional separation of disciplines.

Most current studies in real estate economics utilize valuation models in specific geographic regions to infer the marginal price effect, or the price premium, of a given performance metric, including environmental amenities such as streetscape (Law et al., 2019), waterscape (W. Y. Chen et al., 2019), viewshed (Dai et al., 2023), building morphology (Rong et al., 2020), greenery (Yang et al., 2021), daylighting (Turan et al., 2020a), visual quality (Turan et al., 2021), and landcover (Baranzini & Schaerer, 2011). Yet, to our knowledge, no study has utilized these fitted models to predict the price of newly generated building and urban designs. This would require incorporating pricing models within a generative design or optimization framework or within a risk framework to assess the impact of attribute persistence: An example for the latter would be whether a desirable lake-view is exposed to future obstructions. The challenge arises from the need to additionally generate new building designs, and, for risk assessment studies, to compute the exposure to urban development or land-use change. While parametric design and building simulation are central to architectural design optimization (F. Jiang et al., 2023), limited access to relevant transaction data and model parameters,

hampers efforts to evaluate the preference or value of a generated design, as well its impact on the local context.

To overcome these challenges, this paper introduces an integrated workflow, an augmented valuation model called Automated Design Appraisal (ADA). The ADA algorithm incorporates computational design techniques to generate a city model based on design parameters; geometric computing to simulate building performance; and finally, a fitted econometric model that predicts the value of a building's design. The output is a single value representing the weighted economic preference of the individual attributes defining a single building design concept and its surrounding context. As a structured approach, ADA can be incorporated within various design analytic frameworks, including design optimization, or risk and impact assessment, by perturbing the initial design parameters and subsequently quantifying the effect size of an altered design scenario.

To demonstrate its usefulness, this paper implements ADA within the context of a visual impact and risk assessment. It presents results from two case-studies in Lausanne, Switzerland; (1) the impact due to a single proposed development and (2) the potential value at risk due to nearby land-use changes across an entire commune. Importantly, the effect size is assessed not only at the point of alteration, but also for nearby buildings to capture the imposed cost of a generated design, or put another way, the risk of neighbor property devaluation. The results illustrate the theoretical space of localized costs imposed on the neighborhood due to simulated design scenarios.

To assess both direct and localized effect sizes, it is important to choose an appropriate building performance metric by which to benchmark one urban design against another. Of the environmental performance metrics, a building's view or visual landscape is particularly relevant as high-quality views are considered inherently important to home prices (Ko et al., 2022; Roth et al., 2021). Moreover, visual obstructions and the subsequent risk of devaluation are primary drivers of objection to proposed developments by community members – a sentiment typically referred to as NIMBYism (**n**ot **i**n **m**y **b**ackyard) (Fischel, 2001). We

therefore use a building's Visual Capital (VC), a value that evaluates building level visual landscape quality, in our case study. VC is as an income derived, non-linear weighting of the visible share of landscape elements (A. R. Swietek & Zumwald, 2023), and, importantly, is derived directly from 3D building geometries and is thus sensitive to nearby design changes to the urban environment. Additionally, we fit a pricing model trained on transaction data, provided by Wüest Partner, learning the preferences for VC and other covariates, and subsequently apply this model to gauge the magnitude of change in predicted price with respect to changes in VC across our design scenarios.

The proposed methodology and impact analysis can be further extended to examine the cost/benefit of proposed urban infrastructure, optimized greenery layouts, as well as its effect on other location-based attributes. The proposed design appraisal offers insights into the direct gain and social acceptance of design choices, making it a tool for site-selection and feasibility assessments. Additionally, future design optimization studies can leverage ADA, by converting performance metrics into financial metrics, to aggregate building objectives into a single value, producing a preference ranking of the 'optimized' set of designs.

3.2 Literature Review

3.2.1 Economic Performance Metrics

In the context of architectural design, economic performance has been described as the evaluation of revenue, cost, and profitability (F. Jiang et al., 2023). Commonly used economic performance metrics focus on a cost minimization objective, such as the cost of pedestrian walking routes (Elshani, 2021), or the cost of lighting & heating (or space efficiency) (Baušys & Pankrašovaite, 2005; Weber et al., 2022). For example, Nagy et al utilize a profit metric to explore modular design solutions at the urban scale (Nagy et al., 2018). Using pre-defined values for selling price and project cost for each modular unit type, a generative design procedure produces a set of profit-optimized solutions. However, the approach has specific limitations: When a fixed selling price is applied, it overlooks the significance of the unique spatial qualities within the proposed design. This can

contradict the proven value of the design itself (Rong et al., 2020). In addition, the potential cost imposed on neighbors as a result of new development (Thibodeau, 1990) remains unexplored.

The few studies that have focused on evaluating the preference of a generated design primarily leverage satisfaction questionnaires (Brown, 2020; Villaggi et al., 2018; T.-K. Wang & Duan, 2023). Such stated preference approaches only describes the hypothetical preference which itself may be biased (Fifer et al., 2014). In contrast, revealed preference methods, such as the determining the willingness to pay by regressing attributes on transaction prices, describe actual economic decisions (Rosen, 1974), are considered a superior method to measure preference.

Thus, the current study contributes to the literature in two ways: it provides a new method that leverages revealed preferences using real estate transaction data to ascribe economic value of newly proposed designs, and it simultaneously estimates the economic impact of a design solution on its immediate urban surrounding. It thus allows to assess the devaluation risk due to land-use change.

3.2.2 Devaluation Risk

Devaluation risk, or potential decrease in the value of a property, is a major concern to property owners and lenders. Previous work primarily focused on the devaluation due to climate change (Stroebel & Wurgler, 2021). Typically, the effects of physical risks are estimated by using historical financial and environmental data; where natural disaster shocks, such as flooding (L. A. Bakkensen & Barrage, 2022; Holtermans et al., 2022; Ortega & Taşpınar, 2018; Ouazad & Kahn, 2019) and wildfires (Issler et al., 2020), are used to show persistent negative impacts on housing values. To understand the future and potential impact of climate change on real estate, the generation of hazard exposure maps is essential. For example, high resolution flood hazard maps for the year 2020-2050 (Bates et al., 2021) enabled subsequent studies to assess whether residential properties are over-priced relative to their flood exposure (Gourevitch et al., 2023).

Among the risks to real estate owners is property devaluation due to local land-use change (Fischel, 2001). For example, Thibodeau shows that the development of a high-rise building had a negative effect on the property values of adjacent neighbors (< 2,500 meters) (Thibodeau, 1990). At such a local scale, it is possible to compute exposure maps by leveraging computational design, urban analytics, and micro-climate simulation methods, including energy modeling (Natanian & Wortmann, 2021), solar irradiation (Nault et al., 2015), daylighting (Gagne & Andersen, 2012), and visibility (Florio et al., 2021). Past studies have leveraged these simulations and applied the hedonic pricing model (Rosen, 1974) to assess the marginal price effect of micro-climate performance on real estate valuation (Baranzini et al., 2006, 2008; Inglis et al., 2022b; Turan et al., 2021). Yet, unlike the future flood risk projections example, local risk evaluation methods stop short of examining the sensitivity of a set of building valuations across future urban design scenarios. Thus, this paper extends the literature by taking advantage of a key feature of geometric data, that differentiates it over other urban data types: its mutability. Specifically, a sensitivity analysis which can be applied to generate new design scenarios and to automatically assess the impact of design perturbation on property values.

3.2.3 Visibility Simulation and Visual Capital

Of the factors that drive property devaluation risk, visual impact resulting from land-use change is of particular concern to NIMBYs (Fischel, 2001; Thibodeau, 1990). This concern is driven by the significant influence of attractive views on property values (Dai et al., 2023; Inglis et al., 2022b; Ko et al., 2022; Li et al., 2022) and the localized effect of visual obstructions (Thibodeau, 1990). Views encapsulate an abstract summary of the urban environment from a single perspective, making it easier for individuals to notice changes in the landscape aesthetics compared to aspects such as noise or air pollution. Yet, despite the importance and attention paid to visual impact assessment (Cilliers et al., 2023) and visual landscape research more broadly (Inglis et al., 2022b), access to a structured 3D approach to evaluate visual landscape at the building-level has only

been achieved recently, in the form of the Visual Capital (VC) index (A. R. Swietek & Zumwald, 2023).

The computation of the VC index is composed of three essential parts: (1), the viewpoint visual share simulation, (2) a set of aggregation functions defining building view-metrics, and (3) a machine learning model that predicts net-income, with the latter serving as a proxy for economic preference based on the concept of amenity-based income sorting (Gagné et al., 2022; Vukomanovic & Orr, 2014). The viewpoint visual share simulation leverages the raycasting algorithm originating from a set of façade points to determine the ‘visible’ part of a 3D city model, and recording the attributes of the intersected ray, including distance, obstructions, and landcover category. The generated viewpoint visual share dataset indicates what landcover categories are visible and in what proportion from a single viewpoint, before being aggregated to the building-level. Specifically, viewpoints are grouped by their associated building and a series of aggregation functions are mapped, resulting in a set of 57 view-metrics describing the spatial composition and configuration of visible landcover elements for each building. View-metrics include average sky exposure, maximum visual share of nature, visual access to lake-view, balance of elements in distance, richness of panorama, among others. A neural network then estimates that weighted importance of these building view-metrics in predicting the commune average net-income. And finally, applying the fitted model to out of sample visual share data produces a building’s VC index.

Unlike other view-based building performance metrics, VC is a single value and can be easily integrated within pricing models to determine the price-amenity gradient. In addition, it can easily be derived for newly generated design scenarios, thus providing a direct link between design performance evaluation (the view) and pricing.

3.3 Material and Methods

Automated Design Appraisal (ADA) is the application of a fitted pricing model to evaluate the economic preference of multiple design metrics. We demonstrate the

applicability of ADA by integrating it within a devaluation risk assessment focused on the potential visual impact of a simulated urban development. The workflow includes three parts: (1) pricing model (2) design simulation and (3) parametric design generator. To identify the potential financial impact, we measure the difference in predicted price between the simulated urban design scenarios (*alt*) and the as-built design scenario (*ref*).

3.3.1 Pricing Model

To analyze the relationship between the design attributes of a generated design scenario and real estate sale transactions, I use the hedonic pricing model. The commonly used approach in real estate economics literature quantifies the revealed preference, or the buyer's willingness to pay, for a given characteristic. These building characteristics includes immutable attributes, including year of transaction, year of construction, etc., as well as mutable attributes, which are the variables of interest within parametric design and design evaluation. Eq. 1 presents the functional form of the specified model,

$$\ln(P)_i = \beta_0 + \beta_1(VC)_i + \beta_3(L)_i + \beta_4(M)_i + \beta_5(S)_i + \beta_6(T)_i + \varepsilon_i \quad (1)$$

where the dependent variable $\ln(P)$ is the natural logarithm of the transacted sales prices for building observation i . In this paper we are interested in quantifying the price sensitivity with respect to visual impact, thus we use Visual Capital (VC) as the variable of interest. L is a vector of exogenous location characteristic, including the log-scaled distance to water bodies. M is a vector of neighborhood level characteristics, such as macro-location (Djurdjevic et al., 2008). T is a vector representing time fixed effects, i.e. year of transaction, and ε_i is a vector of the unobservable characteristics.

Given the importance of water-bodies on property valuation and on VC, we further limit the training sample to transactions of buildings located within agglomerations in proximity to a major lake, i.e. Biel/Bienne, Zurich, Lausanne, Geneva, Vevey–Montreux, Luzern, Thun, Neuchatel, and Zug. To control for differences between these urban regions of Switzerland, we condition a building's

VC on agglomeration identity. Transaction data, including 7,651 sales transactions from years 2008 to 2017, and exogenous data points were provided and anonymized by Wüest Partner in compliance with Swiss privacy laws.

3.3.2 Design Simulation

A building's design performance is measured with respect to its visual landscape quality.

3.3.2.1 City Model

To evaluate a building's visual landscape, I first construct a Digital Twin, or 3D city model, using three separate publicly available databases: representing terrain, buildings, and vegetation (Federal Office of Topography swisstopo, 2018a, 2018b; *Vegetation Height Model NFI - 2019 Vegetation Height Model NFI (Current) - EnviDat*, n.d.). The composed city model provides a 3D digital representation of the building stock and is used as the reference scenario (*ref*). Importantly, due to the mutability of 3D data we can subsequently alter the input geometries to represent design changes. The swissBUILDING3D database provides separate 3D geometries for a building's facade and roof, which allowing the modification of the height of an individual building, e.g. add a story, without distorting the roof. The altered design parameters thus lead to a slightly modified city model (*alt*). To represent different design scenarios, I compile a set of structured design alterations that can be compared against one another and against the reference scenario.

3.3.2.2 Performance Metrics

Using the compiled city model, a viewpoint visual share dataset is generated and subsequently used to compute a range of view-metrics and the Visual Capital index, as described in Swietek et al (A. R. Swietek & Zumwald, 2023). Specifically, I compute viewpoints for J buildings (B) indexed by j . The j -th building has n viewpoints (B_{jn}) situated on its façade, spaced apart by 8 meters across each floor. Importantly, only exterior walls are considered. For instance, in the case of two buildings joined by an interior wall (e.g. row of townhomes) they are considered as single joint structure. For each viewpoint B_{jn} with $n = 1, 2, \dots, n$, a 120-degree view

cone composed of 2600 rays is cast outward and the endpoint of intersection within the city model is recorded. The count of rays intersecting the same $l = 1, 2, \dots, 20$ landcover categories at $d = 1, 2, \dots, 4$ distance categories are summed and divided by the total number of rays (i.e. 2600), generating the visual proportions for B_{jn} denoted by z_{ld} . Visible proportions of landcover data for building j are thus represented by a $(n \times 20 \times 4)$ array, denoted by Z_j . The values are derived from the swissTLM3D, COPERNICUS databases, describing whether the view is obstructed by a façade, roof, or vegetation; as well as the distance to visual elements. This procedure is referred to as the viewpoint visual share simulation, or visibility analysis. Next, the generated viewpoint visual share dataset is used to aggregate the land-use proportion viewpoint values to building level view metrics (for details see (A. R. Swietek & Zumwald, 2023)). This results in 57 view metrics describing the visual landscape for a given building, e.g. maximum share of lake-view, sky exposure, etc. Lastly, to generate the Visual Capital index, I apply the pre-trained neural network, from Swietek et al, to the newly constructed vector of view-metrics.

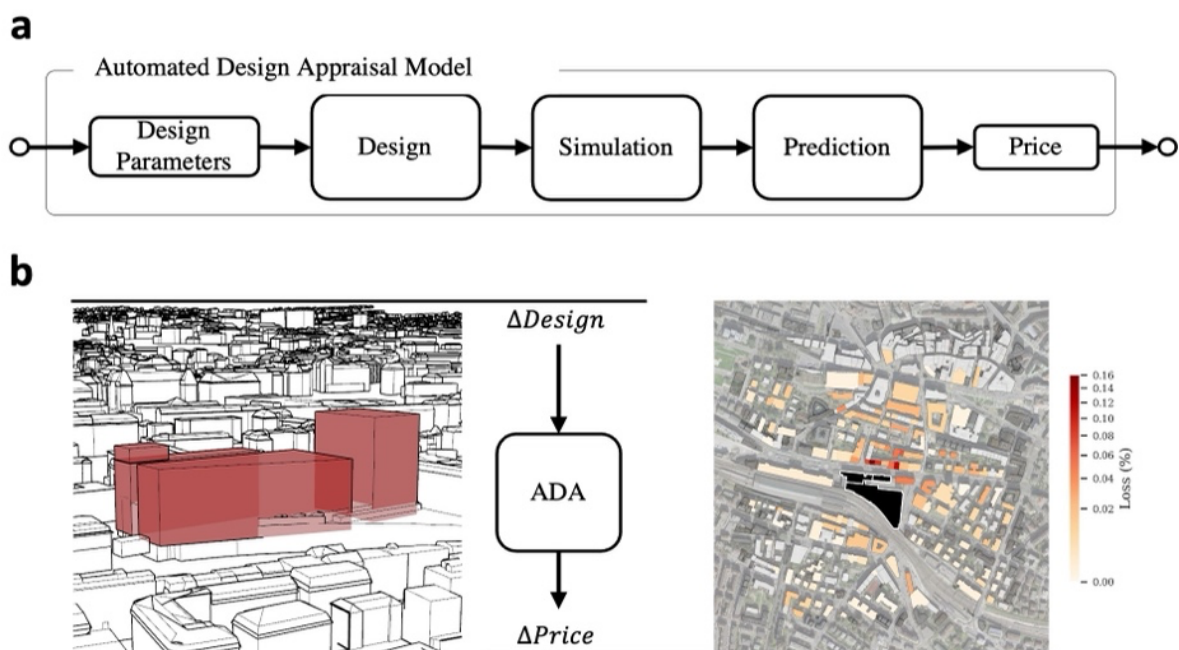


Figure 12 (a) Abstract schematic of the proposed Automated Design Appraisal algorithm: step 1.) define the set of design parameters of interest; step 2.) update buildings within 3D city model according to design parameters, thereby creating an alternative design scenario; step 3.) compute building performance metrics

using building and micro-climate simulations – in this paper, we utilize a viewpoint visual share visibility simulation to generate a set of view-metrics and subsequently calculate the visual landscape quality, i.e. Visual Capital; step 4.) update vector of building attributes to include new performance metrics; step 5.) use fitted model to predict price of building with updated performance metrics. (b) Abstract schematic showing the application of ADA for a visual impact assessment in Lausanne. The proposed development, shown in red, represents the point of modification within a reference 3D city model. The spatial distribution of price impact, computed via ADA, is shown, with darker red representing greater impact on a building's predicted price.

3.3.3 Integrated Impact Assessment

The determinants of risk are the degree of exposure and sensitivity to a given hazard (IPCC, 2023). In the context of this paper, a hazard is a proposed building development that may obstruct the view and degrade the visual landscape quality of nearby buildings. As such, I propose two case-studies: an impact assessment of a single hazard, and of multiple hazards.

To measure the exposure of building j to changes in the urban form, we can iteratively perturb the underlying city model denoted by s^{ref} thereby creating a set of new design scenarios of length S , and measure the persistence of the performance values. The design evaluation procedure consisting of M metrics (here $m = 1, 2, \dots, 57$ view metrics) applied to building j derived from the context of design scenario s , results in a $M \times J \times S$ matrix V^{alt} of design performance values. To express the impact or change in performance metrics in a given building,

$$\Delta V = V^{alt} - V^{ref} \quad (2)$$

Where $\Delta V(m)$ is a $J \times S$ matrix and $V^{ref}(m)$ is a vector of length j , describing the design performance values of metric m in the as-built design scenario s^{ref} across all included buildings j . To standardize the impact to represent the relative change,

$$\Delta V^{rc} = \frac{\Delta V}{V^{ref}} - 1 \quad (3)$$

Thus, $\Delta V(m)_{j_s}^{rc}$ describes the relative change in the value of metric m for building j due to the proposed project s . To express the maximally exposed metric, I take the metric with the largest change for each building and scenario

$$MEVM_j = \text{Max}_M (\Delta V(m)_{js}) \quad (4)$$

To derive the impact on predicted price ΔY , I take the difference in the predicted prices of building j . Where Y is a $J \times S$ matrix. The predicted price is calculated by applying the previously development pricing model to the sample region with updated values for building performance values, V^{alt} . Further, to identify the financial impact due to the effect on a building's visual capital, I simplify the price impact equation by assuming no change across the other building's attributes. Thus,

$$\Delta Y = Y^{alt} - Y^{ref} \approx \beta_{vc} \Delta V(VC) + \varepsilon \quad (5)$$

3.3.3.1 Single Development

The first case study examines the potential visual impact of the Rasude Development within a .5km radius of a proposed 15-story office project near the Lausanne train station (*La Rasude reprend vie au cœur de Lausanne.*, n.d.; *Quartier Rasude à Lausanne – Quinze Étages, «c'est Un Cadeau Aux Promoteurs»*, 2023). Thus, one new design scenario s^{alt} is a modified city model containing the proposed Rasude Development. The proposed massing, containing three distinct structures (*L'association Perirasude*, 2023), is designed in Rhinoceros 3D and added to s^{ref} replacing the existing structures. Next, the design performance simulation with respect to a building's visual landscape quality is initiated (described in section 3.1.2) and spatial view metrics are calculated for both design scenarios.

3.3.3.2 Regional Vulnerability

The second case study pertains to assessing the risk of multiple hazards, the spatial distribution of vulnerability to land-use changes within a sample region. Unlike the first case study, it incorporates multiple design scenarios and contrasts the potential gain in value of the up-zoned building to the potential losses in value of its neighboring buildings. Specifically, using the process iteratively modifies each building in a sample by adding 1 floor (i.e. 5 meters) to the existing building structure. Thus, in a sample region of 204 buildings index by j , this design

augmentation results in 204 alternate design scenarios indexed by s . Using this set of design scenarios, we next compute the visibility performance of buildings in the sample region. Importantly, for each iteration, we dynamically limit the sample region to the point of modification and its nearest 9 buildings. This helps to reduce the compute time, while maintaining the buildings expected to be most vulnerable to the change within a sample. As a result of this procedure, 2244 design performance simulation were executed: where in addition to the reference design scenario (no modifications), the 204 buildings were modified and the visual impact of each modification was assessed either from the perspective of the modified building itself or from the perspective of each of the nearest 9 neighboring buildings. This results in a sparse $J \times S$ matrix ΔV , where each design scenario corresponds to a specific modified building. Hence diagonal entries of the matrix of ΔV represent the impact of the modification on the building itself, or direct effect (DE). DE is a vector of size J that represent the increase (benefit) in a given metric at the modified site.

$$DE(m) = \Delta V(m), \text{ where } s = j \quad (6)$$

Whereas the off-diagonal entries represent the impact of a modification on nearby neighbors, defined as local effects (LE).

$$LE(m) = \Delta V(m), \text{ where } s \neq j \quad (7)$$

As LE maintains a two-dimensional representation, we additionally compute a vector of cumulative local effects and exposure to local effects. Cumulative local effects (CLE) illustrative to collective impact of a single modification on its neighboring buildings.

$$CLE_s(m) = \sum_j \Delta V(m)_s, \text{ where } s \neq j \quad (8)$$

On the other hand, exposure to local effects (ELE ; from the perspective of an unaltered neighbor) denotes the maximum change experienced across all design scenarios s . Put another way, this indicates the potential value at risk attributed to simulated land-use changes in the vicinity of a building.

$$ELE(m)_j = \text{Max}_s(\Delta V(m)_j), \text{ where } s \neq j \quad (9)$$

Figure 13 illustrates the spatial distribution via impact maps portraying maxVSH: Sky, the maximum proportion of sky visible from a single viewpoint. Further, an abstract graph network represents the relationship considered across the impact assessment metrics: ref, DE, CLE, and ELE metrics.

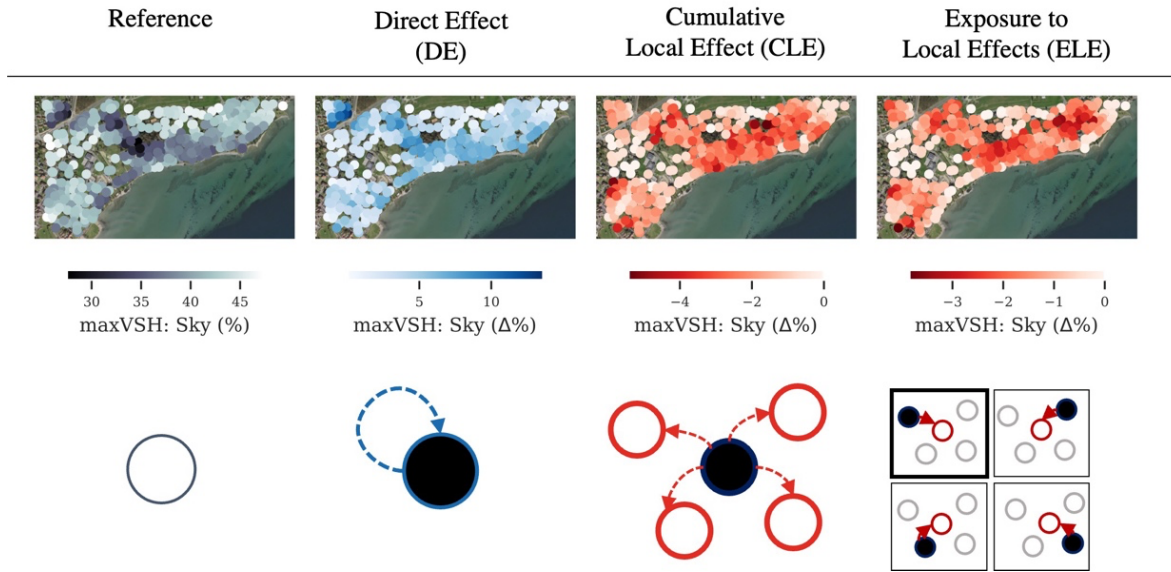


Figure 13: Spatial distribution and abstract representation of the integrated impact assessment metrics used to visualize the distribution of impacts on maxVSH Sky, i.e. the maximum visible proportion of sky from a single viewpoint across all of a building's viewpoints. Reference is the as-built condition of the city, Direct Effect (DE) express the gain in Sky Exposure as a result of the up zoning, Cumulative Local Effects (CLE) describes the gross cost imposed on its neighbors due up zoning at a given building, and Exposure to Local Effects (ELE) expresses the maximum potential loss across all of the unzoning scenarios tested.

3.4 Results

3.4.1 Value of a View

We carry out a hedonic regression to understand the net effect of each included variable (see Methods) in predicting the sales transactions of included buildings. We are particularly interested in the coefficients for Visual Capital, as this learned parameter will drive variability across our integrated impact assessment tool. Table 8 shows parameter estimates across four pricing models where the natural logarithm of transacted prices is used as the dependent variable. We test four specified models (Table 1) to understand the interaction of Visual Capital across

two different location-based scenarios, fitting VC independent (model 1 and 3) or dependent (model 2 and 4) on the agglomeration buildings are located in. In addition, each location-based model excludes (model 1 and 2) or includes (model 3 and 4) agglomeration and a macro-location indices (Djurdjevic et al., 2008) provided by Wüest Partner. The difference between the first and second model (as well as between third and fourth model) helps identify the variable importance VC has across agglomerations. The third and fourth model additionally control for a set of important covariates, including a macro-location index which describes desirability across communes. Thus, the difference between the third and fourth model, highlights the spatial variability of VC after controlling for both building- and macro-level covariates. Importantly, the ranked coefficients for agglomeration-specific VC remain consistent whether macro-location indices are included or not. A similar trend is observed for all model coefficients when comparing the third and fourth models, with the one notable exception being the coefficient associated with the macro-location indicator. This suggests that part of the index is explained by agglomeration-specific VC. The fully specified model, shown in column (4), indicates that the model explains up to 81% of the variability in sales transactions, and, relevant to this study, indicates that Visual Capital has a positive influence on price in the Lausanne agglomeration used for the two design scenarios.

Table 8: Regression results across four models, where the dependent variable is the natural logarithm of the transacted price. Column (1) presents the regression results of the model that includes only the variable of interest, visual capital (VC). Column (2) presents the results of the model containing VC conditional on the agglomeration. Column (3) incorporates the fully specified model with an unconditional VC . Column (4) presents results for the fully specified model with VC conditioned on lake-side agglomeration. Robust standard errors are shown in brackets and statistical significance is denoted at the following levels *** $p < 0.01$, ** $p < 0.05$, * $p < 0.1$.

Parameters	(1)	(2)	(3)	(4)
<i>Intercept</i>	-50.62*** [3.85]	-46.92*** [3.48]	-55.47*** [3.03]	-61.87*** [2.79]
<i>VisualCapital(VC)</i>	1.62*** [0.04]	-	0.27*** [0.03]	-
VC: [Biel/Bienne]	-	1.39*** [0.04]	-	0.29*** [0.03]

Parameters	(1)	(2)	(3)	(4)
<i>Intercept</i>	-50.62*** [3.85]	-46.92*** [3.48]	-55.47*** [3.03]	-61.87*** [2.79]
<i>VisualCapital(VC)</i>	1.62*** [0.04]	-	0.27*** [0.03]	-
VC: [Genève]	-	1.54*** [0.04]	-	0.37*** [0.03]
VC: [Lausanne]	-	1.5*** [0.04]	-	0.35*** [0.03]
VC: [Luzern]	-	1.5*** [0.04]	-	0.34*** [0.03]
VC: [Neuchâtel]	-	1.42*** [0.04]	-	0.3*** [0.03]
VC: [Thun]	-	1.42*** [0.04]	-	0.32*** [0.03]
VC: [Vevey– Montreux]	-	1.49*** [0.04]	-	0.33*** [0.02]
VC: [Zug]	-	1.59*** [0.04]	-	0.4*** [0.03]
VC: [Zürich]	-	1.54*** [0.04]	-	0.39*** [0.03]
<i>Year_{TRANSACTION}</i>	0.03*** [0.0]	0.03*** [0.0]	0.03*** [0.0]	0.03*** [0.0]
<i>logVolume</i>	-	-	0.37*** [0.02]	0.39*** [0.02]
<i>N. Rooms</i>	-	-	0.06*** [0.0]	0.05*** [0.0]
<i>Condition</i>	-	-	0.05*** [0.0]	0.05*** [0.0]
<i>FitoutStandard</i>	-	-	0.16*** [0.0]	0.14*** [0.0]
<i>logDistance_{SEA}</i>	-	-	-0.05*** [0.0]	-0.08*** [0.0]
<i>Age</i>	-	-	0.15 [0.33]	0.34 [0.3]
<i>logPlotArea</i>	-	-	0.13*** [0.01]	0.18*** [0.01]
<i>logMacroLocation</i>	-	-	0.67*** [0.01]	0.4*** [0.01]
Adj. R-squared	0.21	0.36	0.76	0.81
Observations	7651	7651	7651	7651
R-squared	0.21	0.36	0.76	0.81

Figure 14 provides an illustration of the varying price effect of VC across lakeside agglomerations. Additionally, it shows the range of VC values used to train model

4. Lausanne, displayed in red, has the fourth largest coefficient, and third largest maximum VC range.

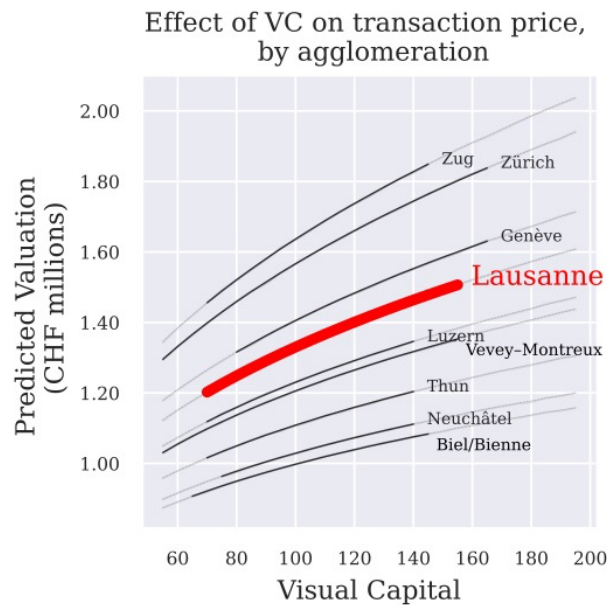


Figure 14: Price Effect of Visual Capital by agglomeration while holding the other model parameters constant. The black line represents the actual range of values used during model training. For comparison, Lausanne (the agglomeration used in the case studies), is shown in red.

The remainder of the paper describes results from two case studies which apply the fitted pricing model: (1) the local visual impact on neighboring buildings due to a single proposed development in central Lausanne, and (2) the visual capital at risk due to localized up-zoning in the commune of Saint-Sulpice.

3.4.2 Single Hazard

The proposed 15-story Rasude development negatively impacts the visual metrics of 50% of buildings within a 500m radius. To understand the extent of visual impact, the largest relative loss across all view-metrics – the maximally exposed view metric (MEVM) – is computed and summarized across all buildings. Figure 15 illustrates that approximately 65% of the buildings have a MEVM of less than 1% relative change and that impact on both MEVM and prices are highly concentrated. Figure 15b shows among the most common negatively exposed view-metrics is sky-exposure, proportion of distant views (>1km), as well as the maximum share on water-body, industrial complexes, and nature, with each being impacted in some capacity for 20% of the sampled buildings. As expected, there are positive gains in view-metrics related to façade and near distance obstructions. Note, that the largest relative losses are for scarce view-metrics, such as

distant views and water-bodies; and the largest absolute changes are for more abundant view-metrics, such as sky-exposure.

To understand how price impact is distributed, I compare the aggregate valuations across all buildings in the sample region. Figure 15c illustrates that 44% of aggregate value lost is held by only 4% of the neighbors. They individually have losses greater than 5%, where the most price sensitive building lost 16% of its original valuation. Nearly 40% of the building stock account for the majority or 63% of aggregate value lost, where each individual loss is between 0-5% of the initial valuation (Figure 15c). Interestingly, 8% of the buildings sampled gain value as a consequence of the change in urban form. An analysis of this building subset shows that they benefit from the development of the sky-line. Specifically, the minimal obstruction of positive views with an increase in the visual complexity of the panorama, results in a gain in visual capital, and, in turn predicted price (Figure 15).

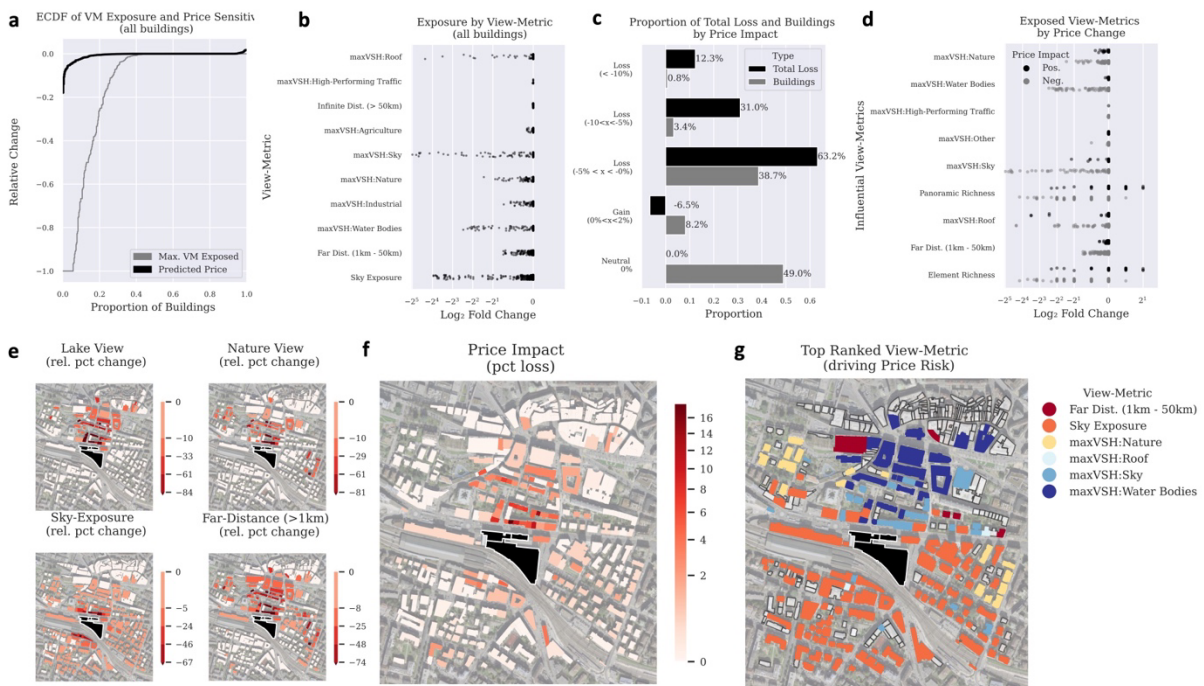


Figure 15: (a) ECDF of relative change of maximally exposed view-metric and predicted price for all buildings in the sample region. Maximum visual impact is defined as the maximum relative change across a building’s vector of view-metrics between the two design scenarios. Heavily skewed distribution indicates concentrated losses. (b) Summary of log fold changes of view-metrics for all buildings between two design scenarios, the design scenario with the proposed development versus the baseline, as-built condition. (c) Barplot of the

proportion of aggregate value lost for each level of price sensitivity, relative to the sample share of corresponding buildings. (d) Dot plot comparing the exposed view-metrics of buildings with Positive and Negative price sensitivity, suggesting some building benefits from additions to the ‘Sky-Line’ (Panoramic and Element Richness). (e) Series of effect-size maps following the developed method: 4-view metrics (lake-view, nature view, far-distance, and sky-exposure). (f) Effect size map of the predicted price impact the proposed development site has on neighboring buildings (development shown in black). (g) Top ranked view-metric contributing to price risk at a given building.

The spatial distribution of price impact expands radially from the proposed development site, yet, a disproportionate share of the aggregate losses is held by the adjacent neighbors to the north (Figure 15f). Figure 15e shows the spatial distribution of effect size for the sample regions for individual view metrics. As expected, the spatial pattern of exposure varies by view-metrics; contingent on the location and abundance of landcover elements. For instance, impacted lake-views are exclusively to the north of the development site (Lake Geneva is directly south on the development site); and impacted nature views are additionally found in pockets in the east and north west of the sample region (Jura Mountains to the west, Swiss Alps to the east, and French Alps to the South); whereas a radial impact zone appears for sky-exposure. Using the weighting importance of view-metric in estimating visual capital, Figure 15g depicts the metric most responsible for driving the change in predicted price. For examples changes to desirable visual qualities – e.g. lake-views, are the driving determinant for the high price impact region.

3.4.3 Multi Hazard

Results from the regional simulation of up-zoning each building in the commune of Saint-Sulpice by one additional floor confirm that neighboring buildings face devaluation risk caused by nearby developments, with estimates as high as 5% of value lost for individual buildings. Despite the predicted price exposure to local effect (ELE) of individual buildings, the direct effect (DE) of most simulated single-story additions results in aggregate housing price gain even after accounting for the cumulative local effects (CLE).

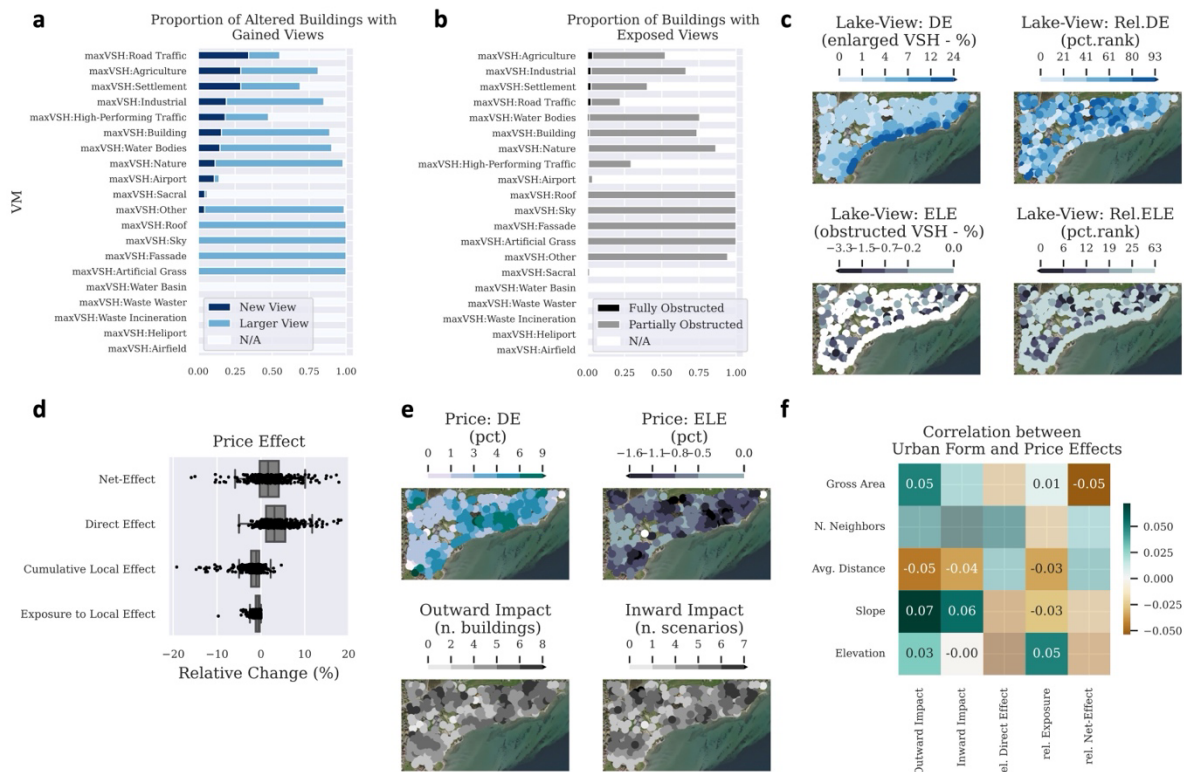


Figure 16 Barplot of the share of (a) altered buildings with newly gained or enlarged existing views (direct effects) of specific landcover elements. (b) Share of exposed buildings with partial or full obstruction by view metric. (c) Spatial distribution of Lake-View direct effects, relative direct effect ranks, local exposure, and relative exposure ranks. (d) Boxplot of the Price effect across all design scenario; including direct (DE), cumulative local (CLE), exposure (ELE), and net effect. (e) Spatial distribution of Price Effects (DE and ELE); illustrating spatial variability of the number of impacted building to a specific hazard and the count of hazards a building is exposed to (Visual Risk). (f) Correlation plot of price effect metric and Urban and Environmental form attributes, with correlation values shown for significant values $p < .05$.

For direct effects (DE) at the site of alteration, the majority of absolute gain is defined by the enlargement of already visible abundant landcovers: vegetation, sky, mid-distance (Figure 16a). The most common new views, or the landcover elements not visible prior to the alteration, are local roads, industrial areas, and agriculture. Of the exposed views: landcover area identified as local roads, industrial areas, and agriculture are most at risk of complete obstruction. Figure 16b shows that abundant view-metrics account for the majority of partial obstructions: including sky exposure and vegetation. The average loss of the maximally exposed view-metric (MEVM) is 10%, whereas 15% of the sample risks completely losing its maximally exposed view-metric. Additionally, potential visual impact is a function of the development’s location. Despite the large DE and

CLE values, the majority of change is explained by abundant and negative sentiment; desirable views account for smaller proportion due to their scarce nature and as such exhibit spatial patterns in change. Figure 16c maps the spatial distribution of lake-view changes, showing that buildings along the shoreline enlarge their lake-view the most, and inland buildings have the greatest relative gain. Whereas the exposed lake-views are distributed in two distinct pockets on the west and eastern edges of the commune. Thus, even though changes to individual view-metrics provide insight to the extent of exposure, they alone do not describe the overall impact, as the importance of the metric, or sensitivity to change in value, have not been accounted for. The following section describe results in terms of price, which can be thought of as weighted combination of building performance metrics according to the learned market preferences.

3.4.3.1 Price Risk

The automated design appraisal model (ADA) captures the price effect with respect to a given design change. The average direct effect of single floor additions in Saint-Sulpice result in a 4.4% price improvement, whereas the highest ranked building gains 12.5%. Interestingly, the rank of direct effect, or price gain, is weakly negatively correlated to both the rank cumulative local effects (CLE), i.e. social cost imposed, and exposure to local effects (ELE), or price vulnerability to local changes. Considering price change, the cumulative local effect (CLE) remains small compared to the direct effect (DE), i.e. price effect at the point of modification effect. Figure 16d shows that the vast majority of design scenarios are a net-positive for Saint-Sulpice, with only 5 locations where the DE is less than the cost imposed through visual obstructions to neighboring buildings. Figure 16f maps the spatial distribution of price changes, showing several distinct pockets of buildings along the shoreline with the largest relative gain in value. Yet, the spatial distribution of value at risk does not follow the same spatial pattern, with multiple clusters forming for both inward and outward impact Figure 16e. To examine the apparent spatial pattern found in the analysis, I subsequently examine the relationship of price impact with characteristics of the urban and natural form. Figure 16f illustrates the correlation between the price effect metrics

and urban environmental form metrics, such as slope, building density, elevation, and spread. Although correlations are weak, they are significant, suggesting that, on average, urban form influences the price effect of simulated modifications. For example, buildings in low-density areas, greater distance to neighbors, correlates with larger benefits to alterations (DE) and smaller value at risk (ELE).

It is additionally useful to understand the individual factors, in this case the view-metrics, driving the spatial patterns in both price gain (DE) and value at risk (ELE) within the region. To examine this, Figure 17 depicts the change in a common set of view-metrics from two properties: one from a region of high price gain (DE), and another from a region of high price vulnerability (ELE). The first property (EGID 796374), sees benefits from the alteration, such as a new lake-view, and increased view of nature with little risk to its view-metrics from neighboring local development. However, the second property (EGID), has its 4% visual share of the lake at risk of obstruction due to a single neighbor's alterations, moreover its view share of nature is at risk of obstruction by multiple potential local developments.

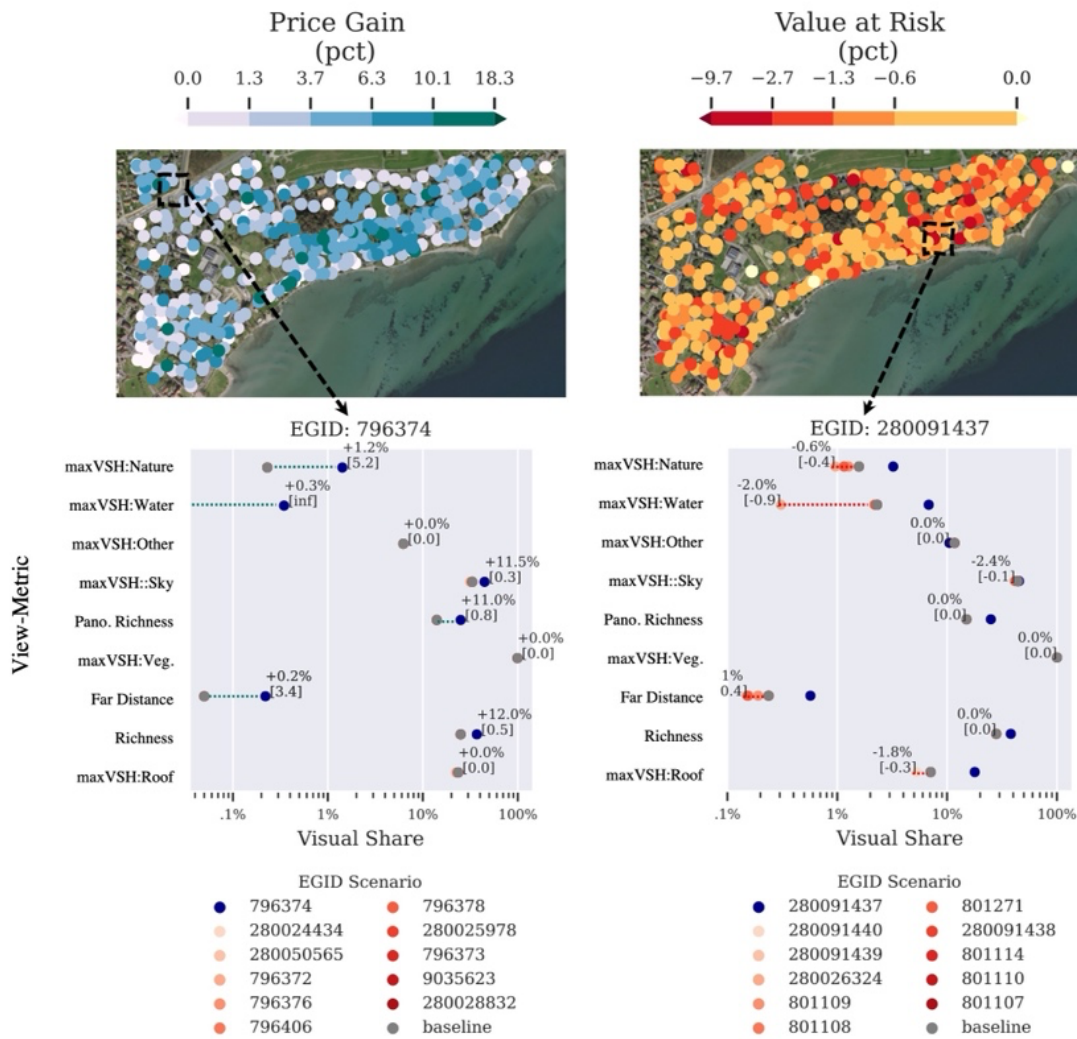


Figure 17: Change in top weighted view-metrics for 2 separate properties, EGID 796374 from a region of high price gain and EGID 280091437 representing a region from high price risk. Points in grey represent the values for the reference scenario, or as-built condition; Blue points represent visual share value after alteration at the property; and the set of Red points represent the values after the modification it's set of neighbors. Change in visual share (%) of view-metric is expressed for DE with green dashed line, and ELE with red dashed line. The relative change in listed in brackets. For example, the maximum visual share of water (maxVSH:Water) for EGID 280091437 in the reference scenario is ~2.3%; whereas it drops to .3% when EGID 280026324 builds up an addition floor, and rises to 8% when EGID 280091437 itself build up an additional floor.

Summarizing the metrics driving price gain and risk, Figure 18 depicts the ranked feature importance for both price gain and risk across all buildings. For Saint-Sulpice, maxVSH of water-bodies is the primary determinant of price gain for most site alterations (Figure 18a,b), and is a within the top 3 factors for nearly 60% of the building stock (Figure 18c). For price risk, due to the long coast, proportionately few buildings have exposed lake-views, thus metrics related to sky

exposure, such as the maximum visual share of sky, are more commonly the primary determinant of price risk to single-story up-zoning in Saint-Sulpice (Figure 18d,f), with exception of properties along the coast, where the gained façade (within Neutral Sentiment index) and lost view of roofs play a bigger role (Figure 18e).

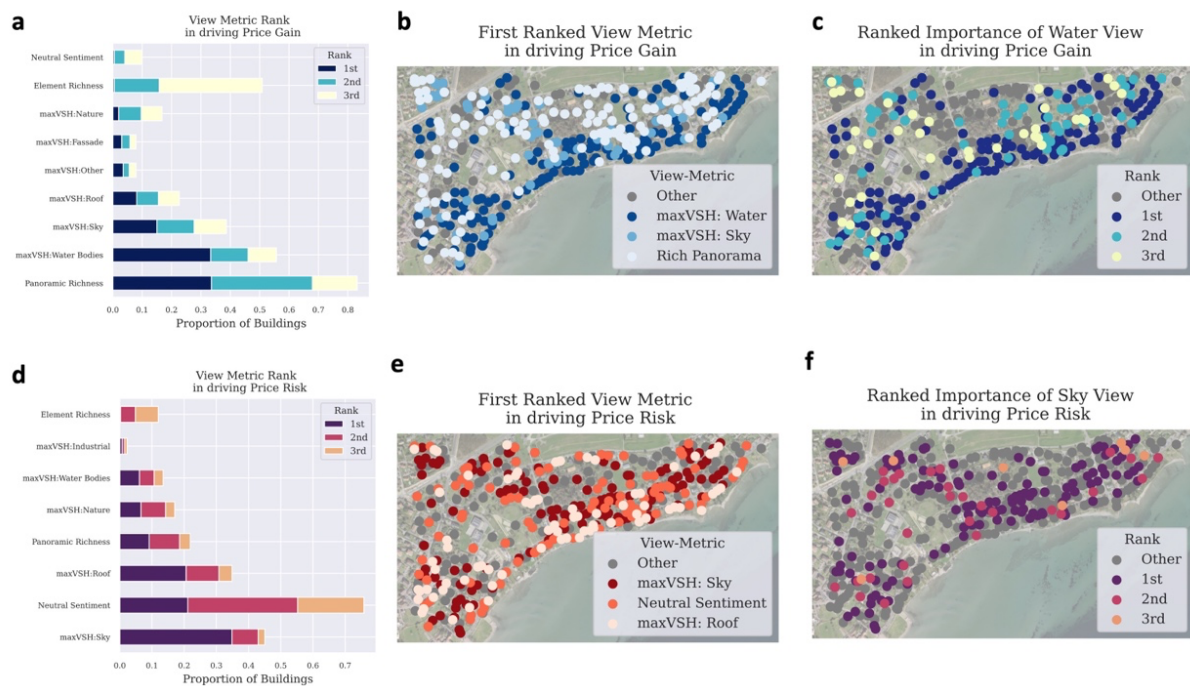


Figure 18: Predictive importance rank of view-metrics in driving (a) price gain and (d) price risk as a proportion of buildings. (b+e) Maps illustrate the spatial distribution of the first ranked view-metric, and the spatial distribution of (c+f) of the view-metric with largest impact on price: (c) maximum visual share of water and (f) and maximum visual share of sky

3.5 Discussion

Integrating large scale geometric computing with econometric methods offers an opportunity to infer the price effect of a proposed design alteration. Hence: this paper extends the literature in two ways: First, it presents a novel approach to estimate the financial value of procedurally-generated designs, which I refer to as Automated Design Appraisal (ADA). Second, it incorporates the ADA algorithm within a 3D urban design simulation to measure devaluation risks with respect to design changes. Further, focusing on the urban scale enables the quantification not just of the benefit of a given development at the site of modification, but also

of the local vulnerability to the proposed development, i.e. the cost imposed on neighbors by the point of modification.

ADA relies on the assumption that the price of a building is the weighted sum of its individual attributes, also known as the hedonic price theory (Rosen, 1974). Though, unlike the vast hedonic pricing literature, this study takes the additional step to apply the fitted models to newly generated building and urban designs. Utilizing computational design and large-scale 3D geodatabases, the as-built city model is systematically perturbed by altering design parameters, thereby creating new urban scenarios. A subsequent analysis of the price changes relative to the initial as-built conditions help to confirm that urban land-use change has localized impact affecting nearby neighbors to a greater extent. An important aspect of this approach is its interpretability. It is possible to not only explore the impact at the point of modification and nearby buildings; but also understand the determinants of the underlying risk. The latter is achieved by investigating the persistence of specific exposed building attributes— such as lake-view, nature-view, sky-exposure, etc.- and the aggregate valuation at risk due to these specific exposures. A common objection to local development is the immediate impact on visual landscape, which supports the use of Visual Capital in this study; however, future studies may extend this method by focusing on other environmental attributes, including noise pollution, thermal comfort, and air-quality, which are commonly used to raise objection to developments by the NIMBY movement, or more generally communities opposed to local development. Thus, this approach may prove beneficial to local communities interested in quantifying and communicating the visual and environmental impact in terms of local real estate valuation.

A streamlined method to infer the price of computer-generated designs may provide further benefits: Generative Design tools may particularly benefit from ADA. Generative Design in architecture is an iterative design process that outputs feasible building designs under specified optimization functions. The proposed algorithm, ADA enables two new types of objective functions for architectural design optimization. First is optimizing valuation, whereby converting building

attributes into monetary terms allows Generative Design procedures to (1) quantify the importance of non-market goods, e.g. environmental quality such as the view, and (2) weigh tradeoffs between seemingly disparate building attributes (e.g. visual quality and programming). The second opportunity, is optimizing for social cost or the cost imposed on its nearby neighbors. It can be reasoned that developments which minimize the localized cost (whether gross cost or count of neighbors negatively impacted) also minimize the risk of local opposition. Evaluating the distribution effects- both direct and localized cost- could be particularly useful for urban planners and property developers who perform pre-development site selection and feasibility studies.

Although the method could be useful for both design optimization and distribution effect exploration, the approach does have its limitations. As with all hedonic analyses, inference is dependent on the specified model. Given that building attributes are highly correlated, results and parameter selection should be approached with care and scrutinized to assure meaningful interpretation. In this paper I study the distribution of price effects of urban development on visual impact. Thus, our results communicate price effects due to visual changes and ignore the changes from other environmental and economic changes that may arise simultaneously. Building upon this work, future studies can incorporate distribution effects stemming from changes to other environmental quality indicators: including noise pollution, thermal comfort, and air-quality.

Lastly, the measures of exposure and sensitivity are ultimately derived from 3D city models. Thus, the level of detail of the underlying 3D model will define the resolution of the building performance metrics. That is, information at a higher fidelity than that of the 3D model will not be included in the evaluation. For instance, building facades in this study are all considered to be the same, ignoring differences in construction materials and textures; lakes are also considered the same, ignoring difference in pollution and geometry. To build upon this limitation, future studies may incorporate images as a way to improve the fidelity of the automated visual impact assessment.

3.6 Conclusion

Economic performance objectives within Architectural Design Optimization have remained challenging to implement, and have thus far been limited to cost minimization, ignoring economic preferences. In this paper, I introduce a novel approach to infer the financial value of a generated design. The proposed Automated Design Appraisal produces building-level price predictions using local-scale environmental performance simulations. Further, I integrate the algorithm within a visual impact framework to understand the property value at risk due to local development.

Results from an impact assessment of a single proposed urban development indicate (1) losses are concentrated to neighbors closest to the point of modification and (2) a subset of buildings benefit from the development of the sky-line, confirming previous findings. Findings from a regional assessment show potential impact -both direct effects and localized costs- are a function of the local urban and environmental form. The spatial pattern of exposure varies by view-metrics; contingent on the location and abundance of landcover elements. Yet, despite the devaluation risk to individual properties, moderate urban development (single-story up-zoning) is estimated to yield aggregate price benefits to low-density regions.

Automated Design Appraisal provides a scalable approach to incorporate economic performance within Architectural Design Optimization procedures. Doing so, enables evaluating generative urban design procedures with respect to both the (1) predicted price and (2) devaluation risk imposed on nearby neighbors. The approach enables future studies to integrate devaluation risk within automated real estate valuation models, reveal mispriced real estate with respect to their local exposure

4 Conclusion & Outlook

As cities continue to digitalize and as more sophisticated tools for assessing and integrating novel forms of data emerge, it becomes feasible to evaluate urban design decisions with respect to two dimensions: economic preference and environmental impact. With growing attention to the physical and transitional risks cities face, methods and tools that account for these two dimensions will be increasingly important to planners and policy makers.

This thesis was motivated by the lack of methods that account for the dynamic relationship between price and amenities, i.e. the price-amenity gradient. As such it set out to develop a method to evaluate the price effect- whether it be a direct gain or a social cost – of a design change at the concept design stage. Furthermore, it sought to apply this approach to model a risk that is particularly relevant to property owners as densification increases: devaluation risk of visual impact due to zoning reform.

4.1 Main Contribution & Findings

This thesis explores the concept of local area risk estimation (Section 1), and introduces GeoAI methods to model the devaluation risk of visual impact due to zoning reform by integrating building performance simulation (Section 2) with property valuation estimation techniques (Section 3). This section presents the unique contribution and findings according to each risk modeling stage:

Performance Simulation: Capturing visual landscape quality at the building level has been a persistent challenge. Existing methods largely focused on lighting, wind, or noise-based simulations. Section 2 introduces a viewpoint visual share simulation that quantifies the visual proportion of unique land elements and obstructions visible from a building's set of viewpoints. To improve the interpretability of the viewpoint visual share geodatabase, Section 2 introduces a comprehensive set of view-metrics which describe both the spatial and aspatial - referred to as the visual composition and configuration- attributes of the building's visual landscape quality. By constructing view metrics for the entire building stock

of Switzerland, Section 2 identifies abundant and scarce visual elements, and reveals the spatial concentration of view-metrics relating to urban typology, natural landscape, and the identity of major agglomerations.

Performance Evaluation: The attribute space for visual landscape quality is far larger than that of other micro-climate and environmental features. The absence of a standardized metric to quantify views has limited derivative works that associate building-level urban environmental metrics with external factors, such as health (Section 6.1), or price (Section 6.2). To overcome this limitation, Section 2 constructs a Visual Capital index, that, based on the concept of income-sorting, depicts the preference for a building's viewpoints. Section 2 goes on to describe the primary drivers of visual capital – water-bodies and elements in the far distance – and illustrates the context-dependent nature of each metric, whereby the importance of a landscape element varies in the presence of another. Importantly, section 2 identifies that on average the visual landscape quality increases in settings of both (1) low density, as well as (2) high density with moderately steep terrain. Further, by applying an unbiased clustering analysis, new boundaries of high visual capital are uncovered, thus identifying potentially undervalued properties – i.e. high visual capital in low-income communes.

Price of Performance: Properties featuring high quality environmental amenities typically command a premium on the market. Vistas and views of water bodies are commonly considered 'luxury-goods' sought after by high-income individuals. However, the lack of standardization in pricing visibility and visual quality – often reduced to 'line-of-sight' indices – impedes our ability to accurately capture non-linear and interaction effects. To address this, Section 3 utilizes the composite Visual Capital indices and estimates revealed preferences using the hedonic pricing model. By limiting the training sample to major lake regions in Switzerland, Section 3 demonstrates that the coefficients for Visual Capital vary by lake region. This variation suggests that additional factors, not captured by the underlying visibility simulation and which differ across lakes, may further influence pricing estimates, such as environmental condition or market supply.

Importantly, Visual Capital serves as a macro-location variable (average listing price) and exerts a positive effect on sales transactions.

Impact of Design Choice: While densification is understood to critically contribute toward the transition to sustainable development, achieving public acceptance for development projects remains challenging. Section 1 and 3 highlight the role of NIMBY (Not In My Backyard) attitudes in public acceptance and the negative externalities associated with increased densification. Existing methods to evaluate the impact of densification and similar urban design choices fall short in quantifying the devaluation risk posed by these negative externalities to property owners. To address this, Section 3 presents an automated visual impact assessment that measures the property valuation at risk due to local land use change. Central to this is Automated Design Appraisal (ADA) – a combination of methods developed in Section 2 and Section 3. ADA measures the change in predicted price across simulated design scenarios, providing both direct and indirect effects. Where indirect effects are the spillover effects onto nearby properties. Applied to a single hazard case-study, a new office tower development, Section 3 illustrates that ‘damages’ are concentrated within the immediate neighborhood of the new development, whereas potential benefits (the improvement to the ‘sky-line’) are observed for buildings at further distances. Simulating multiple-hazards, single-floor additions across an entire commune, the method not only identifies buildings highly vulnerable to local land-use changes, but also distills which view-metrics drive this sensitivity.

5 Future Outlook

This section highlights the outlook and addresses the limitations of each section. Further, it covers two promising future directions made possible by this research.

5.1 Addressing Limitations

This thesis explores the price effect of visual obstructions caused by urban development. As a result, the analysis focuses on how changes in view metrics influence visual landscape quality, therefore deliberately omitting the impact of simultaneous environmental and economic shifts. This provides an opportunity for subsequent studies to investigate how variations in other environmental quality factors, such as noise pollution, thermal comfort, and air quality, affect the underlying dynamics of the price-amenity gradient. Moreover, there is an opportunity to incorporate alternative estimator models to reveal additional predictive efficiency.

Since this research is based on 3D models, the resolutions of these models determine the accuracy and the level of detail of the building performance metrics. As a result, details finer than those provided by the 3D models are not included in our analysis (e.g. composition and condition of façades). To address this limitation, future studies could employ images to refine the precision of automated visual impact assessments. That is, update 3D models with the components and aesthetics captured by each image.

5.2 Towards Preference Driven Design

A novel aspect of this thesis is the introduction of Automated Design Appraisal (ADA) and its role in estimating devaluation risk. Looking forward, there is an opportunity to integrate ADA within architectural design optimization procedures, specifically in Generative Design.

One of the major challenges in the field of Architectural Design Optimization (ADO) is multi-objective optimization. ADO aims to produce a set of design options that satisfy objective functions, i.e., the Pareto front. However, without a clear

approach to weigh the results from each optimization task, ADO struggles to narrow down the design space towards solutions satisfying higher priority objectives. Essentially, to produce a single design recommendation, ADO requires a mechanism to manage trade-offs. As discussed in Section 3, past approaches (including the more recent 'human-in-the-loop' approach (Z. Jiang et al., 2022)) have relied on survey-based or stated preference methods, which can be biased and challenging to scale.

To effectively bypass these hurdles, ADA proposes to solve the multi-objective tradeoff problem by directly using design-induced price alterations. The predicted price for a simulated building design reflects the weighted combination of the design-focused objective functions, where the weight corresponds to the learned market preference for each design parameter. Further, we can use the predicted valuation as a new objective function within a generative design algorithm thereby exploring the design search space along the trajectory of increasing valuations.

This thesis additionally explores the concept of local area devaluation risk. This concept equally applies to ADO. Whereby a Generative Design procedure can evaluate the cost imposed onto the neighborhood, whether as a risk to local valuations or as public goods such as urban environmental quality.

Thus, ADA within ADO enables designs to leverage market data to quantify the financial performance of the design itself, as well as the spillover effects that the design imposes onto its neighbors. In (A. Swietek, 2023), I explain “*While building design concepts are commonly assessed for engineering performance, including structural resilience (Mayencourt & Mueller, 2019), environmental quality (Gagne & Andersen, 2012; Natanian & Auer, 2020) and energy performance (Natanian & Wortmann, 2021; Shi et al., 2017), as well as for cost performance, including material usage (Weber et al., 2022) and sustainability goals (Ameen et al., 2015; Elshani, 2021), current approaches have stopped short of considering the financial value of a given design directly, or more broadly speaking the preference thereof...*”. Figure 19 provides an illustration of the two additional objective functions that emerge as a result: maximize predicted valuation and minimize social cost.

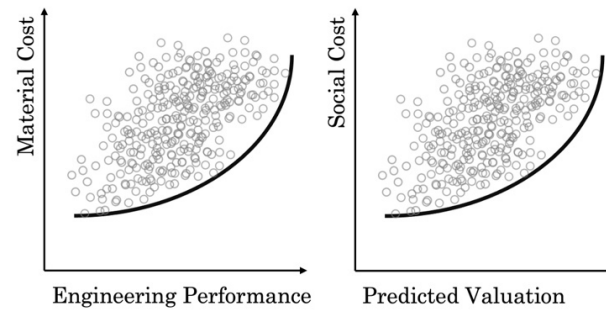


Figure 19: Illustration of the outcome for a Generative Design simulation, where grey circles represent generated building designs and the black line delineates the Pareto Front of optimal designs. The left figure displays the traditional two objective functions found in Architectural Design Optimization literature: minimizing Material Cost (which encompasses efficiency, sustainability, etc.) and maximizing Engineering Performance (encompassing structural, thermal, etc. aspects). The right figure introduces the expanded dimensions made possible by integrating a property valuation model: maximizing property valuation (predicted price) and minimizing social cost (including local devaluation risk, NIMBY acceptability, etc.)

This approach to building design evaluation within a generative design procedure facilitates a more efficient exploration of the design space. A distinctive feature of this method is the ability to quantify the cost and benefits of a marginal unit of a non-market good. For instance, the addition of a tree or vegetation to a proposed development, previously seen merely as a cost, can now be evaluated for its contributions to the design's value. With this approach, the inferred value provided by non-market goods such as urban amenities is documented. Since the interpretation of marginal price effects reflects revealed preferences, this method leads to the creation of building design solutions that are optimized not only for valuation but also for market preference: Preference-Driven Generative Design.

6 Supplements

6.1 Mini-Study: UEQ, Urban Health, Energy Consumption

In this section, I illustrate the usefulness of performance metrics by presenting results from a small case study. It is known that environmental quality of the built environment directly contributes to both the health and quality of life of an individual by reducing stress, improving concentration, and increasing productivity. This can be shown by investigating differences in urban environmental quality (UEQ) indicators across spatial clusters of years of potential life lost or gained (YPLLG), a mortality metric. To do so, we can build on previous socio-economic work on life expectancy inequalities using existing individual-level mortality data in the canton of Geneva, Switzerland (Ladoy et al., 2021), and take advantage of environmental data from the open-source Swiss Topo and SwissBuildings3D database. Specifically; solar irradiation [kWh/m²/Jahr], road traffic noise [db], air temperatures [°C], nitrogen dioxide (NO₂) concentrations [ug/m³], and the visual share of vegetation and visible elements in the far distance [%]; as quantitative measures representing daylighting, noise pollution, thermal comfort, air quality, and visual quality.

Indicator	Measure	unit	Data Provider
Mortality Indicator	Death Age	yr	Cantonal Statistical Office, OCSTAT
	Life Expectancy	yr	Cantonal Statistical Office, OCSTAT
Socio-Economic Indicators	median age	yr	Cantonal Statistical Office, OCSTAT
	median income	CHF	Cantonal Statistical Office, OCSTAT
	Nationality	Swiss/Not-Swiss	Cantonal Statistical Office, OCSTAT
Thermal Comfort	Surface Temp	C	Geneva Territory Information System (SITG)
Daylighting	Solar Irradiation	kWh/m ² /yr	Swiss Federal Office of Energy
Air Quality	Nitrogen Dioxide	ug/m ³	Wuest Partner
	Ozone	ug/m ³	
	PM10	ug/m ³	
Noise Pollution	Road Traffic Noise	db	Swiss Office for the Environment
Visual Quality	Share of Elements	%	Wuest Partner

Table 9 Urban environmental quality metrics and their underlying data source.

Results show YPLLG to have a spatial structure within Geneva, and substantial differences in UEQ are observed across regions of high and low spatial autocorrelation, when computed using robust Local Moran clustering methods. Further, controlling for UEQ covariates reduces the size of these initial high and low Local Moran clusters of YPLLG by 92% and 81%, suggesting that UEQ could explain the spatial pattern of the mortality metric. Based on these results we can infer the benefits of high-resolution UEQ. Public health policy and urban health initiatives could benefit from a greater understanding of a region's UEQ.

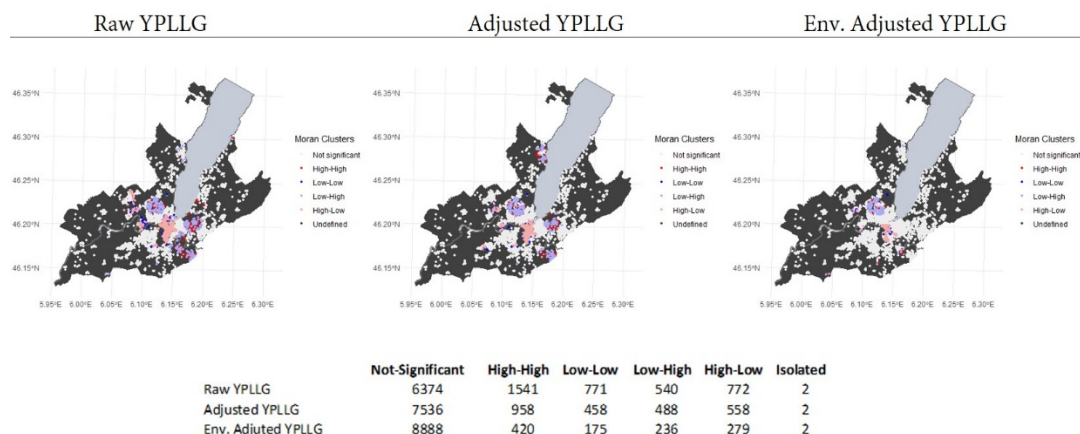


Table 10 Environmental features (including solar irradiance, road noise, air quality, thermal comfort, view metrics) help to partly explain the spatial structure of the YPLLG in Geneva

In a second small case-study, I explore the questions: Does Building Level Urban Environmental Quality influence energy consumption behavior? To do this, I use an 11-year sample of Heat Expenditure for a sample of the Geneva Building Stock, 8641 buildings. Compiling the micro-climate data, I develop UEQ indicators at property level by taking the maximum raster value within a 100m buffer zone. Using a bootstrap approach, we find that building level indicators improve the model’s predictive power, and the solar metrics, daylighting and thermal comfort, have a small, yet, significant influence (when compared to age or size) on a building’s renovation propensity, Figure 20.

Effect of UEQ on Renovation Propensity (RPI)

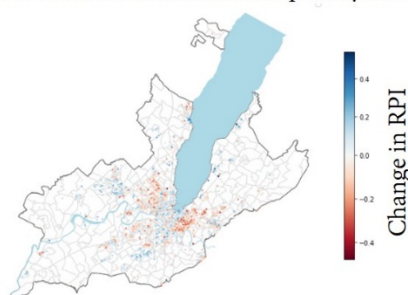


Figure 20: Effect of Building Level Urban Environmental Indicators on Renovation Propensity.

While overall energy consumption declined in the period between 2010 and 2022, we can be seen that buildings in hotter urban areas, e.g. city center, have seen the strongest declines in energy consumption.

6.2 How view determines well-being and value

Adam R. Swietek^{a,*}, Jacqueline Schweizer^b

^a Laboratory of Environmental and Urban Economics (LEURE), École Polytechnique Fédérale de Lausanne (EPFL), Lausanne, Switzerland

^b Wüest Partner, Zurich, Switzerland

Article published with Wüest Partner

Swietek, A. R, M. Zumwald, J. Schweizer "How view determines well-being and value" (2022)*
<https://www.wuestpartner.com/ch-en/2022/11/07/how-view-determines-well-being-and-value/>

Abstract

With a digital twin of Switzerland's building stock, we are able to derive a range of view-metrics, such as a building's visual share of a lake. This allows us to measure the financial impact of visual elements on housing prices at a previously unattained level of resolution. We find that large views of lakes and cities in the far distance have the strongest impact on the sale price; however, we find the financial influence of the studied visual elements are highly-context dependent. The analysis provides a rich picture of how visual quality varies across the Swiss building stock and within a given building.

6.2.1.1 View in Real-Estate

View qualities are commonly understood to play an important role in how individuals perceive landscapes and how they make decisions. Recent neuroscience research highlights for instance the unconscious influence of fractal patterns on visual perception and well-being. Optimal fractal dimensions (i.e. nature scenery) greatly reduces stress and induces the release of endorphins (Briellmann et al., 2022). Further, distant backgrounds (>1km) tend to command a greater share of people's attention than objects in the mid-ground (150-1km) (Hull & Stewart, 1995). Both the aspect of depth perception and visibility of fractal patterns (such as trees) are thus relevant aspects to consider in the context of the built environment. This is backed up by urban health and indoor research

indicating that a high-quality window view improves a worker's mental state and sleep quality, reduces stress, and boosts creativity (Al Horr et al., 2016; Frontczak & Wargocki, 2011).

What we see not only influences our well-being, but can also have an effect on rents or real-estate value. View and visual quality metrics explain price differences in Geneva multi-family (Baranzini et al., 2008), as well as Manhattan office rentals. In the latter case, office spaces with high access to views had a 6% net effective rent premium compared to spaces with low view access (Turan et al., 2021).

While previous analyses have highlighted the revealed preference – higher premiums – for high-quality window views, they have, for the most part, focused on smaller case-studies, relying on simplified proxy variables. Thus, with the new ability to quantify the view with orientation-specific and 3D-based metrics, we have the opportunity to analytically evaluate the financial value of a view at a higher resolution and with larger geographic coverage.

6.2.1.2 Our view data: Derived from a Digital Twin

Digital twins or simulated 3D urban environments allow researchers to capture information based on elevation and orientation, enabling a more comprehensive and quantitative definition of a view. Our view database consists of 32 mio. viewpoints from building facades across Switzerland. Each point represents the visual landscape as seen through a virtual window, allowing the quantification of a view in terms of the composition and configuration of visual elements.

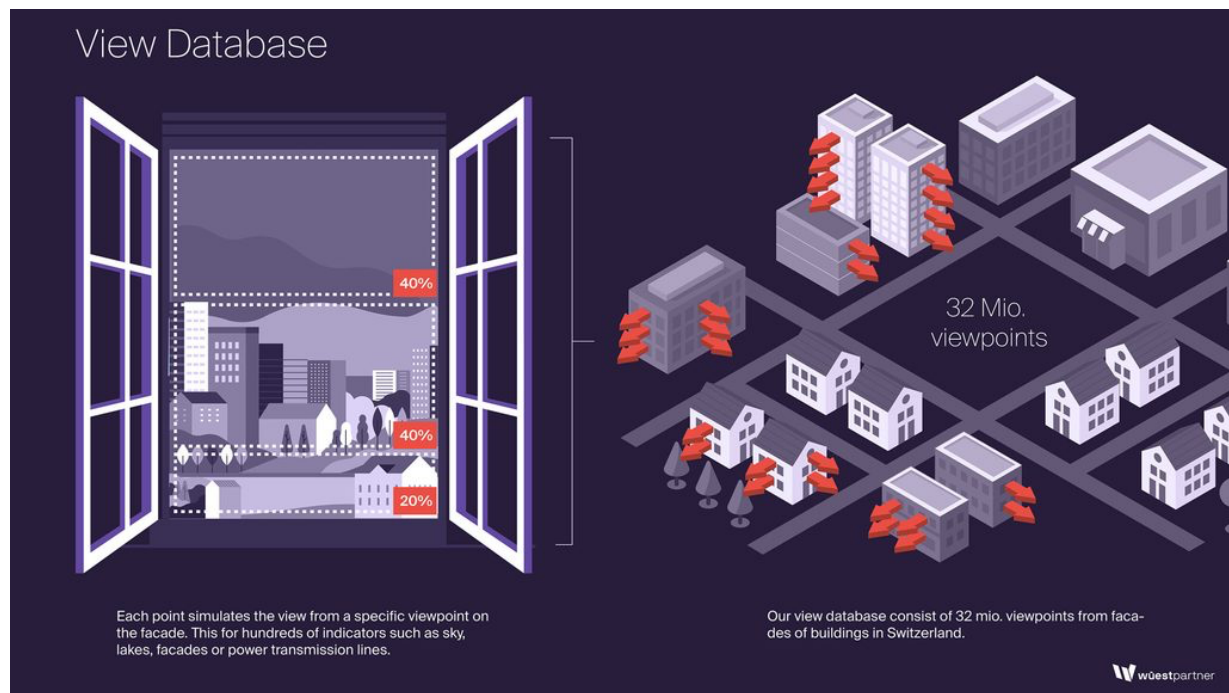


Figure 21 Schematic of the Viewpoint Visual Share geodatabase

Concretely the Digital Twin consists of an exact 3D representation of all buildings and topologies, view-relevant point of interest data, such as mountains, nuclear power plants, power transmission lines, and different land surface types such as roads, forest, lakes etc. This allows us to model what is visible from different floors from every side of the building. One viewpoint contains the information about the share of facades, roofs, lakes, vegetation and undesirable structures, such as high-voltage power transmission lines.

Visual landscape elements can vary in scarcity. For instance, a meager 4.6 % of the Swiss building stock has a 1% view onto a waterbody (e.g. river, lake); whereas 57.6% has a 1% view of nature. Abundance of such visual elements further varies by location; for instance, the average building in Basel will have a 18.7% view of vegetation, compared to 26.7% in Geneva.

Urban form and natural terrain play a significant role in determining the local supply of views. If we consider the coastal cities of Lausanne and Zürich, and examine solely the distribution of lake-views; a few interesting patterns emerge: Buildings in Lausanne are not only more likely to have lake-views, but also tend to have a larger visual share if they do. However, there are proportionately more

buildings in Zürich with exceptionally good lake-views (total share of over 10%), indicating a higher degree of inequality with respect to access to lake-views across these two cities. Considering the location of the buildings with the best lake-views, it becomes evident that, while the hilly topography of the north-eastern shore of Lake Geneva (Lausanne, Lavaux, Vevey, Montreux) increases the propensity of above average views far away from the lake, the clustering within 1.5 km of the lakeshore in Zürich creates a natural scarcity of high-quality lake-views.

Economically, scarcity of goods typically results in a higher willingness to pay which may contribute to the competitiveness of Zürich's housing market. These observations are of course intuitive, however, the ability to quantify the national supply of views opens up new avenues to measure our cities and improve the accuracy of property evaluation models.

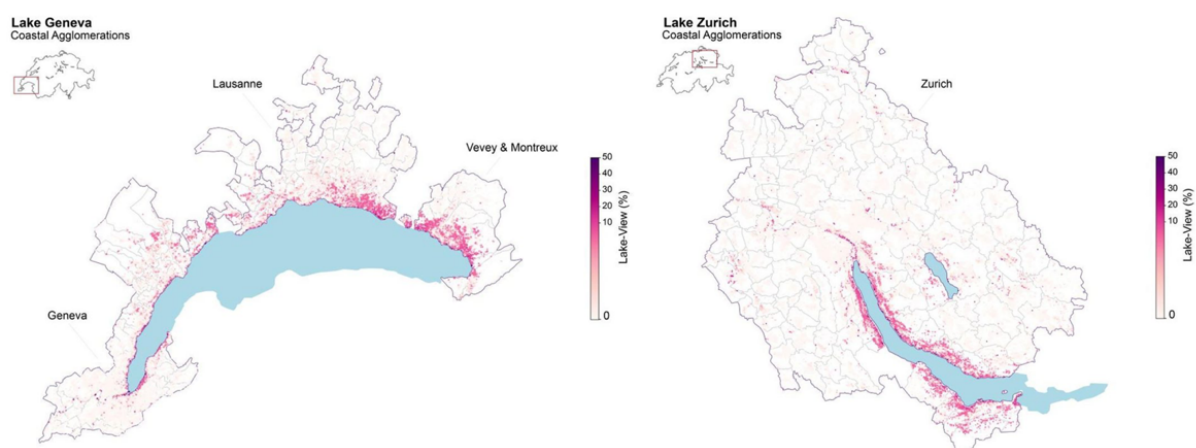


Figure 22 Plotting the geographic footprint of lake-view buildings, colored by the size of their respective largest view, reveals the differences in supply of lake-view buildings, between Lake Geneva and Lake Zürich.

6.2.1.3 View influences Home prices in Switzerland

We examine the effect of different visual elements in Switzerland on house prices. Specifically, we define our set of view attributes as the maximum visible share of a selected variable for a given building; e.g. a 5% lake-view. Controlling for standard structural, accessibility-, and environmental characteristics, we use the hedonic pricing model (Rosen, 1974) to determine the implicit price of our attributes of interest. Under this model, we find that homes with a larger view of

a lake command an 11% premium on average; whereas larger views of nature, on average, trade at a 1.6% discount. Yet, a closer look reveals that while particular visual features, (i.e. lake-view or view of a city in the distance see figure), have large price effects that are globally true, others vary spatially and are highly context-dependent. For instance, larger views of nature trade at a 1% premium in wealthy-urban areas; as opposed to a 1% discount in the peri-urban neighborhoods of mid-sized cities.

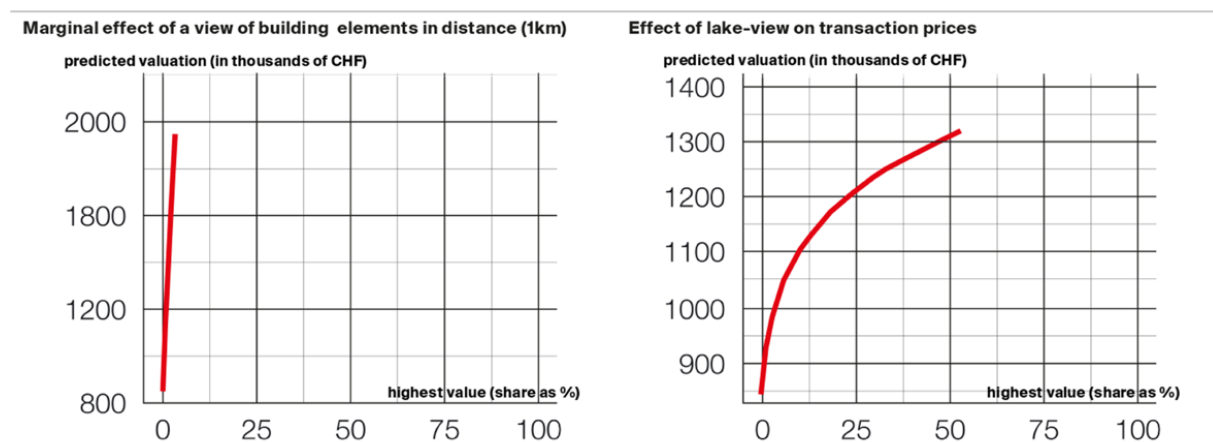


Figure 23 The x-axis shows the highest value (share as %) per building of the respecting view element. The y-axis shows the predicted valuation (in thousands of CHF) of a single-family home with a given visual share, while controlling for other predictors used in our hedonic model. Left: Marginal effect of a view of building elements in distance (1km). Right: Effect of lake-view on transaction prices.

6.2.1.4 From macro- to nano-location

When describing the location of a property, the distinction between macro- and micro-location has been established. In Switzerland, the macro-location, i.e. the large-scale spatial classification, is usually represented by the municipality. The micro-location describes the small-scale location characteristics that differentiate within the macro-location.

In addition to the identification of a location and the assignment of the associated location characteristics, the conversion of this collected information into economic categories is of decisive importance. In this context, the value is derived from the scarcity of the spatial bundle of goods: the rarer a certain combination of desirable site characteristics occurs in an area, the higher its economic value is in principle.

Thus, land with a lake-view fetches significantly higher prices than land without one, because it is rare – at least in Switzerland. A micro-location criterion only becomes price-relevant if it is also an exclusive attribute that is not available in other locations in the same macro-location.

With the growing availability of high-resolution spatial data, a third level of location quality has found its way into the valuation practice: the nano-location. This term is used to define the quality of location of an apartment within the building. E.g. an apartment on the top floor has different views than an apartment on the ground floor and a south-facing apartment has more daily sunlight than a north-facing one. The nano-location introduces an additional spread of willingness to pay within the price level of the macro- and micro-location. Our view database allows for data-driven assessment of the nano-location.

6.3 Supplementary Material for Visual Capital Article

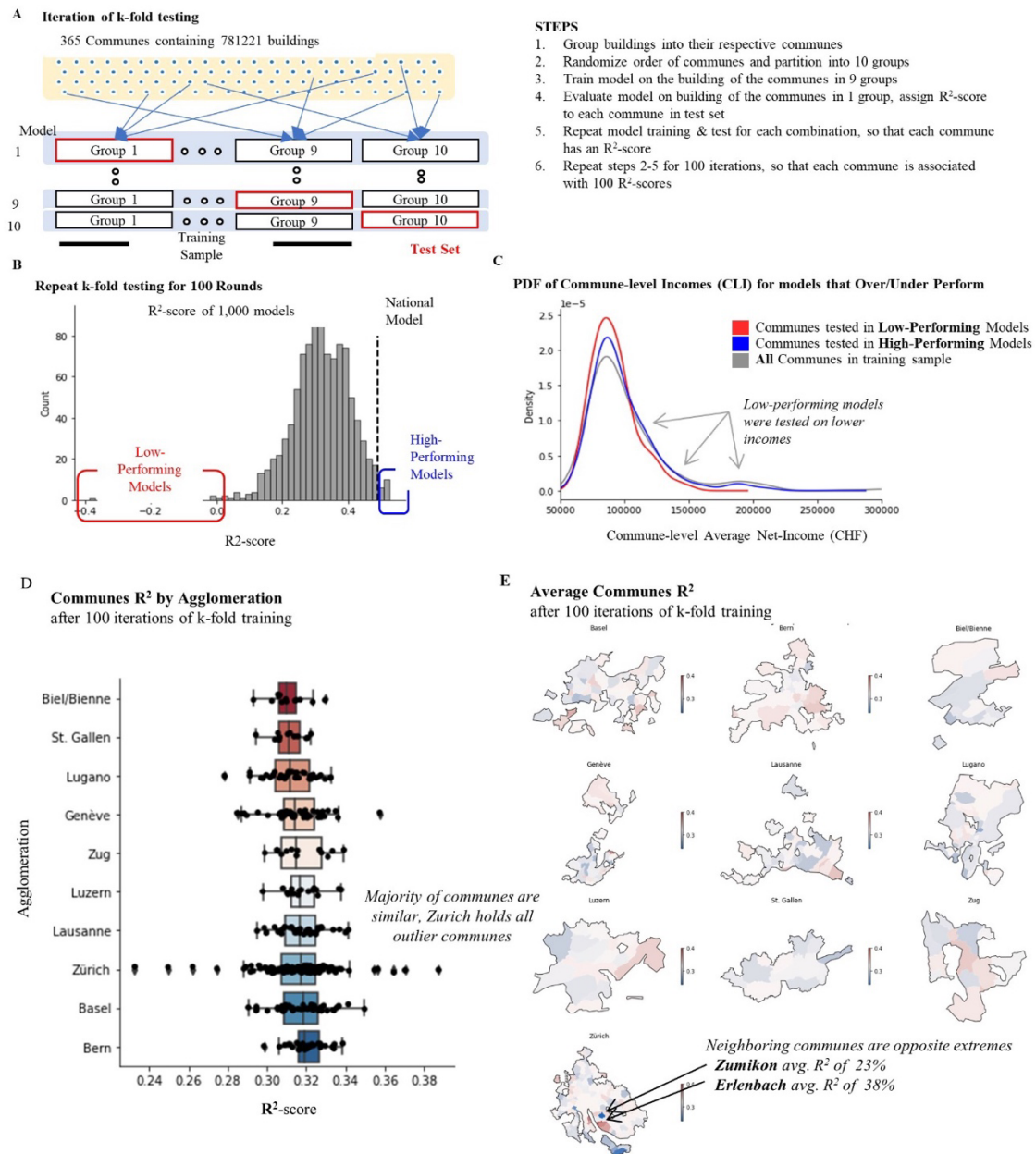


Figure S 1: (A) k-fold cross validation methodology. (B) Model fit results from 100 iterations, i.e. 1000 models. (C) Low performing models were tested on lower income communes, suggesting view-data better explains average income in high-income communes, than in low-income communes. (D) Boxplot of model fit results by Agglomeration. (E) Choropleth plot of average commune R²-score across 100 models. Majority of scores are normally distributed between .28 and .34, and Zurich holds most of the high and low scoring outliers

A k-fold cross validation procedure confirms the robustness of the methodology, with a normally distributed model performance (mean of R²-score = .32, standard deviation = .09) consistent across agglomerations. Communes within the Zurich

agglomeration accounted for most of the high and low scoring outliers where the neighboring communes of Zumikon and Erlenbach represented the lowest and highest R²-scores respectively. The suboptimal performance model was limited to instances where lower-income communes were enriched in the test set



Figure S 2: Figure depicts summary statistics for view-metrics across 10 agglomerations in Switzerland

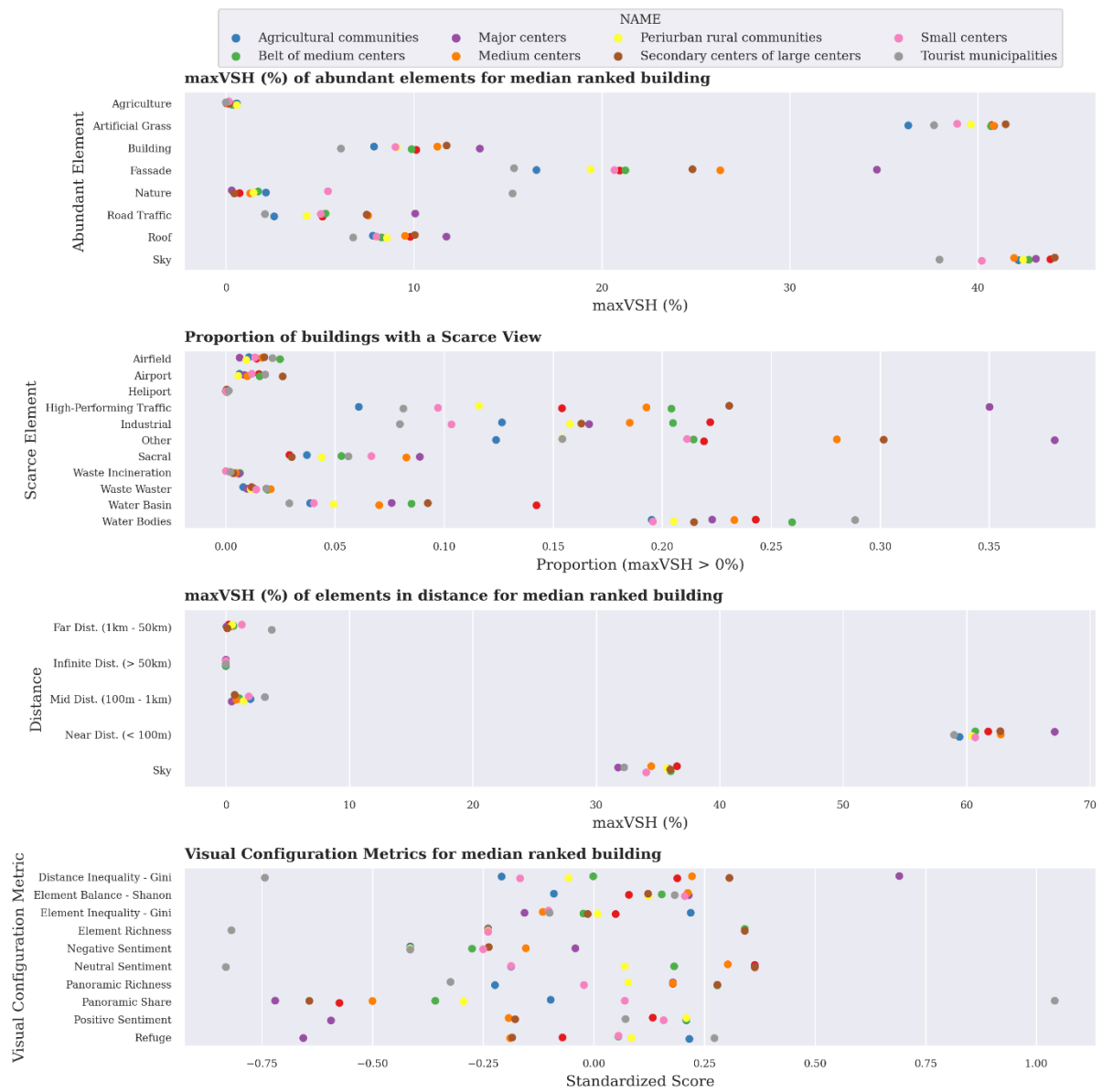


Figure S 3: Figure depicts summary statistics for view-metrics across the 8 major urban typologies in Switzerland

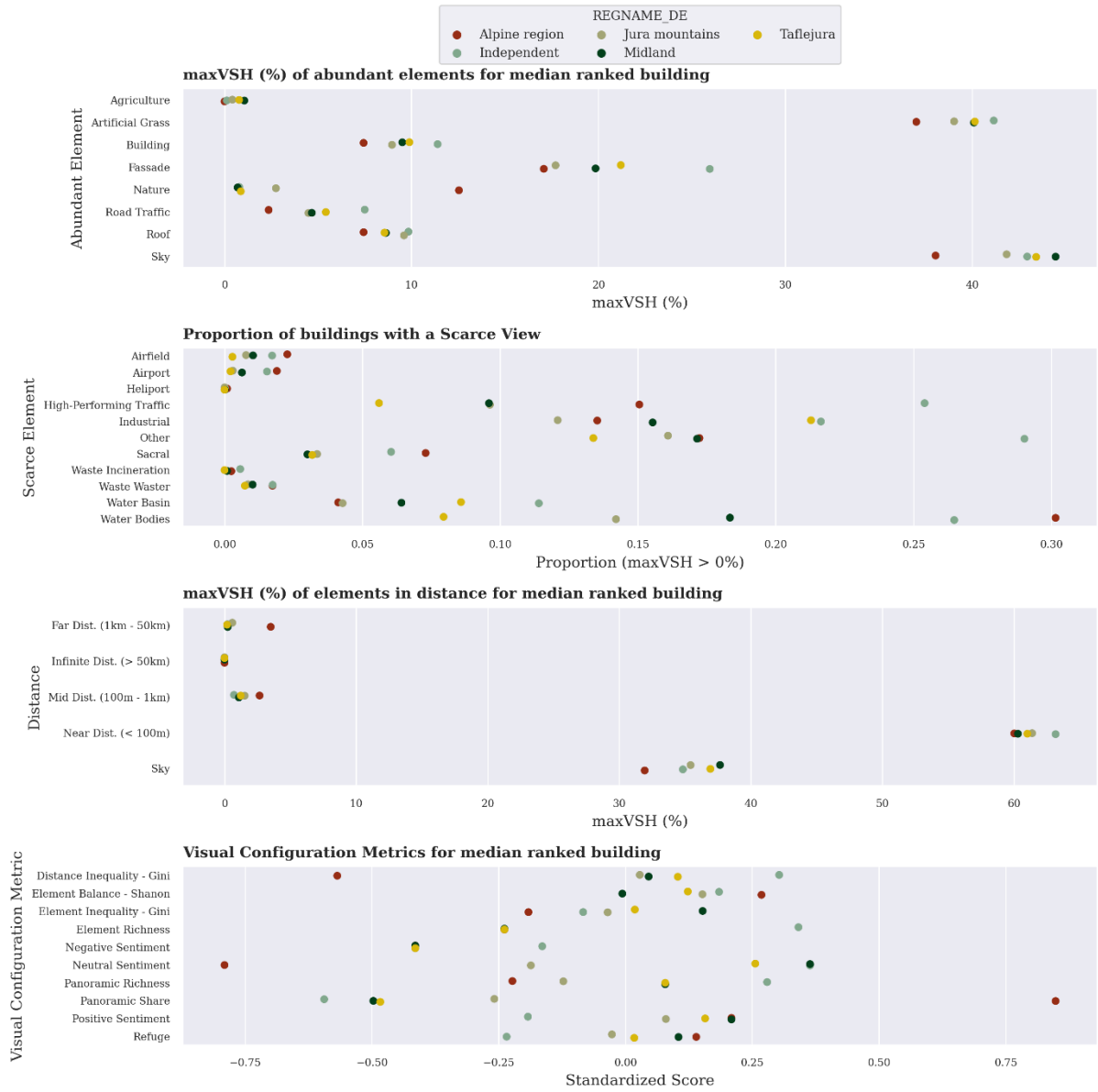


Figure S 4: Figure depicts summary statistics for view-metrics across 5 landscape typologies in Switzerland

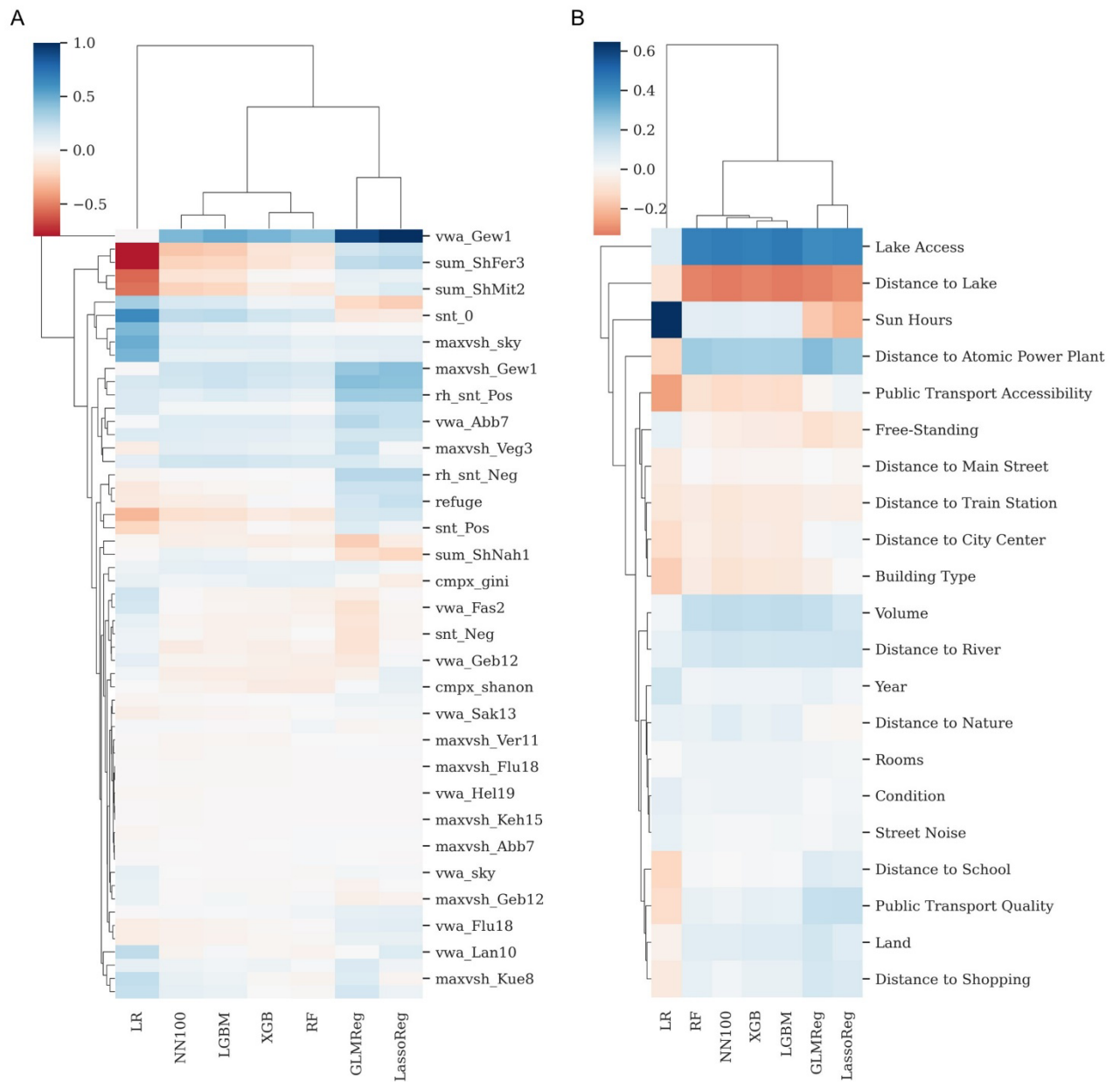


Figure S 5: (A) Heatmap depicts the correlation between view-metrics and prediction results from each of the regression models tested (B) Heatmap depicts the correlation between non-view metrics and the prediction results from each of the regression models tested in this study.

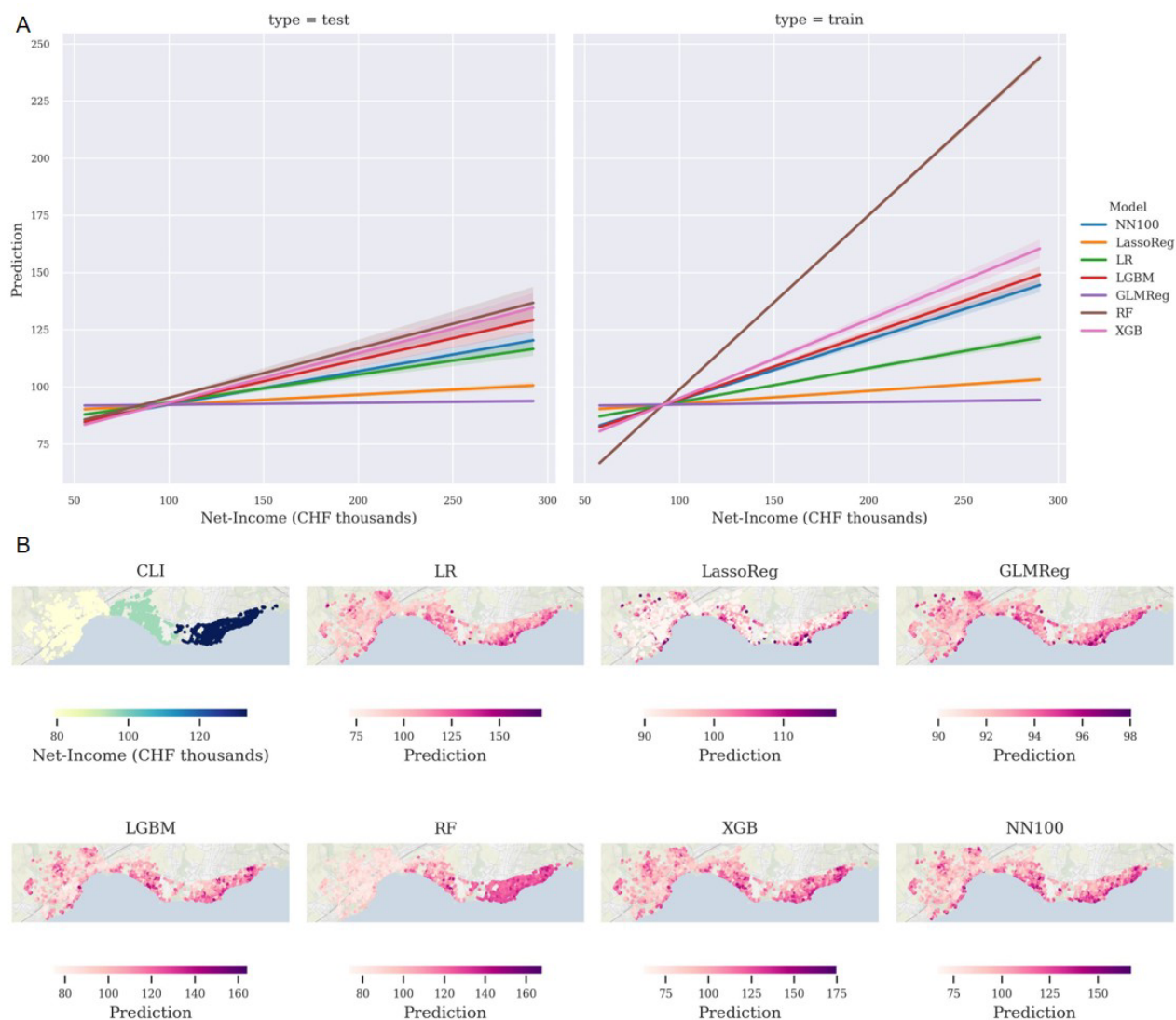


Figure S 6: (A) Comparison of the fitted line on Prediction vs Actual test and training data (B) Choropleth map of fitted values for buildings with 3 adjacent lake-shore communes in Lausanne, for each of the 6 models tested.

We find the results are robust across all tested model architectures. Specifically, the correlation of each model's prediction against individual metrics is consistent across models. XGB/RF Model perform best, having similar test-set results, however, RF does tend to overfit to the training data, with considerably higher training set r^2 indicates. This is most evident in the attached figure showing the spatial distribution of prediction in 3 neighbouring communes of increasing net-income. Our goal is to calibrate scores on the average net-income but extract

distribution of results The RF model's predictions are closely related to the administration boundaries with minimal variance. Importantly, XGB is considerably faster than RF (10 seconds vs 6 minutes), allowing us to perform an extensive k-fold testing (1000 total iterations) to further validate robustness. Considering the promising results obtained, future research can explore the optimization of neural networks to potentially enhance the performance and accuracy of predictions in similar and new contexts, namely floor-level predictions.



Figure S 7: SHAP value summary plot for fully trained XGB, gradient boosted regression model

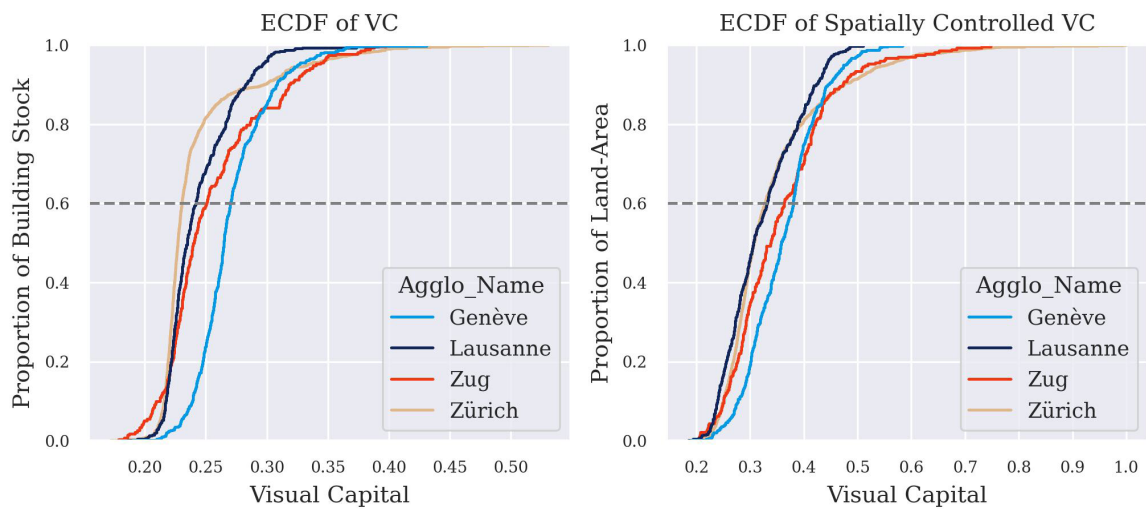


Figure S 8: Comparison of lake shore agglomeration of Zurich, Zug, Lausanne and Geneva's ECDF of Visual Capital. Spatially controlled VC is the maximum value for each 1-km² hexbin aggregation. The figure shows that both the majority of the land and building stock in Zurich has substantially lower VC than Geneva. Yet, some of the highest values appear in Zurich in a small portion of the building stock that take up an equally small portion of the land area.

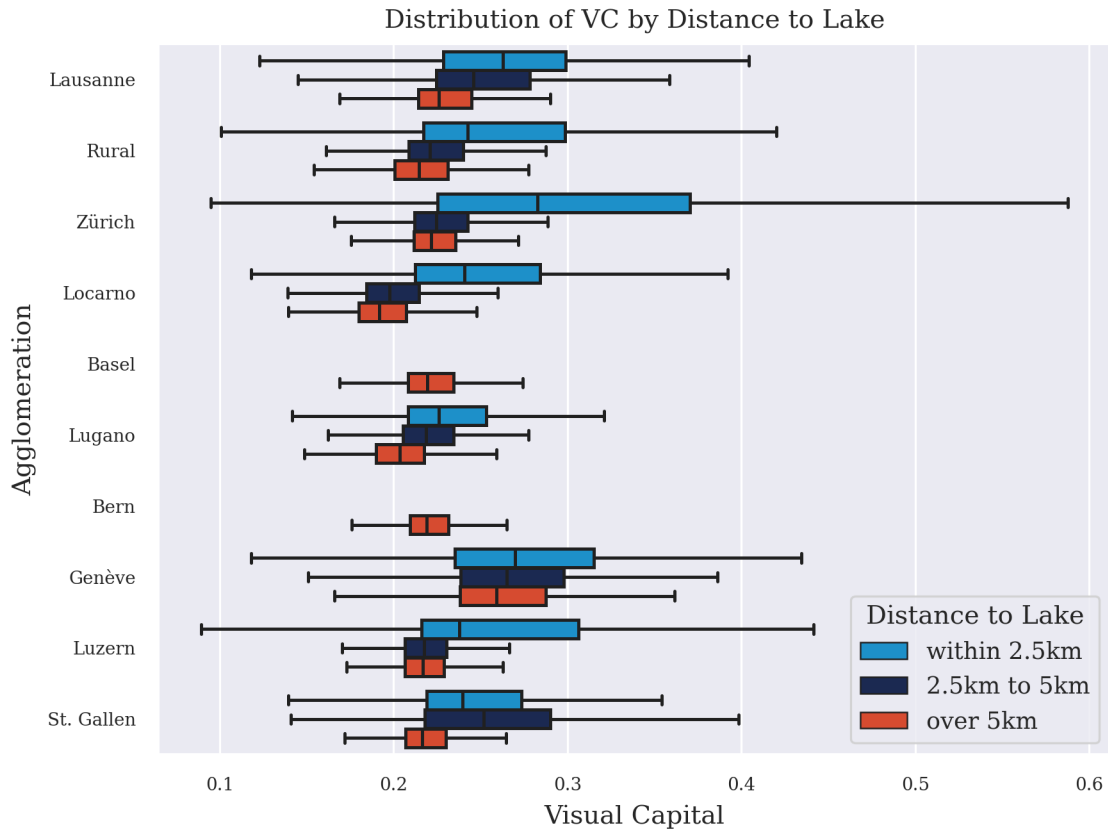


Figure S 9: Boxplot describes the Visual Capital by Distance to the nearest lake for the major agglomerations

CLI Stratified by Building Density and Terrain Slope

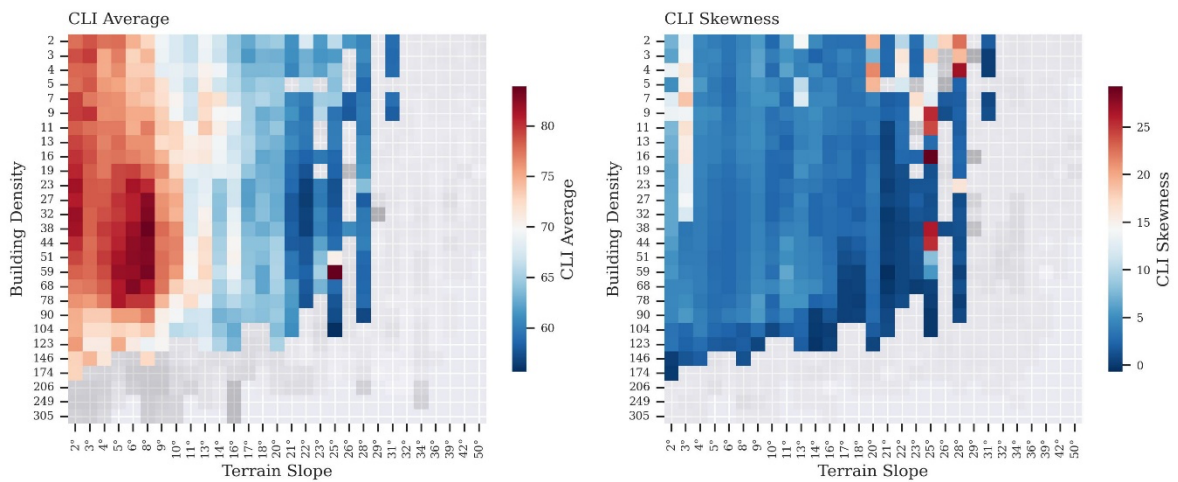


Figure S 10: Heatmap depicts the average and skewness of Commune Level Income (CLI) stratified by Terrain Slope and Building Density

7 References

- Allegrini, J., Orehounig, K., Mavromatidis, G., Ruesch, F., Dorer, V., & Evins, R. (2015). A review of modelling approaches and tools for the simulation of district-scale energy systems. *Renewable and Sustainable Energy Reviews*, *52*, 1391–1404. <https://doi.org/10.1016/j.rser.2015.07.123>
- Ameen, R. F. M., Mourshed, M., & Li, H. (2015). A critical review of environmental assessment tools for sustainable urban design. *Environmental Impact Assessment Review*, *55*, 110–125. <https://doi.org/10.1016/j.eiar.2015.07.006>
- Ander, G. D. (2003). *Daylighting Performance and Design*. John Wiley & Sons.
- Anderegg, W. R. L., Chegwiddden, O. S., Badgley, G., Trugman, A. T., Cullenward, D., Abatzoglou, J. T., Hicke, J. A., Freeman, J., & Hamman, J. J. (2022). Future climate risks from stress, insects and fire across US forests. *Ecology Letters*, *25*(6), 1510–1520. <https://doi.org/10.1111/ele.14018>
- Anderegg, W. R. L., Collins, T., Grineski, S., Nicholls, S., & Nolte, C. (2023). Climate change greatly escalates forest disturbance risks to US property values. *Environmental Research Letters*, *18*(9), 094011. <https://doi.org/10.1088/1748-9326/ace639>
- Anselin, L. (1995). Local Indicators of Spatial Association—LISA. *Geographical Analysis*, *27*(2), 93–115. <https://doi.org/10.1111/j.1538-4632.1995.tb00338.x>
- Aries, M. B. C., Veitch, J. A., & Newsham, Guy. R. (2010). Windows, view, and office characteristics predict physical and psychological discomfort. *Journal of Environmental Psychology*, *30*(4), 533–541. <https://doi.org/10.1016/j.jenvp.2009.12.004>
- Armal, S., Porter, J. R., Lingle, B., Chu, Z., Marston, M. L., & Wing, O. E. J. (2020). Assessing Property Level Economic Impacts of Climate in the US, New Insights and Evidence from a Comprehensive Flood Risk Assessment Tool. *Climate*, *8*(10), Article 10. <https://doi.org/10.3390/cli8100116>
- Assouline, D., Mohajeri, N., & Scartezzini, J.-L. (2017). Quantifying rooftop photovoltaic solar energy potential: A machine learning approach. *Solar Energy*, *141*, 278–296. <https://doi.org/10.1016/j.solener.2016.11.045>
- Bakkensen, L. A., & Barrage, L. (2022). Going Underwater? Flood Risk Belief Heterogeneity and Coastal Home Price Dynamics. *The Review of Financial Studies*, *35*(8), 3666–3709. <https://doi.org/10.1093/rfs/hhab122>
- Bakkensen, L., Nguyen, Q., Phan, T., & Schuler, P. (2023). *Charting the Course: How Does Information About Sea Level Rise Affect the Willingness to Migrate?* (SSRN Scholarly Paper 4580834). <https://doi.org/10.21144/wp23-09>
- Baldauf, M., Garlappi, L., & Yannelis, C. (2020). Does Climate Change Affect Real Estate Prices? Only If You Believe In It. *The Review of Financial Studies*, *33*(3), 1256–1295. <https://doi.org/10.1093/rfs/hhz073>
- Baranzini, A., Ramirez, J. V., Schaerer, C., & Thalmann, P. (2008). Introduction to this Volume: Applying Hedonics in the Swiss Housing Markets. *Swiss Journal of Economics and Statistics*, *144*(4), 543–559. <https://doi.org/10.1007/BF03399265>

- Baranzini, A., & Schaerer, C. (2011). A sight for sore eyes: Assessing the value of view and land use in the housing market. *Journal of Housing Economics*, 20(3), 191–199. <https://doi.org/10.1016/j.jhe.2011.06.001>
- Baranzini, A., Schaerer, C., Ramirez, J. V., & Thalmann, P. (2006). *Feel it or Measure it—Perceived vs. Measured Noise in Hedonic Models* (SSRN Scholarly Paper 937259). <https://papers.ssrn.com/abstract=937259>
- Barrage, L., & Furst, J. (2019). Housing investment, sea level rise, and climate change beliefs. *Economics Letters*, 177, 105–108. <https://doi.org/10.1016/j.econlet.2019.01.023>
- Basolo, V., & Hastings, D. (2003). Obstacles to Regional Housing Solutions: A Comparison of Four Metropolitan Areas. *Journal of Urban Affairs*, 25, 449–472. <https://doi.org/10.1111/1467-9906.00172>
- Bates, P. D., Quinn, N., Sampson, C., Smith, A., Wing, O., Sosa, J., Savage, J., Olcese, G., Neal, J., Schumann, G., Giustarini, L., Coxon, G., Porter, J. R., Amodeo, M. F., Chu, Z., Lewis-Gruss, S., Freeman, N. B., Houser, T., Delgado, M., ... Krajewski, W. F. (2021). Combined Modeling of US Fluvial, Pluvial, and Coastal Flood Hazard Under Current and Future Climates. *Water Resources Research*, 57(2), e2020WR028673. <https://doi.org/10.1029/2020WR028673>
- Baušys, R., & Pankrašovaite, I. (2005). Optimization of architectural layout by the improved genetic algorithm. *Journal of Civil Engineering and Management*, 11(1), Article 1. <https://doi.org/10.3846/13923730.2005.9636328>
- Benson, E. D., Hansen, J. L., Schwartz, A. L., & Smersh, G. T. (1998). Pricing Residential Amenities: The Value of a View. *The Journal of Real Estate Finance and Economics*, 16(1), 55–73. <https://doi.org/10.1023/A:1007785315925>
- Bernstein, A., Billings, S. B., Gustafson, M. T., & Lewis, R. (2022). Partisan residential sorting on climate change risk. *Journal of Financial Economics*, 146(3), 989–1015. <https://doi.org/10.1016/j.jfineco.2022.03.004>
- Bibri, S. E., Krogstie, J., & Kärrholm, M. (2020). Compact city planning and development: Emerging practices and strategies for achieving the goals of sustainability. *Developments in the Built Environment*, 4, 100021. <https://doi.org/10.1016/j.dibe.2020.100021>
- Biljecki, F., & Chow, Y. S. (2022). Global Building Morphology Indicators. *Computers, Environment and Urban Systems*, 95, 101809. <https://doi.org/10.1016/j.compenvurbsys.2022.101809>
- Biljecki, F., & Ito, K. (2021). Street view imagery in urban analytics and GIS: A review. *Landscape and Urban Planning*, 215, 104217. <https://doi.org/10.1016/j.landurbplan.2021.104217>
- Biljecki, F., Stoter, J., Ledoux, H., Zlatanova, S., & Çöltekin, A. (2015). Applications of 3D City Models: State of the Art Review. *ISPRS International Journal of Geo-Information*, 4(4), Article 4. <https://doi.org/10.3390/ijgi4042842>
- Bosker, M., & Buringh, E. (2017). City seeds: Geography and the origins of the European city system. *Journal of Urban Economics*, 98, 139–157. <https://doi.org/10.1016/j.jue.2015.09.003>

- Bourassa, S. C., Hoesli, M., & Sun, J. (2004). What's in a View? *Environment and Planning A: Economy and Space*, 36(8), 1427–1450. <https://doi.org/10.1068/a36103>
- Boustan, L. P., Kahn, M. E., Rhode, P. W., & Yanguas, M. L. (2020). The effect of natural disasters on economic activity in US counties: A century of data. *Journal of Urban Economics*, 118, 103257. <https://doi.org/10.1016/j.jue.2020.103257>
- Boyle, M. A., & Kiel, K. A. (2001). A Survey of House Price Hedonic Studies of the Impact of Environmental Externalities. *Journal of Real Estate Literature*, 9(2), 117–144.
- Breiman, L. (2001). Random Forests. *Machine Learning*, 45(1), 5–32. <https://doi.org/10.1023/A:1010933404324>
- Bretz, L. (2017, October 18). Climate Change and Homes: Who Would Lose the Most to a Rising Tide? *Zillow*. <https://www.zillow.com/research/climate-change-underwater-homes-2-16928/>
- Brielmann, A. A., Buras, N. H., Salingaros, N. A., & Taylor, R. P. (2022). What Happens in Your Brain When You Walk Down the Street? Implications of Architectural Proportions, Biophilia, and Fractal Geometry for Urban Science. *Urban Science*, 6(1), 3. <https://doi.org/10.3390/urbansci6010003>
- Brown, N. C. (2020). Design performance and designer preference in an interactive, data-driven conceptual building design scenario. *Design Studies*, 68, 1–33. <https://doi.org/10.1016/j.destud.2020.01.001>
- Buchak, G., Matvos, G., Piskorski, T., & Seru, A. (2020). *Why is Intermediating Houses so Difficult? Evidence from iBuyers* (Working Paper 28252). National Bureau of Economic Research. <https://doi.org/10.3386/w28252>
- Buffat, R., Froemelt, A., Heeren, N., Raubal, M., & Hellweg, S. (2017). Big data GIS analysis for novel approaches in building stock modelling. *Applied Energy*, 208, 277–290. <https://doi.org/10.1016/j.apenergy.2017.10.041>
- Bunce, S. (2023). From “smart growth” to “frontier” intensification: Density, YIMBYism, and the development of garden suites in Toronto. *Frontiers in Sustainable Cities*, 5. <https://www.frontiersin.org/articles/10.3389/frsc.2023.1196428>
- Burchfield, M., Overman, H. G., Puga, D., & Turner, M. A. (2006). Causes of Sprawl: A Portrait from Space*. *The Quarterly Journal of Economics*, 121(2), 587–633. <https://doi.org/10.1162/qjec.2006.121.2.587>
- Caetano, I., Santos, L., & Leitão, A. (2020). Computational design in architecture: Defining parametric, generative, and algorithmic design. *Frontiers of Architectural Research*, 9(2), 287–300. <https://doi.org/10.1016/j.foar.2019.12.008>
- Chen, M., Liu, Y., Arribas-Bel, D., & Singleton, A. (2022). Assessing the value of user-generated images of urban surroundings for house price estimation. *Landscape and Urban Planning*, 226, 104486. <https://doi.org/10.1016/j.landurbplan.2022.104486>
- Chen, T., & Guestrin, C. (2016). XGBoost: A Scalable Tree Boosting System. *Proceedings of the 22nd ACM SIGKDD International Conference on Knowledge Discovery and Data Mining*, 785–794. <https://doi.org/10.1145/2939672.2939785>

- Chen, W. Y., & Jim, C. Y. (2010). Amenities and disamenities: A hedonic analysis of the heterogeneous urban landscape in Shenzhen (China). *The Geographical Journal*, 176(3), 227–240. <https://doi.org/10.1111/j.1475-4959.2010.00358.x>
- Chen, W. Y., Li, X., & Hua, J. (2019). Environmental amenities of urban rivers and residential property values: A global meta-analysis. *Science of The Total Environment*, 693, 133628. <https://doi.org/10.1016/j.scitotenv.2019.133628>
- Chetty, R., Jackson, M. O., Kuchler, T., Stroebel, J., Hendren, N., Fluegge, R. B., Gong, S., Gonzalez, F., Grondin, A., Jacob, M., Johnston, D., Koenen, M., Laguna-Muggenburg, E., Mudekereza, F., Rutter, T., Thor, N., Townsend, W., Zhang, R., Bailey, M., ... Wernerfelt, N. (2022). Social capital I: Measurement and associations with economic mobility. *Nature*, 608(7921), Article 7921. <https://doi.org/10.1038/s41586-022-04996-4>
- Chinazzo, G., Wienold, J., & Andersen, M. (2019). Daylight affects human thermal perception. *Scientific Reports*, 9(1), 13690. <https://doi.org/10.1038/s41598-019-48963-y>
- Cho, Y., Karmann, C., & Andersen, M. (2023a). A VR-based workflow to assess perception of daylight views-out with a focus on dynamism and immersion. *Journal of Physics: Conference Series*, 2600(11), 112002. <https://doi.org/10.1088/1742-6596/2600/11/112002>
- Cho, Y., Karmann, C., & Andersen, M. (2023b). Dynamism in the context of views out: A literature review. *Building and Environment*, 244, 110767. <https://doi.org/10.1016/j.buildenv.2023.110767>
- Cilliers, D., Cloete, M., Bond, A., Retief, F., Alberts, R., & Roos, C. (2023). A critical evaluation of visibility analysis approaches for visual impact assessment (VIA) in the context of environmental impact assessment (EIA). *Environmental Impact Assessment Review*, 98, 106962. <https://doi.org/10.1016/j.eiar.2022.106962>
- Couture, V., Gaubert, C., Handbury, J., & Hurst, E. (2023). Income growth and the distributional effects of urban spatial sorting. *The Review of Economic Studies*, rdad048. <https://doi.org/10.1093/restud/rdad048>
- Cove.Tools. (2024). *Cove.tool | Sustainable Building Design | Energy Modeling Software*. <https://cove.tools/>
- Dai, X., Felsenstein, D., & Grinberger, A. Y. (2023). Viewshed effects and house prices: Identifying the visibility value of the natural landscape. *Landscape and Urban Planning*, 238, 104818. <https://doi.org/10.1016/j.landurbplan.2023.104818>
- Dambon, J. A., Sigrist, F., & Furrer, R. (2021). Maximum likelihood estimation of spatially varying coefficient models for large data with an application to real estate price prediction. *Spatial Statistics*, 41, 100470. <https://doi.org/10.1016/j.spasta.2020.100470>
- Davidson, P. J., & Howe, M. (2014). Beyond NIMBYism: Understanding community antipathy toward needle distribution services. *International Journal of Drug Policy*, 25(3), 624–632. <https://doi.org/10.1016/j.drugpo.2013.10.012>

- Delve. (2024). *Delve by Sidewalk Labs | Real Estate Generative Design*.
<https://www.sidewalklabs.com/products/delve>
- Djurdjevic, D., Eugster, C., & Haase, R. (2008). Estimation of Hedonic Models Using a Multilevel Approach: An Application for the Swiss Rental Market. *Swiss Journal of Economics and Statistics*, 144(4), Article 4.
<https://doi.org/10.1007/BF03399271>
- EEA. (2015). *Air quality in Europe—2015 report—European Environment Agency* [Publication]. <https://www.eea.europa.eu/publications/air-quality-in-europe-2015#tab-data-references>
- Elshani, D. (2021). Measuring Sustainability and Urban Data Operationalization—An integrated computational framework to evaluate and interpret the performance of the urban form. A. Globa, J. van Ameijde, A. Fingrut, N. Kim, T.T.S. Lo (Eds.), *PROJECTIONS - Proceedings of the 26th CAADRIA Conference - Volume 2, The Chinese University of Hong Kong and Online, Hong Kong, 29 March - 1 April 2021, Pp. 407-416*.
https://papers.cumincad.org/cgi-bin/works/paper/caadria2021_391
- Elzeyadi, I. M. K. (2011). *Daylighting-Bias and Biophilia: Quantifying the Impact of Daylighting on Occupants Health*. 9.
- European Central Bank. (2020). *Guide on climate-related and environmental risks*.
<https://www.bankingsupervision.europa.eu/ecb/pub/pdf/ssm.202011finalguideonclimate-relatedandenvironmentalrisks~58213f6564.en.pdf>
- Fairweather, D., Kahn, M. E., Metcalf, R. D., & Sandoval-Olascoaga, S. (2023). *The Impact of Climate Risk Disclosure on Housing Search and Buying Dynamics: Evidence from a Nationwide Field Experiment with Redfin*.
https://conference.nber.org/conf_papers/f184841/f184841.pdf
- Farley, K. M. J., & Veitch, J. A. (2001). *A Room With A View: A Review of the Effects of Windows on Work and Well-Being: (668402012-001)* [dataset]. American Psychological Association. <https://doi.org/10.1037/e668402012-001>
- Federal Office of Topography swisstopo. (2018a). *swissALTI3D*. Federal Office of Topography Swisstopo.
<https://www.swisstopo.admin.ch/en/geodata/height/alti3d.html>
- Federal Office of Topography swisstopo. (2018b). *swissBUILDINGS3D 2.0*. Federal Office of Topography Swisstopo.
<https://www.swisstopo.admin.ch/en/geodata/landscape/buildings3d2.html>
- Federal Office of Topography swisstopo. (2018c). *swissTLM3D*. Federal Office of Topography Swisstopo.
<https://www.swisstopo.admin.ch/en/geodata/landscape/tlm3d.html>
- Federal Statistical Office. (2000). *Federal Statistical Office*.
<https://www.bfs.admin.ch/bfs/en/home.html>
- Federal Statistical Office. (2022, February 1). *Durchschnittliches steuerbares Einkommen pro Steuerpflichtigem/-r (Kantone/Politische Gemeinden) | Karte*. Bundesamt für Statistik.
<https://www.bfs.admin.ch/asset/de/21324555>
- Fiedler, T., Pitman, A. J., Mackenzie, K., Wood, N., Jakob, C., & Perkins-Kirkpatrick, S. E. (2021). Business risk and the emergence of climate

- analytics. *Nature Climate Change*, 11(2), Article 2. <https://doi.org/10.1038/s41558-020-00984-6>
- Fifer, S., Rose, J., & Greaves, S. (2014). Hypothetical bias in Stated Choice Experiments: Is it a problem? And if so, how do we deal with it? *Transportation Research Part A: Policy and Practice*, 61, 164–177. <https://doi.org/10.1016/j.tra.2013.12.010>
- First Street Foundation. (2023). *First Street Foundation Flood Model 2023 Methodology Addendum*. FirstStreet. <https://firststreet.org/methodology/flood/>
- Fischel, W. A. (2001). Why Are There NIMBYs? *Land Economics*, 77(1), 144–152. <https://doi.org/10.2307/3146986>
- Florio, P., Peronato, G., Perera, A. T. D., Di Blasi, A., Poon, K. H., & Kämpf, J. H. (2021). Designing and assessing solar energy neighborhoods from visual impact. *Sustainable Cities and Society*, 71, 102959. <https://doi.org/10.1016/j.scs.2021.102959>
- FOEN. (2023). *Vollzugshilfe sonROAD18 – Modellempehlungen*. <https://www.bafu.admin.ch/bafu/de/home/themen/thema-laerm/laerm--publikationen/publikationen-laerm/uv-2314-strassenlaerm-berechnungsmodell-sonroad18-modellempehlungen.html>
- Fotheringham, A. S. (2023). Digital twins: The current “Krays” of urban analytics? *Environment and Planning B: Urban Analytics and City Science*, 50(4), 1020–1022. <https://doi.org/10.1177/23998083231169159>
- Gagne, J., & Andersen, M. (2012). A generative facade design method based on daylighting performance goals. *Journal of Building Performance Simulation*, 5(3), 141–154. <https://doi.org/10.1080/19401493.2010.549572>
- Gagné, C., Koster, H. R. A., Moizeau, F., & Thisse, J.-F. (2022). Who lives where in the city? Amenities, commuting and income sorting. *Journal of Urban Economics*, 128, 103394. <https://doi.org/10.1016/j.jue.2021.103394>
- Gao, X., Song, R., & Timmins, C. (2023). Information, migration, and the value of clean air. *Journal of Development Economics*, 163, 103079. <https://doi.org/10.1016/j.jdeveco.2023.103079>
- Garmaise, M. J., & Moskowitz, T. J. (2009). Catastrophic Risk and Credit Markets. *The Journal of Finance*, 64(2), 657–707. <https://doi.org/10.1111/j.1540-6261.2009.01446.x>
- Giraffee. (2024). *Giraffe: Create vibrant cities with simplicity*. <https://www.giraffe.build/>
- Gourevitch, J. D., Kousky, C., Liao, Y. (Penny), Nolte, C., Pollack, A. B., Porter, J. R., & Weill, J. A. (2023). Unpriced climate risk and the potential consequences of overvaluation in US housing markets. *Nature Climate Change*, 13(3), Article 3. <https://doi.org/10.1038/s41558-023-01594-8>
- Grimmond, S. (2007). Urbanization and global environmental change: Local effects of urban warming. *The Geographical Journal*, 173(1), 83–88. https://doi.org/10.1111/j.1475-4959.2007.232_3.x
- Heblich, S., Trew, A., & Zylberberg, Y. (2021). East-Side Story: Historical Pollution and Persistent Neighborhood Sorting. *Journal of Political Economy*, 129(5), 1508–1552. <https://doi.org/10.1086/713101>

- Herweijer, C., Ranger, N., & Ward, R. E. T. (2009). Adaptation to Climate Change: Threats and Opportunities for the Insurance Industry. *The Geneva Papers on Risk and Insurance - Issues and Practice*, 34(3), 360–380. <https://doi.org/10.1057/gpp.2009.13>
- Hino, M., & Burke, M. (2021). The effect of information about climate risk on property values. *Proceedings of the National Academy of Sciences*, 118(17), e2003374118. <https://doi.org/10.1073/pnas.2003374118>
- Holtermans, R., Kahn, M. E., & Kok, N. (2023). *Climate Risk and Commercial Mortgage Delinquency* (SSRN Scholarly Paper 4066875). <https://doi.org/10.2139/ssrn.4066875>
- Holtermans, R., Niu, D., & Zheng, S. (2022). *Quantifying the Impacts of Climate Shocks in Commercial Real Estate Market* (SSRN Scholarly Paper 4276452). <https://doi.org/10.2139/ssrn.4276452>
- Hurst, E., Keys, B. J., Seru, A., & Vavra, J. (2019). *Regional Redistribution Through the U.S. Mortgage Market*. 65.
- Iliyasu, J., Sanusi, A. R., Mamman, S. O., & Abubakar, Y. (2023). Pricing Environmental Amenities and Climate Change Risks in Real Estate Market. *Environmental Modeling & Assessment*, 28(6), 999–1010. <https://doi.org/10.1007/s10666-023-09919-9>
- Inglis, N. C., Vukomanovic, J., Costanza, J., & Singh, K. K. (2022a). From viewsheds to viewsapes: Trends in landscape visibility and visual quality research. *Landscape and Urban Planning*, 224, 104424. <https://doi.org/10.1016/j.landurbplan.2022.104424>
- Inglis, N. C., Vukomanovic, J., Costanza, J., & Singh, K. K. (2022b). From viewsheds to viewsapes: Trends in landscape visibility and visual quality research. *Landscape and Urban Planning*, 224, 104424. <https://doi.org/10.1016/j.landurbplan.2022.104424>
- Intergovernmental Panel On Climate Change (Ippc). (2023a). *Climate Change 2022 – Impacts, Adaptation and Vulnerability: Working Group II Contribution to the Sixth Assessment Report of the Intergovernmental Panel on Climate Change* (1st ed.). Cambridge University Press. <https://doi.org/10.1017/9781009325844>
- Intergovernmental Panel On Climate Change (Ippc) (Ed.). (2023b). Urban Systems and Other Settlements. In *Climate Change 2022—Mitigation of Climate Change* (1st ed., pp. 861–952). Cambridge University Press. <https://doi.org/10.1017/9781009157926.010>
- IPCC. (2023). *Climate Change 2022 – Impacts, Adaptation and Vulnerability: Working Group II Contribution to the Sixth Assessment Report of the Intergovernmental Panel on Climate Change* (1st ed.). Cambridge University Press. <https://doi.org/10.1017/9781009325844>
- Issler, P., Stanton, R., Vergara-Alert, C., & Wallace, N. (2020). *Mortgage Markets with Climate-Change Risk: Evidence from Wildfires in California* (SSRN Scholarly Paper 3511843). <https://doi.org/10.2139/ssrn.3511843>
- Jain, S., Wienold, J., Lagier, M., Schueler, A., & Andersen, M. (2023). Perceived glare from the sun behind tinted glazing: Comparing blue vs. color-neutral tints. *Building and Environment*, 234, 110146. <https://doi.org/10.1016/j.buildenv.2023.110146>

- Jiang, F., Ma, J., Webster, C. J., Chiaradia, A. J. F., Zhou, Y., Zhao, Z., & Zhang, X. (2023). Generative urban design: A systematic review on problem formulation, design generation, and decision-making. *Progress in Planning*, 100795. <https://doi.org/10.1016/j.progress.2023.100795>
- Jiang, Z., Wen, H., Han, F., Tang, Y., & Xiong, Y. (2022). Data-driven generative design for mass customization: A case study. *Advanced Engineering Informatics*, 54, 101786. <https://doi.org/10.1016/j.aei.2022.101786>
- Kahn, M. (2024). *Adaptation in Financial Markets: Climate Risk Pooling in Mortgage-Backed Securities*. San Francisco Fed. <https://www.frbsf.org/economic-research/events/2023/december/matthew-e-kahn-climate-seminar/>
- Kang, N., & Liu, C. (2022). Towards landscape visual quality evaluation: Methodologies, technologies, and recommendations. *Ecological Indicators*, 142, 109174. <https://doi.org/10.1016/j.ecolind.2022.109174>
- Karmann, C., Chinazzo, G., Schöler, A., Manwani, K., Wienold, J., & Andersen, M. (2023). User assessment of fabric shading devices with a low openness factor. *Building and Environment*, 228, 109707. <https://doi.org/10.1016/j.buildenv.2022.109707>
- Katz, L., & Bokhari, S. (2023, July 24). *Migration to Flood-Prone Areas Has More Than Doubled Since 2020*. <https://www.redfin.com/news/climate-migration-real-estate-2023/>
- Ke, G., Meng, Q., Finley, T., Wang, T., Chen, W., Ma, W., Ye, Q., & Liu, T.-Y. (2017). LightGBM: A Highly Efficient Gradient Boosting Decision Tree. *Proceedings of the 31st International Conference on Neural Information Processing Systems*, 3149–3157.
- Keys, B. J., & Mulder, P. (2020). *Neglected No More: Housing Markets, Mortgage Lending, and Sea Level Rise* (Working Paper 27930; Working Paper Series). National Bureau of Economic Research. <https://doi.org/10.3386/w27930>
- Khan, J., Ketzler, M., Kakosimos, K., Sørensen, M., & Jensen, S. S. (2018). Road traffic air and noise pollution exposure assessment – A review of tools and techniques. *Science of The Total Environment*, 634, 661–676. <https://doi.org/10.1016/j.scitotenv.2018.03.374>
- Ko, W. H., Schiavon, S., Altomonte, S., Andersen, M., Batool, A., Browning, W., Burrell, G., Chamilothoni, K., Chan, Y.-C., Chinazzo, G., Christoffersen, J., Clanton, N., Connock, C., Dogan, T., Faircloth, B., Fernandes, L., Hescong, L., Houser, K. W., Inanici, M., ... Wienold, J. (2022). Window View Quality: Why It Matters and What We Should Do. *LEUKOS*, 18(3), 259–267. <https://doi.org/10.1080/15502724.2022.2055428>
- Kousky, C., Kunreuther, H., LaCour-Little, M., & Wachter, S. (2020). Flood Risk and the U.S. Housing Market. *Journal of Housing Research*, 29(sup1), S3–S24. <https://doi.org/10.1080/10527001.2020.1836915>
- Kumar, B., Atey, K., Singh, B. B., Chattopadhyay, R., Acharya, N., Singh, M., Nanjundiah, R. S., & Rao, S. A. (2023). On the modern deep learning approaches for precipitation downscaling. *Earth Science Informatics*, 16(2), 1459–1472. <https://doi.org/10.1007/s12145-023-00970-4>
- La Rasude reprend vie au cœur de Lausanne*. (n.d.). La Rasude. Retrieved October 11, 2023, from <https://la-rasude.ch/>

- Ladoy, A., Vallarta-Robledo, J. R., De Ridder, D., Sandoval, J. L., Stringhini, S., Da Costa, H., Guessous, I., & Joost, S. (2021). Geographic footprints of life expectancy inequalities in the state of Geneva, Switzerland. *Scientific Reports*, *11*(1), 23326. <https://doi.org/10.1038/s41598-021-02733-x>
- L'association Perirasude. (2023, April 5). Association Perirasude. <https://perirasude.com/>
- Law, S., Paige, B., & Russell, C. (2019). Take a Look Around: Using Street View and Satellite Images to Estimate House Prices. *ACM Transactions on Intelligent Systems and Technology*, *10*(5), 1–19. <https://doi.org/10.1145/3342240>
- Lee, C. (2019). Impacts of urban form on air quality in metropolitan areas in the United States. *Computers, Environment and Urban Systems*, *77*, 101362. <https://doi.org/10.1016/j.compenvurbsys.2019.101362>
- Lee, S., & Lin, J. (2018). Natural Amenities, Neighbourhood Dynamics, and Persistence in the Spatial Distribution of Income. *The Review of Economic Studies*, *85*(1), 663–694. <https://doi.org/10.1093/restud/rdx018>
- Lenzholzer, S., Carsjens, G.-J., Brown, R. D., Tavares, S., Vanos, J., Kim, Y., & Lee, K. (2020). Awareness of urban climate adaptation strategies –an international overview. *Urban Climate*, *34*, 100705. <https://doi.org/10.1016/j.uclim.2020.100705>
- Li, M., Xue, F., Wu, Y., & Yeh, A. G. O. (2022). A room with a view: Automatic assessment of window views for high-rise high-density areas using City Information Models and deep transfer learning. *Landscape and Urban Planning*, *226*, 104505. <https://doi.org/10.1016/j.landurbplan.2022.104505>
- Lin, B. B., Ossola, A., Alberti, M., Andersson, E., Bai, X., Dobbs, C., Elmqvist, T., Evans, K. L., Frantzeskaki, N., Fuller, R. A., Gaston, K. J., Haase, D., Jim, C. Y., Konijnendijk, C., Nagendra, H., Niemelä, J., McPhearson, T., Moomaw, W. R., Parnell, S., ... Tan, P. Y. (2021). Integrating solutions to adapt cities for climate change. *The Lancet Planetary Health*, *5*(7), e479–e486. [https://doi.org/10.1016/S2542-5196\(21\)00135-2](https://doi.org/10.1016/S2542-5196(21)00135-2)
- Lindenthal, T. (2020). Beauty in the Eye of the Home-Owner: Aesthetic Zoning and Residential Property Values. *Real Estate Economics*, *48*(2), 530–555. <https://doi.org/10.1111/1540-6229.12204>
- Lindenthal, T., & Johnson, E. B. (2021). Machine Learning, Architectural Styles and Property Values. *The Journal of Real Estate Finance and Economics*. <https://doi.org/10.1007/s11146-021-09845-1>
- Long, J., & Robertson, C. (2018). Comparing spatial patterns. *Geography Compass*, *12*(2), e12356. <https://doi.org/10.1111/gec3.12356>
- Lu, H. (2023). Learning from failure: Breaking the waste incineration NIMBY cycle through participatory governance. *Cleaner Waste Systems*, *5*, 100089. <https://doi.org/10.1016/j.clwas.2023.100089>
- Lundberg, S. M., & Lee, S.-I. (2017). A Unified Approach to Interpreting Model Predictions. *Proceedings of the 31st International Conference on Neural Information Processing Systems*, 4768–4777.
- Masson-Delmotte, V., Zhai, P., Pirani, A., Connors, S. L., Péan, C., Berger, S., Caud, N., Chen, Y., Goldfarb, L., Gomis, M. I., Huang, M., Leitzell, K., Lonnoy, E., Matthews, J. B. R., Maycock, T. K., Waterfield, T., Yelekçi, Ö.,

- Yu, R., & Zhou, B. (Eds.). (2021). *Climate Change 2021: The Physical Science Basis. Contribution of Working Group I to the Sixth Assessment Report of the Intergovernmental Panel on Climate Change*. Cambridge University Press. <https://doi.org/10.1017/9781009157896>
- Mayencourt, P., & Mueller, C. (2019). Structural Optimization of Cross-laminated Timber Panels in One-way Bending. *Structures*, 18, 48–59. <https://doi.org/10.1016/j.istruc.2018.12.009>
- McInnes, L., Healy, J., & Astels, S. (2017). hdbscan: Hierarchical density based clustering. *Journal of Open Source Software*, 2(11), 205. <https://doi.org/10.21105/joss.00205>
- Milojevic-Dupont, N., Wagner, F., Nachtigall, F., Hu, J., Brüser, G. B., Zumwald, M., Biljecki, F., Heeren, N., Kaack, L. H., Pichler, P.-P., & Creutzig, F. (2023). EUBUCCO v0.1: European building stock characteristics in a common and open database for 200+ million individual buildings. *Scientific Data*, 10(1), Article 1. <https://doi.org/10.1038/s41597-023-02040-2>
- Mittal, J., & Byahut, S. (2019). Scenic landscapes, visual accessibility and premium values in a single family housing market: A spatial hedonic approach. *Environment and Planning B: Urban Analytics and City Science*, 46(1), 66–83. <https://doi.org/10.1177/2399808317702147>
- Morillas, J. M. B., Gozalo, G. R., González, D. M., Moraga, P. A., & Vilchez-Gómez, R. (2018). Noise Pollution and Urban Planning. *Current Pollution Reports*, 4(3), 208–219. <https://doi.org/10.1007/s40726-018-0095-7>
- Münch, M., Wirz-Justice, A., Brown, S. A., Kantermann, T., Martiny, K., Stefani, O., Vetter, C., Wright, K. P., Wulff, K., & Skene, D. J. (2020). The Role of Daylight for Humans: Gaps in Current Knowledge. *Clocks & Sleep*, 2(1), 61–85. <https://doi.org/10.3390/clockssleep2010008>
- Nagy, D., Villaggi, L., & Benjamin, D. (2018). Generative urban design: Integrating financial and energy goals for automated neighborhood layout. *Proceedings of the Symposium on Simulation for Architecture and Urban Design*, 1–8.
- Natanian, J., & Auer, T. (2020). Beyond nearly zero energy urban design: A holistic microclimatic energy and environmental quality evaluation workflow. *Sustainable Cities and Society*, 56, 102094. <https://doi.org/10.1016/j.scs.2020.102094>
- Natanian, J., & Wortmann, T. (2021). Simplified evaluation metrics for generative energy-driven urban design: A morphological study of residential blocks in Tel Aviv. *Energy and Buildings*, 240, 110916. <https://doi.org/10.1016/j.enbuild.2021.110916>
- Nault, E., Peronato, G., Rey, E., & Andersen, M. (2015). Review and critical analysis of early-design phase evaluation metrics for the solar potential of neighborhood designs. *Building and Environment*, 92, 679–691. <https://doi.org/10.1016/j.buildenv.2015.05.012>
- NREL. (2017). *EnergyPlus* (EnergyPlus™ (e+); 005462MLTPL00). National Renewable Energy Laboratory (NREL), Golden, CO (United States); Lawrence Berkeley National Laboratory (LBNL), Berkeley, CA (United States). <https://www.osti.gov/biblio/1395882>

- Ögçe, H., Müderrisoğlu, H., & Uzun, S. (2020). Visual impact assessment of the Istanbul Land-wall. *Indoor and Built Environment*, 29(10), 1359–1373. <https://doi.org/10.1177/1420326X19874453>
- Oh, K. (1998). Visual threshold carrying capacity (VTCC) in urban landscape management: A case study of Seoul, Korea. *Landscape and Urban Planning*, 39(4), 283–294. [https://doi.org/10.1016/S0169-2046\(97\)00085-6](https://doi.org/10.1016/S0169-2046(97)00085-6)
- Olick, D. (2023, March 20). *Mortgage giant Fannie Mae tackles climate risk, but changes to underwriting may take several years*. CNBC. <https://www.cnbc.com/2023/03/20/mortgage-giant-fannie-mae-tackles-climate-risk.html>
- Ortega, F., & Taşpınar, S. (2018). Rising sea levels and sinking property values: Hurricane Sandy and New York's housing market. *Journal of Urban Economics*, 106, 81–100. <https://doi.org/10.1016/j.jue.2018.06.005>
- Osland, L., Östh, J., & Nordvik, V. (2022). House price valuation of environmental amenities: An application of GIS-derived data. *Regional Science Policy & Practice*, 14(4), 939–959. <https://doi.org/10.1111/rsp3.12382>
- Ouazad, A., & Kahn, M. (2019). *Mortgage Finance in the Face of Rising Climate Risk* (w26322; p. w26322). National Bureau of Economic Research. <https://doi.org/10.3386/w26322>
- Ouazad, A., & Kahn, M. E. (2022). Mortgage Finance and Climate Change: Securitization Dynamics in the Aftermath of Natural Disasters. *The Review of Financial Studies*, 35(8), 3617–3665. <https://doi.org/10.1093/rfs/hhab124>
- Ouazad, A., & Kahn, M. E. (2023). *Mortgage Securitization Dynamics in the Aftermath of Natural Disasters: A Reply* (arXiv:2305.07179). arXiv. <https://doi.org/10.48550/arXiv.2305.07179>
- Ouazad, A., & Ranci re, R. (2019). *Market Frictions, Arbitrage, and the Capitalization of Amenities* (Working Paper 25701). National Bureau of Economic Research. <https://doi.org/10.3386/w25701>
- Quartier Rasude   Lausanne – Quinze  tages, «c'est un cadeau aux promoteurs»*. (2023, April 24). 24 Heures. <https://www.24heures.ch/quinze-etages-cest-un-cadeau-aux-promoteurs-147843395226>
- Rong, H. H., Yang, J., Kang, M., & Chegut, A. (2020). The Value of Design in Real Estate Asset Pricing. *Buildings*, 10(10), Article 10. <https://doi.org/10.3390/buildings10100178>
- Rosen, S. (1974). Hedonic Prices and Implicit Markets: Product Differentiation in Pure Competition. *Journal of Political Economy*, 82(1), 34–55. JSTOR.
- Roswall, N., H gh, V., Envold-Bidstrup, P., Raaschou-Nielsen, O., Ketznel, M., Overvad, K., Olsen, A., & S rensen, M. (2015). Residential exposure to traffic noise and health-related quality of life—A population-based study. *PloS One*, 10(3), e0120199. <https://doi.org/10.1371/journal.pone.0120199>
- Roth, M., Hildebrandt, S., R hner, S., Tilk, C., Schwarz-von Raumer, H.-G., Roser, F., & Borsdorff, M. (2018). Landscape as an area as perceived by people: Empirically-based nationwide modelling of scenic landscape quality in Germany. *J. Digit. Landsc. Archit*, 3, 129–137.
- Roth, M., Hildebrandt, S., Walz, U., & Wende, W. (2021). Large-Area Empirically Based Visual Landscape Quality Assessment for Spatial Planning—A

- Validation Approach by Method Triangulation. *Sustainability*, 13(4), Article 4. <https://doi.org/10.3390/su13041891>
- Saiz, A. (2010). The Geographic Determinants of Housing Supply*. *The Quarterly Journal of Economics*, 125(3), 1253–1296. <https://doi.org/10.1162/qjec.2010.125.3.1253>
- Sandman, P. (1986). Getting to Maybe: Some Communications Aspects of Siting Hazardous Waste Facilities. *Seton Hall Journal of Legislation and Public Policy*, Vol. 9:(Iss. 2, Article 7.).
- Schively, C. (2007). Understanding the NIMBY and LULU Phenomena: Reassessing Our Knowledge Base and Informing Future Research. *Journal of Planning Literature*, 21(3), 255–266. <https://doi.org/10.1177/0885412206295845>
- Schutte, N. S., & Malouff, J. M. (1986). Preference for Complexity in Natural Landscape Scenes. *Perceptual and Motor Skills*, 63(1), 109–110. <https://doi.org/10.2466/pms.1986.63.1.109>
- Seto, K. C., Fragkias, M., Güneralp, B., & Reilly, M. K. (2011). A Meta-Analysis of Global Urban Land Expansion. *PLoS ONE*, 6(8), e23777. <https://doi.org/10.1371/journal.pone.0023777>
- Shi, Z., Fonseca, J. A., & Schlueter, A. (2017). A review of simulation-based urban form generation and optimization for energy-driven urban design. *Building and Environment*, 121, 119–129. <https://doi.org/10.1016/j.buildenv.2017.05.006>
- Shogren, J. F., & Stamland, T. (2002). Skill and the Value of Life. *Journal of Political Economy*, 110(5), 1168–1173. <https://doi.org/10.1086/341875>
- Sinha, P., Caulkins, M., & Cropper, M. (2021). The value of climate amenities: A comparison of hedonic and discrete choice approaches. *Journal of Urban Economics*, 126, 103371. <https://doi.org/10.1016/j.jue.2021.103371>
- Sirmans, G. S., Macpherson, D. A., & Zietz, E. N. (2005). The Composition of Hedonic Pricing Models. *Journal of Real Estate Literature*, 13(1), 3–43.
- Skoury, L., Trembl, S., Opgenorth, N., Amtsberg, F., Wagner, H. J., Menges, A., & Wortmann, T. (2024). Towards data-informed co-design in digital fabrication. *Automation in Construction*, 158, 105229. <https://doi.org/10.1016/j.autcon.2023.105229>
- Smith, C., & Levermore, G. (2008). Designing urban spaces and buildings to improve sustainability and quality of life in a warmer world. *Energy Policy*, 36(12), 4558–4562. <https://doi.org/10.1016/j.enpol.2008.09.011>
- Sonta, A., Dougherty, T. R., & Jain, R. K. (2021). Data-driven optimization of building layouts for energy efficiency. *Energy and Buildings*, 238, 110815. <https://doi.org/10.1016/j.enbuild.2021.110815>
- Sruthi Krishnan, V., & Mohammed Firoz, C. (2020). Regional urban environmental quality assessment and spatial analysis. *Journal of Urban Management*, 9(2), 191–204. <https://doi.org/10.1016/j.jum.2020.03.001>
- Stroebel, J., & Wurgler, J. (2021). What do you think about climate finance? *Journal of Financial Economics*, 142(2), 487–498. <https://doi.org/10.1016/j.jfineco.2021.08.004>

- Swietek, A. (2023). *Automated Design Appraisal: Estimating Real Estate Price Growth and Value at Risk Due to Local Development* (SSRN Scholarly Paper 4670069). <https://doi.org/10.2139/ssrn.4670069>
- Swietek, A. R., & Zumwald, M. (2023). Visual Capital: Evaluating building-level visual landscape quality at scale. *Landscape and Urban Planning*, *240*, 104880. <https://doi.org/10.1016/j.landurbplan.2023.104880>
- Taylor, Z. J. (2020). The real estate risk fix: Residential insurance-linked securitization in the Florida metropolis: *Environment and Planning A: Economy and Space*. <https://doi.org/10.1177/0308518X19896579>
- Tennessen, C. M., & Cimprich, B. (1995). Views to nature: Effects on attention. *Journal of Environmental Psychology*, *15*(1), 77–85. [https://doi.org/10.1016/0272-4944\(95\)90016-0](https://doi.org/10.1016/0272-4944(95)90016-0)
- Thibodeau, T. G. (1990). Estimating the Effect of High-Rise Office Buildings on Residential Property Values. *Land Economics*, *66*(4), 402–408. <https://doi.org/10.2307/3146622>
- Turan, I., Chegut, A., Fink, D., & Reinhart, C. (2020a). The value of daylight in office spaces. *Building and Environment*, *168*, 106503. <https://doi.org/10.1016/j.buildenv.2019.106503>
- Turan, I., Chegut, A., Fink, D., & Reinhart, C. (2020b). The value of daylight in office spaces. *Building and Environment*, *168*, 106503. <https://doi.org/10.1016/j.buildenv.2019.106503>
- Turan, I., Chegut, A., Fink, D., & Reinhart, C. (2021). Development of view potential metrics and the financial impact of views on office rents. *Landscape and Urban Planning*, *215*, 104193. <https://doi.org/10.1016/j.landurbplan.2021.104193>
- Turner, J. (2016). *Air Pollution Exposure Indicators: Review of Ground-Level Monitoring Data Availability and Proposed Calculation Method*. OECD. <https://doi.org/10.1787/5jlsqs98gss7-en>
- ULI, & Heitmann. (2019). *Climate Risk and Real Estate Investment Decision-Making | ULI Knowledge Finder*. https://knowledge.uli.org/en/reports/research-reports/2019/climate-risk-and-real-estate-investment-decisionmaking?_gl=1*ehqa5*_ga*ODc3Mzg5ODM5LjE2OTc0NTY5NzM.*_ga_68JJQP7N7N*MTY5NzQ1Njk3My4xLjAuMTY5NzQ1Njk3My4wLjAuMA..
- Ulrich, R. S. (1977). Visual landscape preference: A model and application. *Man-Environment Systems*, *7*(5), 279–293.
- Ulrich, R. S. (1981). Natural Versus Urban Scenes: Some Psychophysiological Effects. *Environment and Behavior*, *13*(5), 523–556. <https://doi.org/10.1177/0013916581135001>
- Ulrich, R. S. (1986). Human responses to vegetation and landscapes. *Landscape and Urban Planning*, *13*, 29–44. [https://doi.org/10.1016/0169-2046\(86\)90005-8](https://doi.org/10.1016/0169-2046(86)90005-8)
- US EPA, O. (2022, November 28). *Climate Risks and Opportunities Defined* [Collections and Lists]. <https://www.epa.gov/climateleadership/climate-risks-and-opportunities-defined>

- van der Horst, D. (2007). NIMBY or not? Exploring the relevance of location and the politics of voiced opinions in renewable energy siting controversies. *Energy Policy*, *35*(5), 2705–2714. <https://doi.org/10.1016/j.enpol.2006.12.012>
- Vardoulakis, S., Dear, K., & Wilkinson, P. (2016). Challenges and Opportunities for Urban Environmental Health and Sustainability: The HEALTHY-POLIS initiative. *Environmental Health*, *15*(1), S30. <https://doi.org/10.1186/s12940-016-0096-1>
- Vegetation Height Model NFI - 2019 Vegetation Height Model NFI (current)*—*EnviDat*. (n.d.). Retrieved September 10, 2023, from <https://www.envidat.ch/dataset/vegetation-height-model-nfi/resource/d4f64aef-f65e-4070-a661-dac8c49abc69>
- Vellei, M., Chinazzo, G., Zitting, K.-M., & Hubbard, J. (2021). Human thermal perception and time of day: A review. *Temperature*, *8*(4), 320–341. <https://doi.org/10.1080/23328940.2021.1976004>
- Villaggi, L., Stoddart, J., Nagy, D., & Benjamin, D. (2018). Survey-Based Simulation of User Satisfaction for Generative Design in Architecture. In K. De Rycke, C. Gengnagel, O. Baverel, J. Burry, C. Mueller, M. M. Nguyen, P. Rahm, & M. R. Thomsen (Eds.), *Humanizing Digital Reality: Design Modelling Symposium Paris 2017* (pp. 417–430). Springer. https://doi.org/10.1007/978-981-10-6611-5_36
- Vukomanovic, J., & Orr, B. J. (2014). Landscape Aesthetics and the Scenic Drivers of Amenity Migration in the New West: Naturalness, Visual Scale, and Complexity. *Land*, *3*(2), Article 2. <https://doi.org/10.3390/land3020390>
- Walch, A., Castello, R., Mohajeri, N., & Scartezzini, J.-L. (2020). Big data mining for the estimation of hourly rooftop photovoltaic potential and its uncertainty. *Applied Energy*, *262*, 114404. <https://doi.org/10.1016/j.apenergy.2019.114404>
- Walz, U., & Stein, C. (2018). Indicator for a monitoring of Germany's landscape attractiveness. *Ecological Indicators*, *94*, 64–73. <https://doi.org/10.1016/j.ecolind.2017.06.052>
- Wang, T.-K., & Duan, W. (2023). Generative design of floor plans of multi-unit residential buildings based on consumer satisfaction and energy performance. *Developments in the Built Environment*, *16*, 100238. <https://doi.org/10.1016/j.dibe.2023.100238>
- Wang, Y., Tu, Y., & Fan, Y. (2023). The price of quietness: How a pandemic affects city dwellers' response to road traffic noise. *Sustainable Cities and Society*, *99*, 104882. <https://doi.org/10.1016/j.scs.2023.104882>
- Warren, C. R., Lumsden, C., O'Dowd, S., & Birnie, R. V. (2005). 'Green On Green': Public perceptions of wind power in Scotland and Ireland. *Journal of Environmental Planning and Management*, *48*(6), 853–875. <https://doi.org/10.1080/09640560500294376>
- Wartmann, F. M., Frick, J., Kienast, F., & Hunziker, M. (2021). Factors influencing visual landscape quality perceived by the public. Results from a national survey. *Landscape and Urban Planning*, *208*, 104024. <https://doi.org/10.1016/j.landurbplan.2020.104024>

- Weber, R. E., Mueller, C., & Reinhart, C. (2022). Automated floorplan generation in architectural design: A review of methods and applications. *Automation in Construction*, *140*, 104385. <https://doi.org/10.1016/j.autcon.2022.104385>
- Wikle, C. K., Mateu, J., & Zammit-Mangion, A. (2023). Deep learning and spatial statistics. *Spatial Statistics*, *57*, 100774. <https://doi.org/10.1016/j.spasta.2023.100774>
- World Health Organization. (2021). *WHO global air quality guidelines: Particulate matter (PM_{2.5} and PM₁₀), ozone, nitrogen dioxide, sulfur dioxide and carbon monoxide*. World Health Organization. <https://apps.who.int/iris/handle/10665/345329>
- Wortmann, T., Cichocka, J., & Waibel, C. (2022). Simulation-based optimization in architecture and building engineering—Results from an international user survey in practice and research. *Energy and Buildings*, *259*, 111863. <https://doi.org/10.1016/j.enbuild.2022.111863>
- Wunderli, J. M. (2012). *sonRAIL - from the scientific model to an application in practice* (pp. 475–480). <https://www.dora.lib4ri.ch/empa/islandora/object/empa%3A9231/>
- Wunderli, J. M., Zellmann, C., Köpfl, M., Habermacher, M., Schwab, O., Schlatter, F., & Schäffer, B. (2018). sonAIR - a GIS-integrated spectral aircraft noise simulation tool for single flight prediction and noise mapping. *Acta Acustica United with Acustica*, 440–451. <https://doi.org/10.3813/AAA.919180>
- Yamagata, Y., Murakami, D., Yoshida, T., Seya, H., & Kuroda, S. (2016). Value of urban views in a bay city: Hedonic analysis with the spatial multilevel additive regression (SMAR) model. *Landscape and Urban Planning*, *151*, 89–102. <https://doi.org/10.1016/j.landurbplan.2016.02.008>
- Yang, J., Rong, H., Kang, Y., Zhang, F., & Chegut, A. (2021). The financial impact of street-level greenery on New York commercial buildings. *Landscape and Urban Planning*, *214*, 104162. <https://doi.org/10.1016/j.landurbplan.2021.104162>
- Ye, V. Y., & Becker, C. M. (2018). The Z-axis: Elevation gradient effects in Urban America. *Regional Science and Urban Economics*, *70*, 312–329. <https://doi.org/10.1016/j.regsciurbeco.2017.10.002>
- Yu, S., Chen, Z., Yu, B., Wang, L., Wu, B., Wu, J., & Zhao, F. (2020). Exploring the relationship between 2D/3D landscape pattern and land surface temperature based on explainable eXtreme Gradient Boosting tree: A case study of Shanghai, China. *Science of The Total Environment*, *725*, 138229. <https://doi.org/10.1016/j.scitotenv.2020.138229>
- Yu, S., Yu, B., Song, W., Wu, B., Zhou, J., Huang, Y., Wu, J., Zhao, F., & Mao, W. (2016). View-based greenery: A three-dimensional assessment of city buildings' green visibility using Floor Green View Index. *Landscape and Urban Planning*, *152*, 13–26. <https://doi.org/10.1016/j.landurbplan.2016.04.004>
- Zekar, A., Milojevic-Dupont, N., Zumwald, M., Wagner, F., & Creutzig, F. (2023). Urban form features determine spatio-temporal variation of ambient temperature: A comparative study of three European cities. *Urban Climate*, *49*, 101467. <https://doi.org/10.1016/j.uclim.2023.101467>

Curriculum Vitae

Adam R. SWIETEK

Avenue d'Ouchy 58

CH-1006 Lausanne

+41 78 659 77 41

adam.swietek@epfl.ch

December 13, 1990

American and Polish citizen

Education

EPFL, PhD, 04/2024

Thesis: "Spatial Modeling for Building Design Evaluation: from visual landscape quality assessment to devaluation risk estimation", Prof. Dr. Philippe Thalmann

Defense: April 12, 2024: Committee members: Philippe Thalmann, Marilyne Andersen, Alexandre Alahi, Lint Barrage, Silvia Tobias

Nominated for Thesis Distinction

Columbia University, M.Sc. Real Estate Development & Finance, 05/2019

Georgia Tech, B.Sc. Mechanical Engineering, Energy Systems Minor, 12/2013

Employment

EPFL, Laboratory of Environmental and Urban Economics

since 2019: Marie Curie Fellow, Researcher, Teaching Assistant

Wüest Partner, Geneva

2021-2023: PhD researcher, Geospatial Data Scientist

Faithful & Gould, New York City

2015-2018: Project Management Analyst

Olympic Construction, New York City

2013-2015: Assistant Project Manager

Graduate Researcher: Metaprop Venture Capital (2019), Gilbane Virtual Design & Construction (2019)

Supervision of junior researchers

Master's Thesis: Yannick Neypatraiky, "Data-Driven Assessment of the Swiss Building Stock: Characterising Building Typologies for Energy Retrofit Prioritization", 2023

Master's Thesis: Esteban Requena, "Identifying Geographical Clusters of High or Low Sustainability Ratings and Their Implications", 2024

Machine Learning Course: Paul Habert, Yannick Neypatraiky, Thomas Rimbot, "Best Place for You to Live", 2022, [paper](#)

Teaching Activity

Teaching Assistant, 'Economic Growth & Sustainability I & II', HUM-470/471, EPFL

Awards

Marie-Curie Fellowship: EU Horizon 2020

Blaze Accelerator Grant

Circular Economy Transition Incubator

ENAC Innovation Seed Grant

Presentation and Talks

Spatial Statistics Conference: Climate and the Environment, University of Colorado at Boulder, July 2023, poster

Doc.Days, EDAR, EPFL, April 2023, presentation

Publications

Swietek, A.R., (2024). Using Automated Design Appraisal to model Building-specific Devaluation Risk due to Land-use Change, in-review *Sustainable Cities & Society*, <https://doi.org/10.2139/ssrn.4670069>

Swietek, A. R., & Zumwald, M. (2023). Visual Capital: Evaluating building-level visual landscape quality at scale. *Landscape and Urban Planning*, 240, 104880. <https://doi.org/10.1016/j.landurbplan.2023.104880>

Swietek, A.R., & Schweizer, J. (2022) "How view determines well-being and value", Wüest Partner, <https://www.wuestpartner.com/ch-en/2022/11/07/how-view-determines-well-being-and-value/>